

ACCELERATED DISTRIBUTION DEMONSTRATION SYSTEM

REGULATORY INFORMATION DISTRIBUTION SYSTEM (RIDS)

ACCESSION NBR: 8907250083 DOC. DATE: 89/07/18 NOTARIZED: NO DOCKET #
 FACIL: 50-275 Diablo Canyon Nuclear Power Plant, Unit 1, Pacific Ga 05000275
 50-323 Diablo Canyon Nuclear Power Plant, Unit 2, Pacific Ga 05000323

AUTH. NAME AUTHOR AFFILIATION
 SHIFFER, J.D. Pacific Gas & Electric Co.
 RECIP. NAME RECIPIENT AFFILIATION
 Document Control Branch (Document Control Desk)

See list

SUBJECT: Forwards addl info re PRA for maint duration used in diesel generator allowed outage time study.

DISTRIBUTION CODE: A001D COPIES RECEIVED: LTR 1 ENCL 1 SIZE: 184
 TITLE: OR Submittal: General Distribution

NOTES:

	RECIPIENT ID CODE/NAME	COPIES LTTR	ENCL	RECIPIENT ID CODE/NAME	COPIES LTTR	ENCL
	PD5 LA	1	1	PD5 PD	1	1
	ROOD, H	5	5			
INTERNAL:	ACRS	1	1	NRR/DEST/ADS 7E	1	1
	NRR/DEST/CEB 8H	1	1	NRR/DEST/ESB 8D	1	1
	NRR/DEST/ICSB	1	1	NRR/DEST/MTB 9H	1	1
	NRR/DEST/RSB 8E	1	1	NRR/DOEA/TSB 11	1	1
	NUDOCS-ABSTRACT	1	1	OC/LEMB	1	0
	OGC/HDS2	1	0	REG FILE 01	1	1
	RES/DSIR/EIB	1	1			
EXTERNAL:	LPDR	1	1	NRC PDR	1	1
	NSIC	1	1			

NOTE TO ALL "RIDS" RECIPIENTS:

PLEASE HELP US TO REDUCE WASTE! . CONTACT THE DOCUMENT CONTROL DESK,
 ROOM P1-37 (EXT. 20079) TO ELIMINATE YOUR NAME FROM DISTRIBUTION
 LISTS FOR DOCUMENTS YOU DON'T NEED!

TOTAL NUMBER OF COPIES REQUIRED: LTR 28 ENCL 26

R
I
D
S
/
A
D
D
S

R
I
D
S
/
A
D
D
S

20
26
not a

1944

1944

Pacific Gas and Electric Company

77 Beale Street
San Francisco, CA 94106
415/972-7000
TWX 910-372-6587

James D. Shiffer
Vice President
Nuclear Power Generation

July 18, 1989

PG&E Letter No. DCL-89-191



U.S. Nuclear Regulatory Commission
ATTN: Document Control Desk
Washington, D.C. 20555

Re: Docket No. 50-275, OL-DPR-80
Docket No. 50-323, OL-DPR-82
Diablo Canyon Units 1 and 2
Probabilistic Risk Assessment

Gentlemen:

As requested by the NRC Staff in a meeting on June 13-14, 1989, PG&E is submitting the enclosed additional information pertaining to the Diablo Canyon probabilistic risk assessment (PRA). Enclosure 1 provides additional PRA information for the maintenance duration used in the Diesel Generator Allowed Outage Time Study, submitted on May 11, 1989 in PG&E Letter DCL-89-126. Enclosure 2 consists of Appendix F.5, Other External Events, and Appendix H.2, Data Analysis Approach.

Kindly acknowledge receipt of this material on the enclosed copy of this letter and return it in the enclosed addressed envelope.

Sincerely,

A handwritten signature in cursive script, appearing to read 'J. D. Shiffer for'. The signature is written in dark ink and is positioned above the printed name of the signatory.

J. D. Shiffer

cc: J. B. Martin
M. M. Mendonca
P. P. Narbut
H. Rood
B. H. Vogler
CPUC
Diablo Distribution (w/o Enc.)

Enclosures

2791S/0070K/GCW/538

*A001
11*

8907250083 890718
PDR ADOCK 05000275
P PDC



1

2

ENCLOSURE 1

2791S/0070K

...8907250083



PACIFIC GAS AND ELECTRIC COMPANY

DIESEL GENERATOR ALLOWED OUTAGE TIME STUDY

SUPPLEMENTAL INFORMATION
ON DG MAINTENANCE DURATION





Vertical text on the left side of the page, possibly bleed-through from the reverse side. The text is faint and difficult to read, but appears to be organized into several lines.

The maintenance duration data for diesel generators was developed by combining in a Bayesian Update the cumulative experience from a population of nuclear power plants with the plant specific data developed from a review of the Diablo Canyon operation records. The diesel generators currently have a 72-hour Allowed Outage Time (AOT). In order to estimate how diesel generation maintenance practices might change under a 7-day AOT, the plant staff was consulted and a point estimate of the maintenance duration was developed.

Prior Maintenance Duration Distribution (72 Hour AOT)

A prior maintenance duration distribution was developed through review, analysis, and tabulation of the available generic data. The basis for this distribution is described in the PLG proprietary data book (1). Table 1 contains the discretised prior distribution and the cumulative probability for the diesel generator generic maintenance duration distribution. Figure 1 shows the cumulative probability distribution. The following are the parameters of this distribution.

Percentiles

<u>Mean</u>	<u>5th</u>	<u>50th</u>	<u>95th</u>
10.5	.507	6.85	23.7

Posterior Maintenance Duration Distribution (72 Hour AOT)

The posterior maintenance duration distribution was developed by using a Bayesian update to combine the prior distribution with plant specific data.

Information about component unavailabilities due to maintenance at Diablo Canyon Unit 1 was found in the "Clearance Requests." The plant-specific maintenance data was derived from a review of all switching and tagging orders written during non-cold shutdown conditions between May 1985 and July 1986.

24 diesel generator maintenance events were found with a mean duration of 10.2 hours. The BEST4(2) computer code was used to update the prior distribution with this plant specific data to generate a posterior distribution.

Table 2 contains the discretised posterior distribution and the cumulative probability for the diesel generator plant specific maintenance duration distribution. Figure 2 shows the cumulative probability distribution. The following are the parameters of this distribution.

Percentiles

<u>Mean</u>	<u>5th</u>	<u>50th</u>	<u>95th</u>
10.06	6.65	9.74	10.3

The cumulative curve and the tabulated values, may be used to estimate the probability of a maintenance event taking a specified number of hours to complete.

7-Day AOT Maintenance Duration

In order to estimate how DG maintenance practices at DCPD might change under a 7-day AOT, the plant staff was consulted. It was the staff's consensus that

The cumulative curve and the tabulated values, may be used to estimate the probability of a maintenance event taking a specified number of hours to complete.

7-Day AOT Maintenance Duration

In order to estimate how DG maintenance practices at DCPD might change under a 7-day AOT, the plant staff was consulted. It was the staff's consensus that very little change in the maintenance and operations practices and, consequently, the mean maintenance duration, is expected with a 7-day AOT. The following key observations support this conclusion:

- o With a DG unavailable, the ability to perform maintenance on other systems is essentially precluded by Technical Specifications (discussed below). This restriction can have a significant impact on plant maintenance scheduling and planning. In general, other maintenance activities may be postponed until the DG is operable. Hence, there is significant motivation to return the DG to operate status as soon as possible.
- o Technical Specification 3.8.1.1 Action Statement, part 1 requires that if one DG is inoperable then verify that "All required systems, subsystems, trains, components and devices that depend on the remaining operable DG as a source of emergency power are also operable". If these conditions are not met, then action must be initiated within two hours to place the unit in Hot Standby. The plant maintenance staff must assure that this 2-hour Action Statement is met in order to avoid plant shutdown. Thus, unforeseen equipment failures provide incentive to complete any repair work on the inoperable DG.
- o As part of its corporate goals and activities, PG&E has implemented the INPO performance indicator program. In this regard, PG&E management is committed to minimizing DG unavailability and monitors DG unavailability data to assure this commitment is implemented.

DG unavailability is a performance indicator parameter reported by PG&E to INPO on a quarterly basis and is reviewed by PG&E senior corporate and plant management. The data reported includes demand, start, load-run, out-of-service durations, and hour-of-operations data. This management commitment provides a further incentive to minimize DG unavailability time.

Based on these considerations, changing to a 7-day AOT is not expected to cause a significant increase in the mean DG maintenance duration. However, to use a conservative value, an increase of six hours is assumed. Thus, the mean maintenance duration would increase from 10 to 16 hours. In



11
12
13



evaluating the system unreliability results for a 7-day AOT, a point estimate of 16 hours was used, a distribution was not developed.

REFERENCES

- 1) Mosleh, A., et. al., "A Data Base for Probabilistic Risk Assessment of LWRs," Pickard, Lowe and Garrick, Inc., PLG-0500, 1987.
- 2) Pickard, Lowe and Garrick, Inc., "Bayesian Estimation Computer Code 4 (BEST4) User Manual", PLG-0460, December 1985.



PRIOR DISTRIBUTION

		PROBABILITY	CUMULATIVE PROBABILITY
1)	2.15E+00	2.12E-01	2.12E-01
2)	4.24E+00	2.20E-01	4.31E-01
3)	6.48E+00	5.63E-02	4.88E-01
4)	7.25E+00	2.54E-02	5.13E-01
5)	7.75E+00	2.37E-02	5.37E-01
6)	8.25E+00	2.22E-02	5.59E-01
7)	8.75E+00	2.07E-02	5.80E-01
8)	9.15E+00	1.18E-02	5.92E-01
9)	9.45E+00	1.13E-02	6.03E-01
10)	9.80E+00	1.44E-02	6.17E-01
11)	1.01E+01	1.04E-02	6.28E-01
12)	1.04E+01	9.97E-03	6.38E-01
13)	1.08E+01	1.27E-02	6.50E-01
14)	1.12E+01	1.50E-02	6.65E-01
15)	1.17E+01	1.41E-02	6.80E-01
16)	1.22E+01	1.33E-02	6.93E-01
17)	1.27E+01	1.25E-02	7.05E-01
18)	1.40E+01	4.34E-02	7.49E-01
19)	1.64E+01	4.97E-02	7.98E-01
20)	2.61E+01	2.02E-01	1.00E+00

Table 1



Prior Distribution

Cumulative Probability

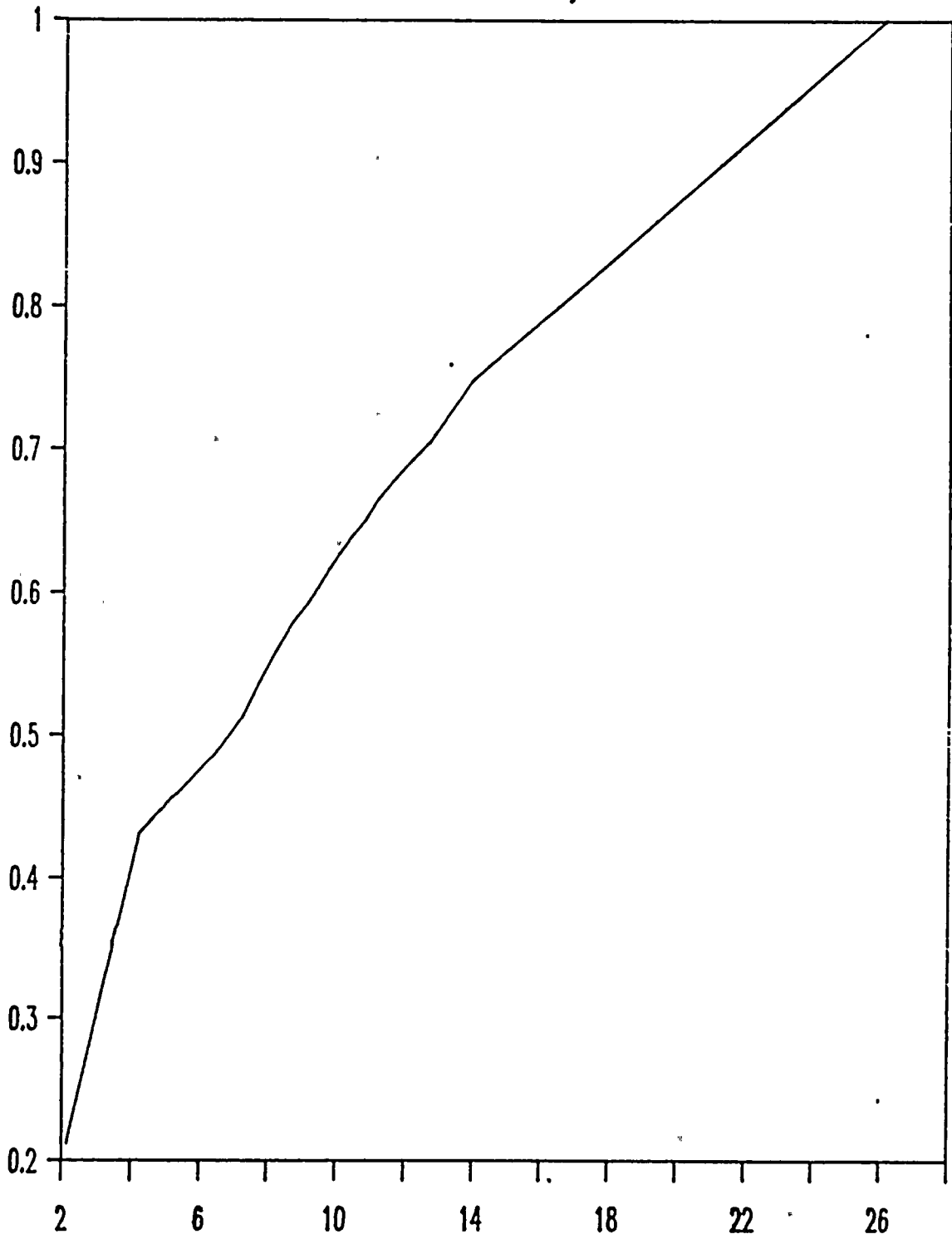


Figure 1



POSTERIOR DISTRIBUTION

		PROBABILITY	CUMULATIVE PROBABILITY
1)	2.15E+00	1.43E-08	1.43E-08
2)	4.24E+00	1.20E-03	1.20E-03
3)	6.48E+00	3.94E-02	4.06E-02
4)	7.25E+00	4.23E-02	8.29E-02
5)	7.75E+00	6.01E-02	1.43E-01
6)	8.25E+00	7.73E-02	2.20E-01
7)	8.75E+00	9.12E-02	3.11E-01
8)	9.15E+00	5.91E-02	3.71E-01
9)	9.45E+00	6.07E-02	4.31E-01
10)	9.80E+00	8.11E-02	5.12E-01
11)	1.01E+01	5.91E-02	5.72E-01
12)	1.04E+01	5.65E-02	6.28E-01
13)	1.08E+01	6.96E-02	6.98E-01
14)	1.12E+01	7.59E-02	7.74E-01
15)	1.17E+01	6.25E-02	8.36E-01
16)	1.22E+01	4.93E-02	8.85E-01
17)	1.27E+01	3.74E-02	9.23E-01
18)	1.40E+01	6.60E-02	9.89E-01
19)	1.64E+01	1.13E-02	1.00E+00
20)	2.61E+01	4.55E-07	1.00E+00

Table 2



Posterior Distribution

Cumulative Probability

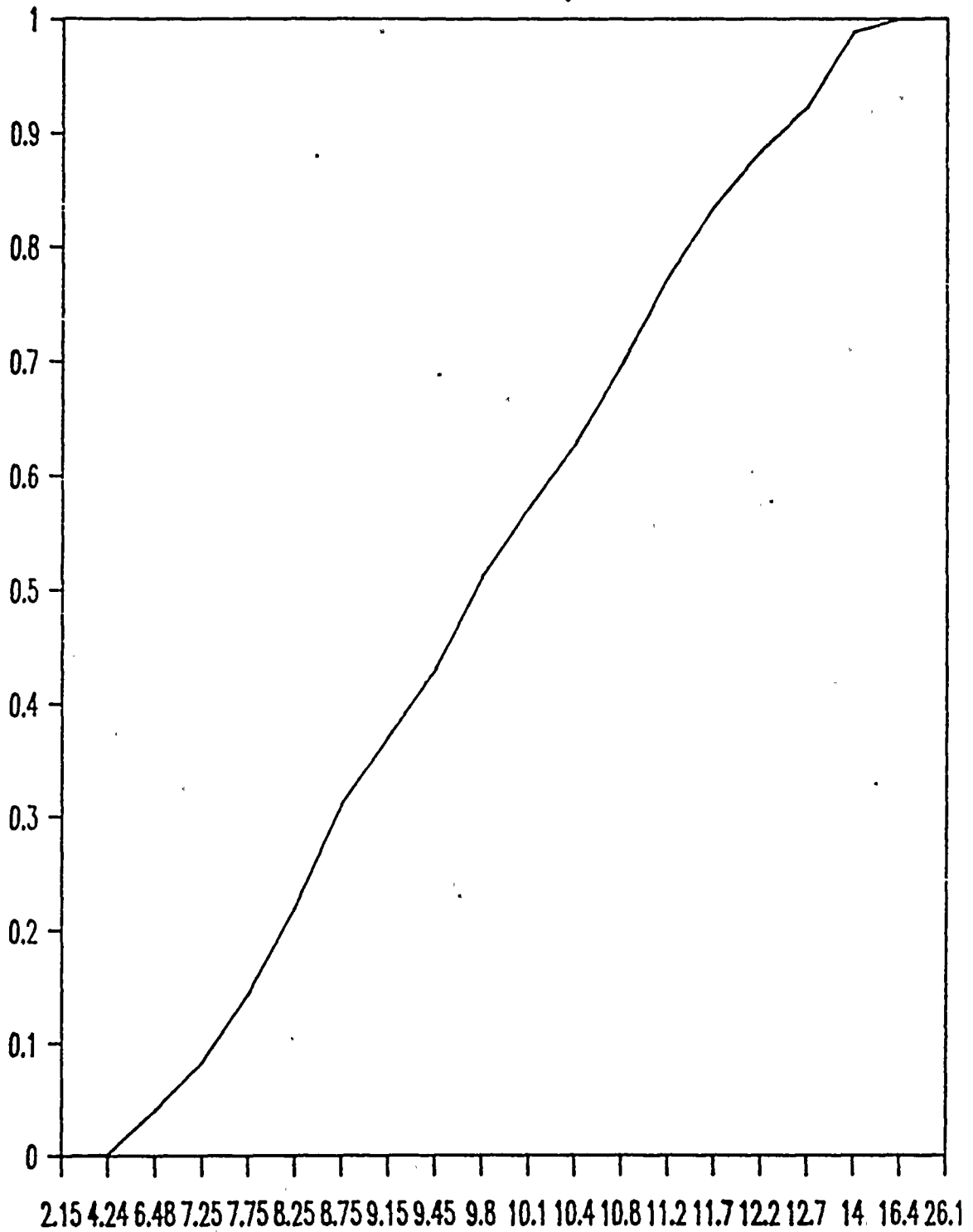


Figure 2



ENCLOSURE 2



1

2

3

4

5

6

7

8

9

10

F.5 OTHER EXTERNAL EVENTS

F.5.1 ANALYSIS OF AIRCRAFT CRASH AND OTHER FALLING OBJECTS

F.5.1.1 Introduction

An analysis of the risk from aircraft crashes on the Diablo Canyon Nuclear Power Plant (DCNPP) is presented here. The annual frequency of aircraft impact on various critical structures is provided, and the consequences of such impacts are studied. This section also presents a discussion of the hazard from other falling objects.

F.5.1.2 Description of Airports and Airways

There is one airport at San Luis Obispo (SLO) and there are several airways in the vicinity of DCNPP (see Figure F.5.1-1). The airport is a general aviation county airport with some scheduled commercial service. The airways include low-level federal airways used by small general aviation type aircraft, high-level jet routes used by large air carriers, and military training routes used by fighter type aircraft.

San Luis Obispo County Airport is located approximately 12.5 miles east-northeast of DCNPP. The airport has two asphalt runways: a smaller one measuring 3,529 feet by 100 feet, and a larger one measuring 4,799 feet by 150 feet. SLO is primarily a general aviation type airport. The airport manager estimated a total of 214,000 operations (one operation is one landing or one takeoff) in 1986. Approximately 10% of these were scheduled commercial flights. The largest commercial



Vertical text on the left side of the page, possibly bleed-through from the reverse side. The characters are faint and difficult to read, but appear to be arranged in a single column.

aircraft normally accommodated are 19-passenger, 14,000-pound maximum weight planes (Reference F.5.1-1). The Federal Aviation Administration (FAA) estimates that 5,840 flights per year operate randomly in the vicinity of the airport (Reference F.5.1-2). There were 190 single-engine aircraft and 35 multi-engine aircraft based there in 1986 (Reference F.5.1-3). According to Reference F.5.1-4, the majority of approaches to the airport use a route that is approximately 8 miles away from DCNPP and is separated from the site by the surrounding coastal mountains. An infrequently used approach route passes within 4 miles of the site and is not shielded by the mountains. The aircraft using this latter route maintain an altitude of at least 3,000 feet near the plant. Of the 214,000 total operations, only those using the approach route near the plant present a possible hazard. Assuming that 50% of operations are approaches for landings at the airport, this reduces the potential number of operations to 107,000. Assuming that only 1% of landings use the approach route near the plant, the number of operations that can present a hazard to the plant is 1,070 per year.

J6/501 and J88/126 are high altitude jet routes used by large commercial air carriers. Aircraft using these routes travel at altitudes of, at least 18,000 feet. The FAA estimates that 59,495 flights per year use route J6/501 and that 28,105 flights per year use route J88/126 (Reference F.5.1-2).

V27 and V113 are low altitude federal airways. They are used primarily by general aviation type aircraft. Aircraft using these airways travel at altitudes below 18,000 feet. The FAA estimates that 10,200 flights



Vertical text on the left side, possibly bleed-through from the reverse side of the page. The characters are faint and difficult to decipher, but appear to be arranged in a single column.

per year use V27 and that 5,840 flights per year use V113 (Reference F.5.1-2).

There is an offshore FAA test route located about 1 mile offshore from the plant and approximately parallel to Federal Airway V27. This route is new and has not yet appeared on aeronautical charts. This route services aircraft from the San Francisco Bay Area to the Los Angeles Basin Area. Aircraft using this route are commercial jet aircraft and high performance turbo-props. Flight is restricted between 16,000 feet and 24,000 feet. The FAA estimates 28,280 flights per year use this route (Reference F.5.1-5).

Morro Bay VORTAC is located about 7 miles east-northeast of DCNPP. The FAA estimates 5,840 flights per year operate randomly within 10 miles of this VORTAC (Reference F.5.1-2).

There are two military training routes in the vicinity of the plant. These are VR249 and IR203. Both are operated by the U.S. Navy. VR249 handled 140 flights in 1986 according to Reference F.5.1-6. A "flight" usually involves one to two aircraft. In this analysis, we will assume an average value of 1.5 aircraft per flight, resulting in a total of 210 aircraft. The aircraft that use VR249 are mainly tactical jets (F-14, F-4, A-4, T-6, and T-38). The heaviest aircraft that use VR249 are the F-14s. These aircraft can weigh up to 60,000 pounds. The altitude bounds of VR249 are 3,000 feet and 5,000 feet. Military training route IR203 handled 219 aircraft in 1986. Again, these were



Vertical text on the left side of the page, appearing as a column of small, faint characters.

mainly tactical jets. The altitude bounds of IR203 are 7,000 feet and 12,000 feet (Reference F.5.1-7).

Helicopters are occasionally operated by the company and its contractors at the plant site. However, helicopters of the type normally used do not constitute a hazard to the safety-related buildings. It may however be able to damage the main transformers or the transmission lines. A brief analysis will show that loss of offsite power due to helicopter crashes are small relative to other causes of loss of offsite power. It is assumed that a helicopter that crashes near the plant will crash within a 3,000 foot diameter circle that encloses the Unit 1 main transformers. The transformers will be conservatively modeled as a 200-foot diameter circle. If the helicopter crashes within this area, it is assumed to destroy the transformers. The transmission lines within the larger 3,000-foot diameter circle are roughly 1,000 feet by 100 feet. Therefore, the conditional probability of striking either the main transformers or the transmission lines is

$$[\pi(100)^2 + 1,000 \cdot 100]/\pi \cdot (1,500)^2 = 0.0186$$

The initiating crash frequency depends on the number of helicopter operations per year. We will assume 365 takeoffs and 365 landings per year. Helicopter crash rates are roughly 2×10^{-4} /landing or takeoff. This gives an initiating crash frequency of 0.146 per year. Finally, the frequency of loss of offsite power due to helicopter crash is $0.146 \cdot 0.0186 = 0.0027$ per year. Since loss of offsite power due to other causes is already 0.135 per year, the helicopter contribution is



.

.

...

...

.

...

...

...

small and will not be included. Furthermore, the number of helicopter operations per year is probably quite conservative for further operations at the plant.

Small general aviation aircraft can also be seen regularly near the plant. These aircraft occasionally violate the FAA minimum altitude requirements of 1,000 feet above ground level for operations over property or people (Reference F.5.2-5). It will be estimated that there are 1,000 such aircraft per year and that they fly at an average height of 500 feet near the plant.

F.5.1.3 Aircraft Hazard Analysis

F.5.1.3.1 Analytical Model

The frequency of aircraft crashes into different structures of the plant is estimated using the following model (Reference F.5.1-8):

$$f_k = \sum_{i=1}^K \sum_{j=1}^L N_{ij} \lambda_j d_j \frac{A_{kj}}{A_{pj}} \quad (\text{F.5.1.1})$$

where

f_k = annual frequency of impact on the kth structure
(events per year).



N_{ij} = annual number of operations of aircraft of type j to or from airport i or along airway i .

λ_j = crash rate of aircraft of type j (accident/mile flown).

d_j = distance traveled by the aircraft while the plant site is within its potential impact area (miles).

A_{pj} = potential impact area for aircraft type j (square miles).

A_{kj} = effective impact area of the k th structure of the plant for aircraft of type j (square miles).

n_j = number of different flight paths that take aircraft past the site.

L = number of different types of aircraft that pass the site.

Except for the variables that are determined geometrically, all the other variables are assigned distributions representing our state of knowledge about their values.

The product, $N_{ij}\lambda_j d_j$, is the number of aircraft accidents of type j within the defined distance segment, d_j , per year that could potentially affect the plant from the i th airway or airport. The ratio, A_{kj}/A_{pj} , is the probability of hitting a particular structure, given that the aircraft accident is in the vicinity of the site.



200

1
2
3
4
5

6

The quantities d and A_p (the aircraft type index j is dropped for convenience) can be calculated by assuming that any given time a crash-initiating malfunction occurs, there is an equal probability of crash termination anywhere in a sector of radial length gh and angular width ϕ that is located directly in front of the aircraft, where g is the glide distance per unit of altitude lost and h is the altitude. The situation is shown in Figure F.5.1-2 where b is defined as the distance of closest lateral approach between the normal flight path of the aircraft and the site.

From Figure F.5.1-2 it can be seen that the distance, d , is given by

$$d = \left[(gh)^2 - b^2 \right]^{\frac{1}{2}} + b/\tan B \quad (F.5.1.2)$$

This quantity can be averaged over all allowable values of b . The result is

$$d = \frac{1}{2} gh \left(\frac{\phi}{2} \right) / \sin \left(\frac{\phi}{2} \right) \quad (F.5.1.3)$$

A_p is the area of the sector defined by angle ϕ and radius gh

$$A_p = (gh)^2 \left(\frac{\phi}{2} \right) \quad (F.5.1.4)$$



1
2
3
4
5
6
7
8
9
10
11
12
13
14
15
16
17
18
19
20
21
22
23
24
25
26
27
28
29
30
31
32
33
34
35
36
37
38
39
40
41
42
43
44
45
46
47
48
49
50
51
52
53
54
55
56
57
58
59
60
61
62
63
64
65
66
67
68
69
70
71
72
73
74
75
76
77
78
79
80
81
82
83
84
85
86
87
88
89
90
91
92
93
94
95
96
97
98
99
100



F.5.1.3.2 Crash Rates

Crash rate statistics are provided either in the form of the number of crashes in the total number of miles flown or the number of hours flown by a particular type of aircraft. The latter can be converted into the former by multiplying the number of hours by an average speed for the type of aircraft under consideration.

Table F.5.1-1 shows 10 years of statistics for fatal accidents involving air carriers (Reference F.5.1-9). The mean and variance of the annual in-flight crash rates are 1.51×10^{-9} and 4.39×10^{-19} , respectively.

These values are used to fit a lognormal distribution by the matching moments method. Other characteristics of the distribution are:

5th Percentile : 6.95×10^{-10}

50th Percentile: 1.39×10^{-9}

95th Percentile: 2.76×10^{-9}

The accident rates for general aviation aircraft are given in Table F.5.1-2 (Reference F.5.1-10). The classification into single and multiple engine aircraft is due to the difference in the effects of their impact on the plant structures. The following values characterize the lognormal distribution chosen to represent our uncertainty concerning these rates.



Vertical text or markings on the left side of the page, possibly bleed-through from the reverse side.

CRASHES PER MILE FLOWN

Characteristics of Distribution	Single Engine	Multiple Engine
5th Percentile	1.91×10^{-7}	5.54×10^{-8}
50th Percentile	2.27×10^{-7}	7.14×10^{-8}
95th Percentile	2.70×10^{-7}	9.20×10^{-8}
Mean	2.28×10^{-7}	7.23×10^{-8}

The distribution in each case is derived by using the mean and variance of the crash rates, based on Table F.5.1-2, as the mean and variance of a lognormal distribution.

The crash rates for military fighter aircraft are based on the analysis of Reference F.5.1-11. That analysis resulted in a lognormal distribution for crash rate, with a mean crash rate of 2.41×10^{-5} accidents per hour, a 5th percentile of 9.30×10^{-6} accidents per hour, a median of 2.12×10^{-5} accidents per hour, and a 95th percentile of 4.62×10^{-5} accidents per hour. Using a mean accident rate of 2.41×10^{-5} accidents per hour and assuming a cruising speed of 400 miles per hour, the accident rate becomes 5.36×10^{-8} accidents per mile flown.

F.5.1.3.3 Number of Operations (N)

The number of aircraft operations is given in Section F.5.1.1. General aviation aircraft are assumed to be composed of 80% single-engine and



一
二
三
四

五
六

七
八

20% multi-engine aircraft unless data were available that indicated otherwise. Of the 5,840 aircraft operating randomly near SLO, the single-engine planes are out of glide range of the plant and are hence excluded from the analysis. This is based on an assumed glide ratio of 17 to 1 and an initial height of 3,000 feet. Multi-engine planes usually operate higher than single-engine planes, and are judged to be within glide range of the plant. Half of these planes, however, would be heading away from the plant when the crash initiating malfunction occurs and their operations would not apply. Therefore, the total number of aircraft operating randomly near SLO that could present a hazard to the plant is $5,840 \times 0.20 \times 0.50 = 584$.

F.5.1.3.4 Exposure Parameters d and A_p

To quantify the exposure parameters d and A_p , as defined by Equations (F.5.1.3) and (F.5.1.4), several other parameters (namely, g , the glide ratio; h , the altitude; and ϕ , the exposure angle) are needed for each category of aircraft.

The mean value of h for general aviation aircraft is assumed to be 3,000 feet for single-engine aircraft and 4,000 feet for multi-engine aircraft, except for the approach route to SLO where h is 3,000 feet for both types. For military aircraft operating on VR249, the mean value of h is 4,000 feet, and, for aircraft operating on IR203, the mean value of h is 9,500 feet. For commercial aircraft operating on J6/501 and J88/126, the mean value of h is assumed to be 30,000 feet. For aircraft



operating on the offshore test route, the mean value of h is 20,000 feet. The relevant aircraft parameters are summarized in Table F.5.1-3.

In this analysis, a glide ratio of 17 is used for general aviation and commercial aircraft, and a glide ratio of 8 is used for military aircraft.

F.5.1.3.5 Impact Area and Fragility of Different Structures

The structures considered as targets are listed in Table F.5.1-3. The effective impact area of a target structure is calculated as the combination of the roof area of the structure and a "shadow" area based on a 30° terminal crash angle of the aircraft (see Figure F.5.1-3). The target areas are presented in Table F.5.1-4. No credit is given for shielding by adjacent structures.

Two types of fragilities are considered. The first is the perforation mode of damage. In this mode, the aircraft engine penetrates the structural component and enters the building or structure. The second type of fragility is the collapse mode. In this mode, the structural component collapses and falls into the building with debris from the aircraft. The fragilities are determined in terms of conditional probability, given an aircraft strike.

Both types of fragility depend on aircraft type, distance from originating airport, and the wall thickness of the target. Table F.5.1-5



*

*

*

*

*

*

*

*

*

*

summarizes the fragilities used in this analysis. It is based on Reference F.5.1-12 and the data on Table F.5.1-6.

F.5.1.4 Results of Aircraft Crash Calculations

The results of applying Equation (F.5.1.1) are summarized in the impact frequency column of Tables F.5.1-7, F.5.1-8, and F.5.1-9. The perforation and collapse frequencies were arrived at by multiplying the impact frequency by the appropriate fragility from Table F.5.1-5.

General aviation aircraft have a greater impact frequency on the plant than do large commercial air carriers. The effects of a general aviation aircraft strike are, however, much smaller. The damage caused by small, light aircraft will be confined to the local area of impact in buildings with multiple walls and floors. It is assumed that these small aircraft can only penetrate through the first wall encountered. Larger commercial aircraft are assumed to destroy all contents in the building if penetration occurs.

Military aircraft flying on VR249 have sometimes been observed flying below the assumed average height of 4,000 feet used on this analysis. However, sensitivity analysis on the results show that even if we assume all aircraft on VR249 fly as low as 2,000 feet, the maximum increase in collapse and penetration frequencies will only be about 6%.



第

一

卷

之

第

一

章

第

一

節

As can be seen, the damage and impact frequencies are low, and, even if we assume that any damage leads to core melt, the frequency of core melt from aircraft crashes would be dominated by other core melt scenarios.

F.5.1.5. Hazard from Other Falling Objects

Potential hazards from other falling objects originated outside of the Diablo Canyon Nuclear Power Plant were also investigated. These included meteorite impact and potential danger to the site from vehicles launched from Vandenberg Air Force Base (VAFB), located approximately 35 miles southeast of the DCNPP site. Based on the screening analysis, the likelihood of these sources posing any risk to the site were determined to be negligible and no further analysis was deemed necessary.

F.5.1.6 References

- F.5.1-1. Gimer, P., Airport Manager, San Luis Obispo County Airport, personal communication, February 1987.
- F.5.1-2. Debelak, R., U.S. Department of Transportation, Federal Aviation Administration, letter to F. Gee, Pacific Gas and Electric Company, March 1987.
- F.5.1-3. U.S. Department of Transportation, Federal Aviation Administration, Airport Master Record for San Luis Obispo County Airport for 12 Months of Operation Ending June 11, 1986, July 15, 1986.
- F.5.1-4. Pacific Gas and Electric Company, Diablo Canyon Power Plant Units 1 and 2, Final Safety Analysis Report Update, Sections 2.2.1 and 3.5.1.4, September 1986.
- F.5.1-5. Debelak, R., U.S. Department of Transportation, Federal Aviation Administration, personal communication, September 1987.
- F.5.1-6. Lt. Stambaugh, COMFITAEW - WINGPAC Scheduling Office, Miramar Naval Air Station, personal communication, September 1987.



2
3
4
5
6
7
8
9
10
11
12
13
14
15
16
17
18
19
20
21
22
23
24
25
26
27
28
29
30
31
32
33
34
35
36
37
38
39
40
41
42
43
44
45
46
47
48
49
50
51
52
53
54
55
56
57
58
59
60
61
62
63
64
65
66
67
68
69
70
71
72
73
74
75
76
77
78
79
80
81
82
83
84
85
86
87
88
89
90
91
92
93
94
95
96
97
98
99
100



- F.5.1-7. Lt. Commander Grant, AIR OPS LOGISTICS and SCHEDULING, COMLATWINGPAC, Lemoore Naval Air Station, personal communication, September 1987.
- F.5.1-8. U.S. Atomic Energy Commission, "Aircraft Consideration Preapplications Site Review by the Directorate of Licensing," in the matter of Portland General Electric Company, Boardman Nuclear Plant, Boardman, Oregon, Project Number 485.
- F.5.1-9. U.S. Department of Transportation, Federal Aviation Administration, "FAA Statistical Handbook of Aviation, Calendar Year 1979," December 1979.
- F.5.1-10. National Transportation Safety Board, "Annual Review of Aircraft Accident Rates, Calendar Year 1980," NTSB-ARG-80-1, May 1980.
- F.5.1-11. Pickard, Lowe and Garrick, Inc., "Seabrook Station Probabilistic Safety Assessment," prepared for Public Service Company of New Hampshire and Yankee Atomic Electric Company, PLG-0300, December 1983.
- F.5.1-12. Chelapati, C.V., R.P. Kennedy, and I.B. Wall, "Probabilistic Assessment of Aircraft Hazard for Nuclear Power Plants," Nuclear Engineering and Design, No. 19, 1972.



84

1

2

3



TABLE F.5.1-1. AIRCRAFT ACCIDENTS AND ACCIDENT RATES:
U.S. AIR CARRIERS, 1970 THROUGH 1979

Year	Number of Fatal Accidents		Aircraft Miles Flown (10 ³)	In-Flight Crash Rates*
	In-Flight	Landing and Takeoff		
1970	4	4	2,684,552	1.49-9
1971	6	2	2,660,731	2.25-9
1972	3	5	2,619,043	1.14-9
1973	5	4	2,646,669	1.89-9
1974	7	2	2,464,295	2.84-9
1975	1	2	2,477,764	0.40-9
1976	2	2	2,568,113	0.78-9
1977	4	1	2,684,072	1.49-9
1978	4	2	2,742,860	1.46-9
1979	4	2	2,889,131	1.36-9

*Accidents per aircraft mile flown.

NOTE: Exponential notation is indicated in abbreviated form;
i.e., 1.49-9 = 1.49 x 10⁻⁹.

22

21

20



TABLE F.5.1-2. FATAL ACCIDENT RATES
FOR U.S. GENERAL AVIATION AIRCRAFT

Year	Fatal Accident Rates per Miles Flown		
	Single Engine	Multiple Engine	All Types
1972	2.63-7	8.7-8	2.11-7
1973	2.52-7	8.2-8	2.09-7
1974	2.45-7	7.6-8	1.88-7
1975	2.30-7	6.9-8	1.71-7
1976	2.02-7	6.4-8	1.66-7
1977	2.03-7	5.1-8	1.59-7
1978	2.02-7	7.7-8	1.59-7

NOTE: Exponential notation is indicated
in abbreviated form;
i.e., 2.63-7 = 2.63×10^{-7} .



TABLE F.5.1-3. AIRCRAFT PARAMETERS

Item	Air Carrier I (j=1)	Air Carrier II (j=2)	General Aviation					
			Single Engine I (j=3)	Single Engine II (j=4)	Multi-Engine I (j=5)	Multi-Engine II (j=6)	Military I (j=7)	Military II (j=8)
g_j (glide ratio)	17	17	17	17	17	17	8	8
h_j (feet)	30,000	20,000	3,000	500	3,000	4,000	4,000	9,500
$g_j \cdot h_j$ (mile)	96.59091	64.39394	9.659091	1.609848	9.659091	12.87879	6.060606	14.39394
ϕ_j (radians)	3.141593	3.141593	3.141593	3.141593	3.141593	3.141593	3.141593	3.141593
λ_j (one per mile)	1.51-9	1.51-9	2.28-7	2.28-7	7.23-8	7.23-8	5.36-8	5.36-8
d_j (mile)	75.86232	50.57488	7.586232	1.264372	7.586232	10.11498	4.759989	11.30497
A_{p_j} (square mile)	14,655.22	6,513.432	146.5522	4.070895	146.5522	260.5373	57.69683	325.4462
Weight (pounds)	>100,000	>100,000	<12,500	<12,500	<12,500	<12,500	60,000	60,000
N_{ij} for path i (operations per year):								
J6/501 (i=1)	59,495	0	0	0	0	0	0	0
J88/126 (i=2)	28,105	0	0	0	0	0	0	0
V27 (i=3)	0	0	8,160	0	0	2,040	0	0
V113 (i=4)	0	0	4,672	0	0	1,168	0	0
SLO Random (i=5)	0	0	0	0	0	584	0	0
SLO Approach (i=6)	0	0	856	0	214	0	0	0
Morro Bay Random (i=7)	0	0	4,672	0	0	1,168	0	0
Offshore Test Route (i=8)	0	26,280	0	0	0	0	0	0
VR 249 (i=9)	0	0	0	0	0	0	210	0
IR 203 (i=10)	0	0	0	0	0	0	0	219
Low Flights over Plant (i=11)	0	0	0	1,000	0	0	0	0

NOTE: Exponential notation is indicated in abbreviated form; i.e., 1.51-9 = 1.51 x 10⁻⁹.



11
12
13
14
15



TABLE F.5.1-4. UNIT 1 TARGET AREAS

Target	Area (square feet)		Area (square miles)		Effective* Target Area (square miles)
	Roof	Wall	Roof	Wall	
Turbine Building - Above 140 Feet	51,708	29,760	1.855-3	1.067-3	3.704-3
Turbine Building - Below 140 Feet	51,708	20,460	1.855-3	7.339-4	3.126-3
Auxiliary Building	13,806	3,068	4.952-4	1.100-4	6.858-4
Containment	24,336	35,880	8.729-4	1.287-3	3.102-3
Fuel Handling Building	14,168	18,975	5.082-4	6.806-4	1.687-3
Outdoor Water Storage Tanks	10,600	8,000	3.802-4	2.870-4	8.773-4
Intake Structure	16,200	2,835	5.811-4	1.017-4	7.572-4
Main Transformers	3,600	3,600	1.291-4	1.291-4	3.528-4

*Roof Area + Wall Area/Tan (30 degrees)

NOTE: Exponential notation is indicated in abbreviated form; i.e., 1.855-3 = 1.855 x 10⁻³.



1
2
3
4
5
6
7
8
9
10
11
12
13
14
15
16
17
18
19
20
21
22
23
24
25
26
27
28
29
30
31
32
33
34
35
36
37
38
39
40
41
42
43
44
45
46
47
48
49
50
51
52
53
54
55
56
57
58
59
60
61
62
63
64
65
66
67
68
69
70
71
72
73
74
75
76
77
78
79
80
81
82
83
84
85
86
87
88
89
90
91
92
93
94
95
96
97
98
99
100

1

2

3

TABLE F.5.1-5. FRAGILITY OF TARGETS

Target	Collapse Fragility		Perforation Fragility	
	Heavy Aircraft* j=1,2,6,7	Light Aircraft j=3-5	Heavy Aircraft* j=1,2,6,7	Light Aircraft j=3-5
Turbine Building Above 140 Feet	1	0	1	1
Turbine Building Below 140 Feet	.86	0	1	.4
Auxiliary Building	.86	0	1	.06
Containment	.86	0	.84	.009
Fuel handling Building	1	0	1	1
Outdoor Water Storage Tanks	1	.5	1	.52
Intake Structure	.86	0	1	.06
Power Transformers	1	1	1	1

*heavy aircraft are greater than 12,500 lbs.

1

2

3

4

5

6

TABLE F.5.1-6. WALL THICKNESS OF TARGETS

Target	Concrete Thickness (inches)		Thickness Used To Determine Fragilities
	Roof	Wall	
Turbine Building Above 140 Feet	Nil	Nil	0
Turbine Building Below 140 Feet	10-12*	16-29	10
Auxiliary Building	18-40	36	18
Containment	30	44	30
Fuel Handling Building	2		0
Outdoor Water Storage Tanks	8	12-36	8
Intake Structure	18-24	24	18
Main Transformers	Nil	Nil	0

*Floor thickness.



1000

1000

1000

TABLE F.5.1-7 STRUCTURES CONSIDERED AND
IMPACT FREQUENCIES BY TARGET - ALL TYPES

Structure	Impact Area (square miles)	Mean Impact Frequency (impacts per year)	Mean Collapse Frequency (per year)	Mean Perforation Frequency (per year)
Turbine Building Above 140 Feet	3.704-3	1.128-6	6.316-8	1.128-6
Turbine Building Below 140 Feet	3.126-3	1.077-6	4.584-8	4.629-7
Auxiliary Building	6.858-4	2.089-7	1.006-8	2.353-8
Containment	3.102-3	9.448-7	4.549-8	5.246-8
Fuel Handling Building	1.687-3	5.138-7	2.877-8	5.138-7
Outdoor Water Storage Tanks	8.773-4	2.672-7	1.411-7	1.461-7
Intake Structure	7.572-4	2.306-7	1.110-8	2.598-8
Main Transformers	3.528-4	1.074-7	1.074-7	1.074-7

Note: Exponential notation is indicated in abbreviated form; i.e., 3.704-3 = 3.704 x 10⁻³.

F.5.1-21



TABLE F.5.1.8. STRUCTURES CONSIDERED AND
IMPACT FREQUENCIES BY TARGET - GENERAL AVIATION

Structure	Impact Area (square miles)	Mean Impact Frequency (impacts per year)	Mean Collapse Frequency (per year)	Mean Perforation Frequency (per year)
Turbine Building Above 140 Feet	3.704-3	1.119-6	5.453-8	1.119-6
Turbine Building Below 140 Feet	3.126-3	1.070-6	3.958-8	4.556-7
Auxiliary Building	6.858-4	2.073-7	8.684-9	2.193-8
Containment	3.102-3	9.375-7	3.928-8	4.639-8
Fuel Handling Building	1.687-3	5.099-7	2.484-8	5.099-7
Outdoor Water Storage Tanks	8.773-4	2.651-7	1.390-7	1.441-7
Intake Structure	7.572-4	2.289-7	9.588-9	2.421-8
Main Transformers	3.528-4	1.066-7	1.066-7	1.066-7

NOTE: Exponential notation is indicated in abbreviated form; i.e., 3.704-3 = 3.704 x 10⁻³.

F.5.1-22



TABLE F.5.1.9. STRUCTURES CONSIDERED AND
IMPACT FREQUENCIES BY TARGET - AIR CARRIER AND MILITARY

Structure	Impact Area (square miles)	Mean Impact Frequency (impacts per year)	Mean Collapse Frequency (per year)	Mean Perforation Frequency (per year)
Turbine Building Above 140 Feet	3.704-3	8.627-9	8.627-9	8.627-9
Turbine Building Below 140 Feet	3.126-3	7.281-9	6.262-9	7.281-9
Auxiliary Building	6.858-4	1.597-9	1.374-9	1.597-9
Containment	3.102-3	7.226-9	6.214-9	6.069-9
Fuel Handling Building	1.687-3	3.930-9	3.930-9	3.930-9
Outdoor Water Storage Tanks	8.773-4	2.043-9	2.043-9	2.043-9
Intake Structure	7.572-4	1.764-9	1.517-9	1.764-9
Main Transformers	3.528-4	8.22-10	8.22-10	8.22-10

NOTE: Exponential notation is indicated in abbreviated form; i.e., 3.704-3 = 3.704 x 10⁻³.

F.5.1-23



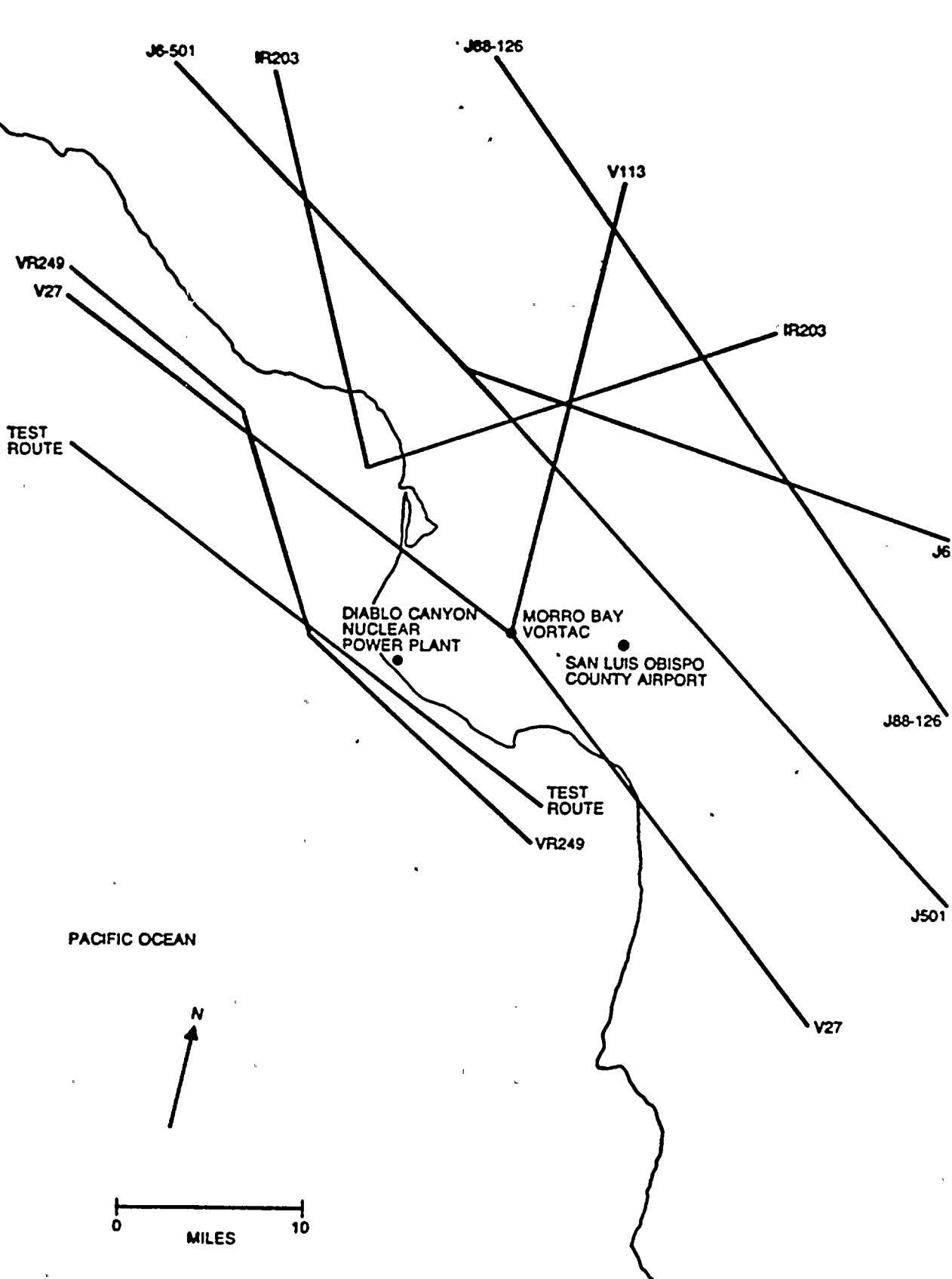


FIGURE F.5.1-1. AIRPORTS AND AIRWAYS NEAR THE SITE



11



12



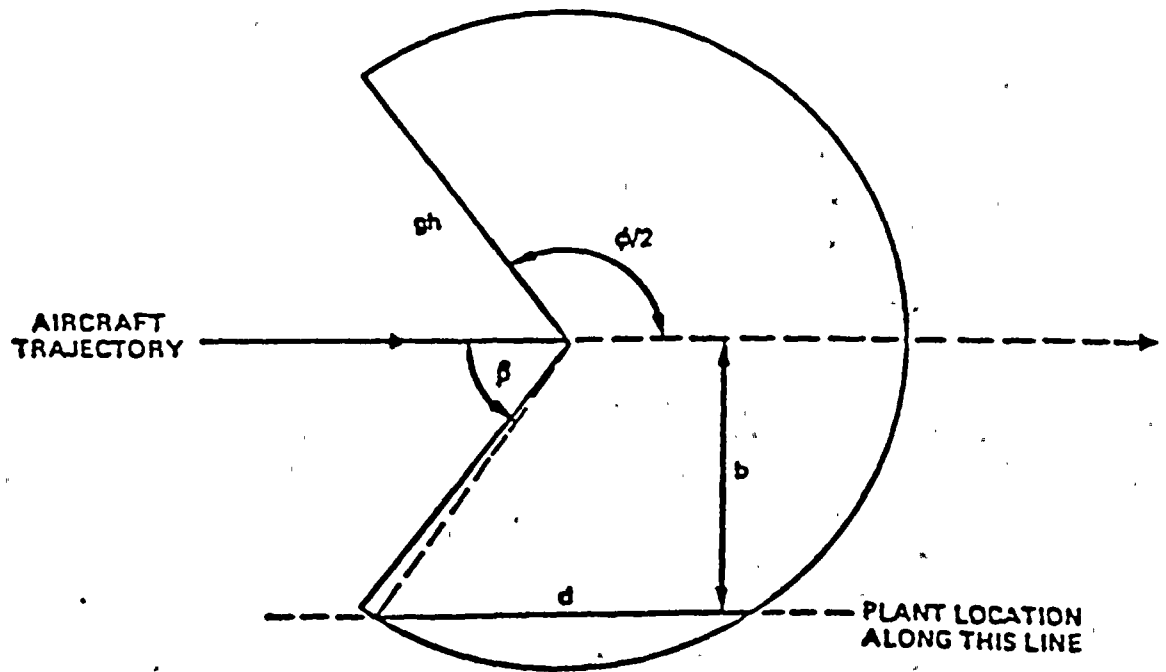
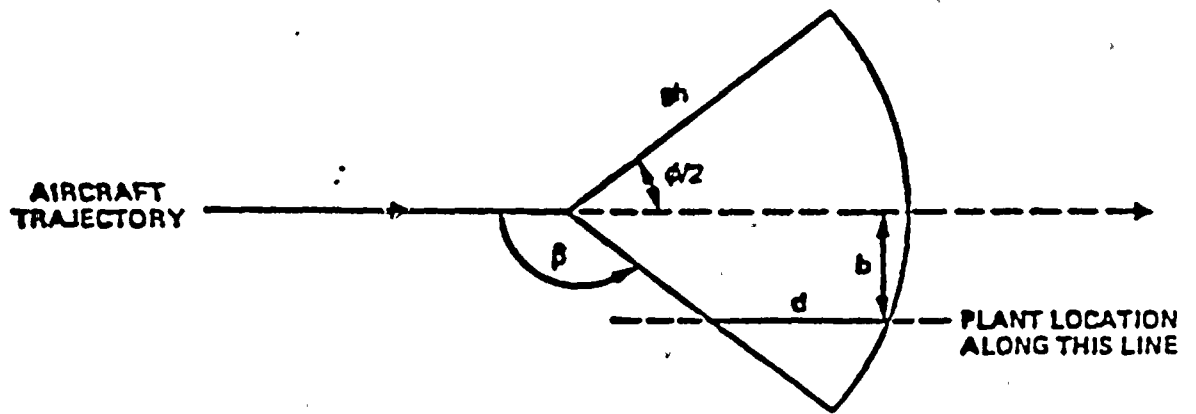
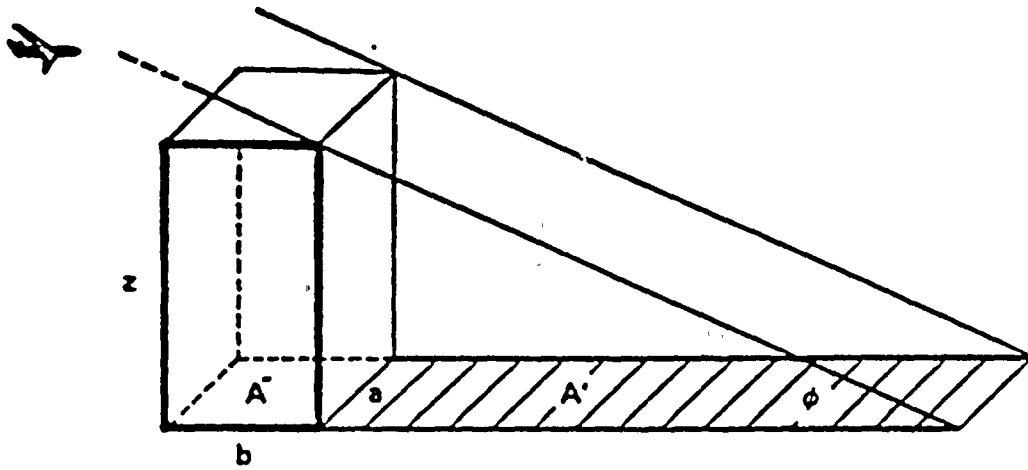


FIGURE F.5.1-2. GEOMETRY FOR IMPACT PROBABILITY MODEL





$$A'' = ab$$

$$A' = (az)/\tan \phi$$

ϕ = GLIDE ANGLE OF AIRCRAFT (ASSUMED $\phi = 30^\circ$)

$$A'' + A' = \text{EFFECTIVE TARGET AREA}$$

FIGURE F.5.1-3. CALCULATION OF EFFECTIVE TARGET AREA



天
地
人
三
才

一
二
三
四
五

六

F.5.2 EXTERNAL FIRES

A review of the plant layout shows that the hazard to the plant from external fires is not significant except for the hillside area to the east of the plant. This was reconfirmed in a plant visit by the analysts of this external event. A fire from brush near the 230-kV switchyard occurred in 1982 during construction (Reference F.5.8-1). Santa Ana winds were present at the time. Under these conditions, hot winds blow from the hills toward the ocean. These winds carried the smoke and products of combustion to the plant site, approximately 1,500 feet away to the southwest. Smoke detectors at the plant picked up the smoke and generated alarms at the control room. The operators then successfully isolated the control room. This protected the operators from the smoke.

Since the smoke detectors at the plant were detecting and alarming the presence of smoke, there was the possibility of a fire occurring somewhere at the plant and going unnoticed, at least initially. To guard against this danger, watches were placed in the plant for fire surveillance. There was also concern that cinders in the wind might set the temporary onsite trailers on fire. Therefore, watches were placed there also.

The initial fire at the 230-kV switchyard occurred in the evening. Power from the 230-kV lines was lost the next morning because of the smoke from the fire. The 500-kV lines were also lost later that morning when an aerial tanker plane dropped flame retardant on the lines in an effort to suppress the fire beneath. The 500-kV lines were energized, and the fire



Vertical text or markings along the left edge of the page, possibly bleed-through from the reverse side.

retardant material caused phase to phase and phase to ground arcing to occur.

Power to the plant was then supplied by diesel generators until the fire was put out. After the fire, the power lines were inspected, and no major damage was found except for burned silicone insulators, which were replaced. A fire of this magnitude is unlikely to reoccur since the brush that supplied the fuel for the fire was removed by the fire itself. The brush near the 230-kV switchyard was very heavy before the fire occurred. However, to guard even further against this hazard, a program of controlled burning is being implemented to keep brush growth down. Brush fires elsewhere around the plant itself are not expected to be significant because of the limited amount of brush and the large cleared area surrounding the plant site.

Nevertheless, if an external fire of the 1982 type and magnitude were to reoccur at the site, the most likely impact would be limited to loss of offsite power. This type of event is considered as a contributor to the loss of offsite power initiating event, which is quantified and analyzed separately.

Based on the above discussion, it is judged that the hazard from external fires to the plant is remote and bounded by other core damage scenarios.

REFERENCES

- F.5.2-1. Kohout, R., Pacific Gas and Electric Company, personal communication, February 1988.



1000

1000

1000

F.5.3 TURBINE MISSILES HAZARD

F.5.3.1 Introduction

Missiles that might be generated in the event of turbine failure can potentially damage safety-related systems. In this section, the likelihood of generating turbine missiles is estimated, and the most probable consequences are analyzed.

The fundamental equation used to find the annual frequency, f , of serious damage to a specific system is

$$f = f_1 \cdot f_2 \cdot f_3 \quad (F.5.3.1)$$

where f_1 is the annual frequency of missile generation due to turbine failure; f_2 is the conditional probability of a missile striking a barrier to an essential system, given that a turbine missile has been generated; and f_3 is the conditional probability of penetrating the barrier, striking system components, and causing unacceptable damage to the system, given that a missile strikes the barrier.

F.5.3.2 Frequency of Turbine Missile Generation, f_1

The Diablo Canyon Nuclear Power Plant (DCNPP) uses Westinghouse Corporation turbine generators. Westinghouse has performed an analysis to determine the frequency of turbine missile generation, based on turbine valve test frequency (Reference F.5.3-1). Bush and Heasler



Vertical text on the left side of the page, possibly bleed-through from the reverse side. The characters are faint and difficult to read, but appear to be arranged in a column.

(Reference F.5.3-2) have also estimated the frequency of turbine missile generation by the analysis of statistical records of failures relevant to turbine generators of the type used in nuclear power plants. The frequency given by Bush and Heasler is greater than those given in Reference F.5.3-1. To be conservative, Bush and Heasler's results (Table F.5.3-1) will be used in this analysis.

As can be seen from Table F.5.3-1, there are two general categories of turbine missile releases: (1) failure at or near operating speed and (2) overspeed failure. Each category has its own failure frequency.

F.5.3.3 Conditional Probability of Missile Impact, f_2

To obtain f_2 , the conditional probability of a missile striking a barrier to an essential system, given turbine failure, one must analyze the behavior of potential missiles ejected from the turbine, taking into account the kinetic energy and possible trajectories of the missiles and the location of potential barriers.

Detailed analysis of the impact frequencies was beyond the scope of this screening analysis. Instead, the simple method of Reference F.5.3-3 is used in conjunction with conservative assumptions to achieve a bounding analysis.

Potential missiles are assumed to fall into the categories of high trajectory or low trajectory. Reference F.5.3-3 provides the following



4

4

4

4

4

4



simple approximations for the impact frequency of missiles in the two categories:

$$\text{High Trajectory} = f^H = \frac{220}{\theta_2^\circ - \theta_1^\circ} \times \frac{A_{\text{roof}}}{v^4} \quad (\text{F.5.3.2})$$

$$\text{Low Trajectory} = f^L = \frac{9.1}{\theta_2^\circ - \theta_1^\circ} \times \frac{A_{\text{wall}}}{d^2} \quad (\text{F.5.3.3})$$

where

v = missile velocity at ejection (m/s).

d = distance of the target from turbine axis (m).

A_{roof} = roof area of the target (m^2).

A_{wall} = wall area of the target (m^2).

\ominus = horizontal angular deviation of the missile (degrees).

θ_2° and θ_1° are two bounds beyond which missile distribution is assumed to be zero. Uniform missile distribution is assumed for angles between θ_2° and θ_1° .

Based on review of the plant layout and turbine orientation, and assuming realistic values of θ_2 and θ_1 ($\theta_2 = -\theta_1 = 25^\circ$), the following barriers



24
25
26
27
28
29
30
31
32
33
34
35
36
37
38
39
40
41
42
43
44
45
46
47
48
49
50
51
52
53
54
55
56
57
58
59
60
61
62
63
64
65
66
67
68
69
70
71
72
73
74
75
76
77
78
79
80
81
82
83
84
85
86
87
88
89
90
91
92
93
94
95
96
97
98
99
100

to essential systems and direct system components are targets for high trajectory missiles (HTM) and for low trajectory missiles (LTM):

HTM Targets	LTM Targets
Containment Building	Containment Building
Auxiliary Building	Auxiliary Building
Fuel Handling Building	Fuel Handling Building
Outdoor Water Storage Tanks	
Turbine Building Elevation 140' Deck	

To calculate f_2 using Equations (F.5.3.2) and (F.5.3.3), values of A_{roof} and A_{wall} are calculated for each of the above targets. Only that portion of the target building that is within the ejection angles, θ_1 and θ_2 , is included. For high trajectory missiles, the following ejection velocities are considered, corresponding to failures at operating speed as well as to overspeed failures.

Failure Mode	Ejection Velocity (m/s)
Operating Speed	91
Overspeed	155

These values are estimated from Reference F.5.3-4.

Tables F.5.3-2 and F.5.3-3 summarize the results of the f_2 calculations for the high and low trajectory missiles respectively.



1
2
3
4
5



6
7
8

9



F.5.3.4 Turbine Missile Fragility of Structures, f3

In general, such thick, reinforced concrete walls and roofs as those in place in nuclear power plants provide a powerful barrier against turbine-generated missiles. The likelihood of perforation or back scabbing for a missile depends on such missile characteristics as weight, ejection speed, shape, angle of ejection, and angle of impact and on such target characteristics as concrete thickness, degree of reinforcement, etc.

Some full-scale concrete impact tests indicate that, for typical turbine missiles, 4 to 5-foot thick concrete walls show no perforation or back scabbing (Reference F.5.3-5). Scale model test (1/11) of 4.5-foot thick heavily reinforced wall (Reference F.5.3-6) also indicates that such walls can contain missiles of an impact velocity of up to 650 feet per second (198 meters per second).

Test results from Reference F.5.3-6 show that 3.5-foot thick walls will contain a 3,250-pound turbine missile at an impact velocity as high as 650 feet per second. When the missile weight is increased to 4,000 pounds, it will be contained for a velocity of 520 feet per second (159 meters per second), but perforation will occur at an impact velocity of 650 feet per second.

The DCNPP containment building has side walls that are 3.67 feet thick; based on the above discussions, it is judged that perforation from a low trajectory missile on the side wall would be highly unlikely. However,



to be conservative in this analysis, we will assume the following (lognormal) distribution of f_3 for missile penetration of the containment building by a low trajectory missile:

5th percentile = 0.01

50th percentile = 0.05

95th percentile = 0.25

Mean = 0.08

For high trajectory missiles on the containment building and other concrete structures listed in Section F.5.3.3, we will use a higher likelihood of penetration because of thinner roof thicknesses. For those structures, the following distribution (truncated lognormal) will be used for f_3 :

5th percentile = 0.50

95th percentile = 0.95

Mean = 0.70

It will also be assumed that $f_3 = 1$ for the fuel handling building and the outdoor water storage tanks.

The auxiliary building can only be hit at a glancing angle of 25° from the horizontal by low trajectory missiles. The walls are 3 feet thick. It is judged that a turbine missile will have little chance of



1
2
3
4
5
6
7
8
9
10

penetrating the auxiliary building side walls. The following distribution is conservatively assumed for this case:

5th percentile = 0.01
50th percentile = 0.05
95th percentile = 0.25
Mean = 0.08

F.5.3.5 Turbine Missile Scenarios

The mean annual frequency of damage to different structures due to turbine missile strike are listed in Table F.5.3-4. Frequency is calculated from Equation (F.5.3.1) by using the appropriate numbers for f_1 , f_2 , and f_3 for operating speed or overspeed conditions, and for high and low trajectory missiles. The total damage frequency for each structure is obtained by adding the contribution of each trajectory and speed category to get the total damage frequency for each structure.

As can be seen, the frequency of damage due to turbine missiles is quite low and even if we assume that any damage results in core melt this hazard is still dominated by other core melt scenarios.

F.5.3.6 References

- F.5.3-1. Rodibaugh, R. K., et al., "Probabilistic Evaluation of Reduction in Turbine Valve Test Frequency," WCAP-11529, Westinghouse Electric Corporation, Power Systems, June 1987.
- F.5.3-2. Bush, S., and P. Heasler, "Probability of Turbine Missile Generation," presented at Electric Power Research Institute Steam Turbine Missile Disc Integrity Seminar, New Orleans, Louisiana, April 6-8, 1981.

11
12
13
14
15
16
17
18
19
20
21
22
23
24
25
26
27
28
29
30
31
32
33
34
35
36
37
38
39
40
41
42
43
44
45
46
47
48
49
50
51
52
53
54
55
56
57
58
59
60
61
62
63
64
65
66
67
68
69
70
71
72
73
74
75
76
77
78
79
80
81
82
83
84
85
86
87
88
89
90
91
92
93
94
95
96
97
98
99
100



- F.5.3-3. Niessner, H., "A Simple Method of Estimating Impact Probabilities of Turbine Missiles," Brown Boveri Review, Vol. 66, No. 6, pp. 394-400, Baden Switzerland, June 1979.
- F.5.3-4. Patton, E. M., "Estimates of Missile Exit Conditions," Battelle Pacific Northwest Laboratory, presented at Electric Power Research Institute Seminar on Turbine Missile Effects in Nuclear Power Plants, Palo Alto, California, October 25-26, 1982.
- F.5.3-5. Woodfin, R. L., "Full Scale Concrete Impact Tests," Sandia National Laboratory, presented at Electric Power Research Institute Seminar on Turbine Missile Effects in Nuclear Power Plants, Palo Alto, California, October 25-26, 1982.
- F.5.3-6. Romander, C. M., "Scale Model Tests of Turbine Missile Containment by Reinforced Concrete," presented at Electric Power Research Institute Seminar on Turbine Missile Effects in Nuclear Power Plants, Palo Alto, California, October 25-26, 1982.

10

11

12

13



TABLE F.5.3-1. ESTIMATE OF THE MEAN ANNUAL FREQUENCY OF TURBINE MISSILE GENERATION

Failure Mode		Total
Operating Speed (f_1)	Overspeed (f_1')	
1.1×10^{-4}	4.3×10^{-5}	1.6×10^{-4}

224
21
20
19
18
17
16
15
14
13
12
11
10
9
8
7
6
5
4
3
2
1



TABLE F.5.3-2. CONDITIONAL FREQUENCY
OF IMPACT FOR HIGH TRAJECTORY MISSILES

Target	Roof Area (m ²)	Conditional Impact Frequency	
		Operating Speed	Overspeed
Containment Building	1.78+3	1.14-4	1.36-5
Auxiliary Building	1.28+3	8.21-5	9.76-6
Fuel Handling Building	1.01+3	6.48-5	7.70-6
Outdoor Water Storage Tanks* (per tank)	1.17+2	7.51-6	8.92-7
Turbine Building Elevation 140' Deck	1.95+3	1.25-4	1.49-5

*Primary Water Storage Tank
Condensate Storage Tank
Refueling Water Storage Tank
Transfer Storage Tank/Firewater Tank

NOTE: Exponential notation is indicated in abbreviated form;
i.e., 1.78+3 = 1.78 x 10³.

TABLE F.5.3-3. CONDITIONAL FREQUENCY
OF IMPACT FOR LOW TRAJECTORY MISSILES

Target	Wall Area (m ²)	Distance from Turbine Axis (m)	Conditional Impact Frequency
Containment Building	8.12+2	29.0	1.76-1
Auxiliary Building	2.60+2	48.8	1.99-2
Fuel Handling Building	3.02+2	76.2	9.47-3

NOTE: Exponential notation is indicated in abbreviated form;
i.e., 8.12+2 = 8.12 x 10².



TABLE F.5.3-4. ANNUAL FREQUENCY OF TURBINE MISSILE PENETRATION

Target	High Trajectory		Low Trajectory		Total
	Operating Speed	Overspeed	Operating Speed	Overspeed	
Containment Building	8.79-9	4.08-10	1.55-6	6.05-7	2.16-6
Auxiliary Building	6.32-9	2.94-10	1.75-7	6.85-8	2.50-7
Fuel Handling Building	7.13-9	3.31-10	1.04-6	4.07-7	1.46-6
Outdoor Water Storage Tanks	8.26-10	3.84-11	0	0	8.64-10
Turbine Building Elevation 140' Deck	9.63-9	4.47-10	0	0	1.01-8

NOTE: Exponential notation is indicated in abbreviated form; i.e., 8.79-9 = 8.79×10^{-9} .

F.5.3-12



Vertical text on the left side of the page, possibly bleed-through from the reverse side. The characters are small and difficult to read, but appear to be arranged in a column.

F.5.4 SHIP IMPACT ANALYSIS

F.5.4.1 Introduction

The plant intake structure, which houses the safety-related auxiliary saltwater pumps, is located on the coastline. This section analyzes the potential hazard to the intake structure and the auxiliary saltwater system (ASW) from maritime vessels.

There are several conceivable ways a ship could present a hazard to the plant. A ship that approaches the breakwaters will probably run aground and stop. If this occurs, the damage to the plant will be minimal and will not involve core damage. However, the function of the ASW pumps may be impaired if the ship grounds in the open channel area and if in settling into this area it manages to seal off the cove from the ocean. The cove contains a large but finite supply of water, which may not be enough to supply the ASW pumps for the required time to safely shut down the plant.

Another scenario involves a large ship traveling at high speed. Such a ship might not be stopped by the breakwater on impact. It may be possible for it to break through a section of the breakwater and continue into the intake cove area. If it hits the intake structure, it may damage the ASW pumps or block the flow of water into the structure.



10
11
12
13
14



15
16
17



Another possibility is based on the observed availability of the breakwaters. From Reference F.5.4-1, the breakwaters were in a damaged state for approximately 2 years from the fall of 1981 to the fall of 1983 because of storm damage. The original Diablo Canyon breakwaters were built in 1971. Therefore, the observed availability of the breakwaters is about 90%. If a ship should approach the intake area while the breakwaters are in a damaged state, it may be possible for the ship to cross over rather than run aground on the breakwater. This would be even more of a possibility if the ship were to approach during high storm wave conditions, which could help sweep the ship over. Once across the breakwaters, the ship could collide with the intake structure and damage the AS_h pumps or crash into the structure in such a way that the flow of water is blocked.

There are two breakwaters, one on the west and one on the east side of the intake area (See Figure F.5.4-1). There is an open channel area between the breakwaters that allows access to the ocean from the south. It is conceivable for a ship to negotiate the open channel between the east and west breakwater arms and enter into the intake cove, depending on the ships dimensions and orientation. Once across the breakwater, the ship does not necessarily hit the intake structure since it may ground at some other point in the cove.

A final hazard is the potential spillage and subsequent interaction of vessel cargo with the intake structure. Each of these hazard modes will be presented in greater detail in the following sections. The frequency and consequences of these scenarios will now be calculated.



.

8

8

8

.

6

.

8

8

8



F.5.4.2 Frequency of Ship Arrival at Breakwater

F.5.4.2.1 Frequency of Shipping Near Plant

Coastal shipping lanes are approximately 20 miles offshore of the plant. Local tankers to Avila Beach and Estero Bay would come within 5 to 10 miles of the plant (Reference F.5.4-1).

An analysis of shipping traffic near the plant was made in 1981 (Reference F.5.4-2). The results are summarized in Table F.5.4-1. The number of ships passing will be escalated to account for shipping traffic growth during the lifetime of the plant.

According to Reference F.5.4-2, the shipping traffic in any subsequent year after 1981 can be estimated by using the following model:

$$N_t = N_{1981} \cdot e^{t \cdot r} \quad (F.5.4.1)$$

where

t = calendar year - 1981.

N_t = number of vessels in year 1981 + t .

N_{1981} = number of vessels estimated for year 1981.

r = annual growth rate of shipping.

To calculate the average shipping traffic for the remaining lifetime of the plant, a time integral average of Equation (F.5.4.1) can be taken



between the present time (t_p) and the time at which the plant will be retired (t_R).

$$N_{avg} = \frac{\int_{t_p}^{t_R} N_t dt}{\int_{t_p}^{t_R} dt} = \frac{N_{1981} \cdot \frac{1}{r} \cdot [e^{t_R \cdot r} - e^{t_p \cdot r}]}{t_R - t_p} \quad (F.5.4.2)$$

where N_t is defined by Equation (F.5.4.1). The lower limit t_p corresponds to the present time, which will be taken to be 1988. In terms of Equation (F.5.4.1), $t_p = 1988 - 1981 = 7$. The retirement time of the plant will be taken to be the year 2025. Therefore $t_R = 2025 - 1981 = 44$. An annual growth rate of $r = 1.5\%$ will be used (Reference F.5.4-2). Using Equation (F.5.4.2) for each vessel category, we arrive at the time average shipping level that the plant will see in its remaining life. The results are tabulated on Table F.5.4-2.

Vessels less than 250 tons are not included in the analysis because these small vessels are not capable of causing significant damage to the intake structure according to Reference F.5.4-2.

F.5.4.2.2 Ship Arrival Frequency at Breakwater

Using the approach of Reference F.5.4-2, the ship arrival frequency at the breakwater can be calculated by

$$A_i = N_i \cdot G_i \cdot W \quad (F.5.4.3)$$



8

8

8

8



where

A_i = arrival frequency at breakwater of vessels in category i
(groundings/year).

N_i = number of passages of vessels in category i in the vicinity of
Diablo Canyon (vessels/year).

G_i = grounding rate of vessels in category i
(groundings/vessel-mile).

W = length of breakwater exposure (miles).

The N_i for each vessel category are the time average values of shipping traffic levels from Table F.5.4-2.

From the analysis in Reference F.5.4-2, the vessel grounding rate for all vessel categories is 2.9×10^{-8} groundings/vessel-mile.

The length of exposure of the breakwater is about 0.2 miles.

The results of the calculation for A_i are summarized on Table F.5.4-3.



Vertical text or markings along the left edge of the page, possibly bleed-through from the reverse side.

F.5.4.3 Scenarios Involving Ship Arrival at Intake Cove

F.5.4.3.1 Arrival Through Breakwater Channel or Crossing a Degraded Breakwater

The analysis of Reference F.5.4-2 shows that the frequency with which ships cross the breakwater is only a fraction of the ships that arrive at the breakwater. Under normal conditions, the breakwaters would provide a substantial barrier to ships entering the intake basin, unless the ship crosses between the breakwaters. In the analysis of Reference F.5.4-2, the breakwaters are assumed to be degraded by previous wave action, down to the mean lower low water level (about a 20-foot degradation of the breakwater). This would make it easier for vessels to be swept over the breakwaters by wave action.

The probability of crossing the breakwater (either by being swept over or passing through the open channel) was calculated in Reference F.5.4-2 for two cases: storm independent and storm dependent. In the first case, ship groundings are assumed to occur independently of storms; in the second case, it is assumed that storms occur coincident with ship groundings. The probabilities F_i , from Reference F.5.4-2, are summarized in Tables F.5.4-4a and F.5.4-4b. Notice that when storms are assumed to coexist with ship grounding events, the probability of crossing the breakwater increases because the higher wave heights associated with storm conditions make it easier to carry the ship over the breakwater.



To calculate the arrival frequency of the vessels in the intake cove, we use the following equation:

$$C_i = A_i \cdot [A_{BW} \cdot F_{Ii} + (1 - A_{BW}) \cdot F_i] \quad (F.5.4.4)$$

whereas before, A_i is the ship arrival frequency at the breakwater and

C_i = ship arrival frequency in intake cove (ships/year).

F_{Ii} = conditional probability of ship arrival in intake cove via negotiating channel, given breakwater is in normal nondegraded state.

F_i = conditional probability of ship arrival in intake cove via negotiating channel or by being swept over degraded breakwaters.

A_{BW} = likelihood of breakwater being in normal (nondegraded state).

The results of this calculation are summarized in Table F.5.4-5.

Since, according to Reference F.5.4-2, there is no correlation between ship groundings and sea conditions (e.g., storm versus calm seas), we will assume that ship groundings are uniformly distributed during the year. The success with which a ship crosses the breakwater is however dependent on the sea conditions. In this analysis, it is assumed that stormy sea conditions prevail approximately 25% of the year.



4

2

2

2

2

2

2

2

2

2

2

2

2

2

Considering this occurrence of storm conditions, the weighted average ship arrival frequency is

$$C_i = 0.75 (C_i)_{SI} + 0.25 (C_i)_{SD} \quad (F.5.4.5)$$

where

C_i = weighted average ship arrival frequency in intake cove.

$(C_i)_{SI}$ = storm-independent arrival frequency.

$(C_i)_{SD}$ = storm-dependent arrival frequency.

The results of this calculation for each ship category are summarized in Table F.5.4-6. The total is $C = 1.83 \times 10^{-6}$ arrivals per year.

Figure F.5.4-1 shows that even if a ship manages to cross the breakwater, the ship does not automatically impact the intake structure. Those ships that manage to negotiate the channel between the breakwaters will have a good chance of hitting the intake structure. However, the ships that are swept over will have a lower probability of hitting the intake. Most of the ships that arrive in the intake cove arrive by being swept over the breakwaters. It will be conservatively assumed that there is an 80% chance of hitting the intake structure given that a ship arrives in the intake by whatever means. The impact frequency for all the ships combined is then $0.8 \times 1.84 \times 10^{-6} = 1.47 \times 10^{-6}$ impacts per year.

If a ship impacts the intake structure, it is conceivable that the collision would damage the structure extensively enough to disable the

Vertical text on the left margin, possibly bleed-through from the reverse side of the page.



ASW pumps. This could be due either to the force of the collision or blockage of the water path to the ASW pumps (although unlikely since the ship would have to achieve a fairly good seal in front of the structure). Ship impact does not, however, guarantee disablement of the ASW system. Moreover, only one of the four ASW pumps is needed for safe shutdown.

In this analysis, however, we will conservatively assume that ship impact leads to failure of all four pumps. Given the loss of ASW pumps, it is still possible to provide seal cooling to the RCP seals and thus prevent a core damage. This is possible by aligning fire water to the charging pumps; an action with a failure frequency of 1.27×10^{-2} .

Consequently, core damage frequency due to the loss of ASW pumps because of ship impact is $\phi_c = C (1.27 \times 10^{-2}) = 1.87 \times 10^{-8}$.

F.5.4.3.2 Breakwater Breakthrough

As mentioned earlier, the analysis of Section F.5.4.3.1 involved two mechanisms for ship arrival in the intake cove when the breakwater is in the degraded state (ship negotiating channel and ship swept over breakwater) and only one mechanism (ship negotiating channel) when the breakwater is in the normal (nondegraded) state. It is implied that when the breakwater is in the normal state that a ship cannot physically go past the breakwater if it strikes anywhere except through the channel. In this section this assumption is analyzed and it will be shown that vessel breakthrough of a fully intact breakwater is highly unlikely.

1
2
3
4
5
6
7
8
9
10
11
12
13
14
15
16
17
18
19
20
21
22
23
24
25
26
27
28
29
30
31
32
33
34
35
36
37
38
39
40
41
42
43
44
45
46
47
48
49
50
51
52
53
54
55
56
57
58
59
60
61
62
63
64
65
66
67
68
69
70
71
72
73
74
75
76
77
78
79
80
81
82
83
84
85
86
87
88
89
90
91
92
93
94
95
96
97
98
99
100



In order for a ship to get past the breakwater without negotiating the channel, the ship will have to physically cross over the intact breakwater. In this analysis, the collision will be idealized as the combination of two different events. First the ship will remove part of the breakwater due to the force of impact. Then it will ride over the damaged breakwater section as the ship loses its momentum. It will be assumed that the ship removes a section of the breakwater equivalent to the beam of the ship in width, and from the MSL to the top of the breakwater in height. It is assumed that if it can move this breakwater section a distance equivalent to the width of the breakwater a path will be established for the ship to continue over the breakwater.

It will be conservatively assumed that the vessel approaches the breakwater at a 90° angle. The analysis will calculate the energy and thus the speed required by the ship in order to (1) breach the top of the and (2) ride over the breakwater.

The energy required to breach the top of the breakwater is assumed to be equal to the energy required to move the breakwater material in front of the ship 90 feet (approximate width of breakwater). The density of the breakwater material is assumed to be about 100 lbm/ft³ (including the effect of voids). The energy required will also depend on the beam (width) of the ship involved. Table F.5.4-7 summarizes the assumed characteristics of ships that are considered large enough to breach the breakwater. It is also conservatively assumed that the draft of the vessels are small enough so as not to ground before reaching the breakwaters. On initial contact with the bottom of the breakwater, the



Vertical text on the left side of the page, possibly bleed-through from the reverse side. The characters are faint and difficult to decipher, but appear to be arranged in a column.

ship rises up and forward. It then continues forward to breach the top part of the breakwater (above MSL). The energy required to move the breakwater material is taken to be force required multiplied by the distance moved. The force required is taken to be the frictional force between the top section of the breakwater with the bottom section. The coefficient of friction is assumed to be 1.0. The results of the energy required calculation are shown in Table F.5.4-8. The required ship speed can be calculated from the energy requirement. The results are shown in the first row of Table F.5.4-9. Note that these are relatively high speeds, if the ship drifts onto the breakwaters. However, if the ship is moving under power, this result could be obtainable.

The second obstacle that the ship would have to overcome would be frictional resistance of the hull with the breakwater. This resistance will decrease the momentum of the ship until it either stops or enters the intake cove. It will be assumed that if at least half the length of the ship crosses the breakwater, the ship will be considered free to enter the intake structure. The closest distance from a point on the breakwater to the intake structure is about 350 feet. Therefore, if the length of a ship is such that 350 feet of it has crossed the breakwater, it is also assumed that the ship can strike the intake structure, even though half of the vessel may not have crossed. A frictional coefficient of 0.5 is assumed between the hull of the ship and the breakwater. The



22



23



frictional energy required to meet one of the two above mentioned criteria is calculated using the following expression

$$E_{fr} = \int_0^D k \cdot N(x) \cdot dx \quad (F.5.4.6)$$

where we assume the normal contact force between the ship and the breakwater, $N(x)$, increases linearly from zero, at initial contact with the breakwater, to the value of the weight of the ship when half of the vessel is across. Therefore

$$N(x) = \frac{mgx}{(1/2 L)}, \text{ for } 0 \leq x \leq 1/2 L \quad (F.5.4.7)$$

m = mass of ship.

g = gravity constant.

L = length of ship.

The value of D is 350 feet or $0.5 \cdot L$, whichever is least.

The speed that the ship must possess in order to meet this frictional energy requirement can be calculated by equating E_{fr} with the kinetic energy,

$$\frac{1}{2} mV^2$$



The results are given in the second row of Table F.5.4-9. The total kinetic energy required for the vessel to enter the intake cove is the sum of the breach energy and the friction energy. The total velocity required is therefore the square root of the sum of the squares of the speed required for the breach and friction components.

$$v_{\text{total}} = \sqrt{v_{\text{breach}}^2 + v_{\text{friction}}^2} \quad (\text{F.5.4.8})$$

The results are shown in the final row of Table F.5.4-9.

As these speeds are higher than what these vessels normally travel at, it is concluded that vessels of the type that use routes near the plant are not able to break through a fully intact breakwater.

F.5.4.4 Breakwater Blockage

Ships that arrive at the breakwaters, but fail to cross into the intake cove, may still present a hazard to the successful operation of the ASW pumps by effectively blocking the channel between the east and west breakwaters. However, to do this the ship must first be oriented correctly so as to ground in the channel; second, it must achieve a nearly watertight seal (allowing less than the suction rate of one ASW pump to flow past). Furthermore, even if the ship meets these criteria, the plant would still have some time to take action. The intake cove is shown in Figure F.5.4-1. The maximum depth is about 44 feet below MSL. The suction level of the ASW pumps is at 20 feet below MSL. The amount



Vertical text on the left side, possibly bleed-through from the reverse side of the page.

of useful water held by the intake cove (before ASW pump draw down) is conservatively bounded by a rectangular block with dimensions 400 feet wide by 800 feet long by 10 feet deep. This gives a total water volume of about 24 million gallons. The suction rate of one ASW pump is about 11,000 gpm. This gives about .36 hours for the plant to respond. Since loss of ASW flow would constitute an extreme emergency, it may be possible for the plant personnel to rig an alternate method to allow water to flow into the intake cove. This could be done possibly by pumps or by using explosives to destroy part of the breakwater, or a part of the ship. Also, if tugs are available, an attempt could be made to remove the grounded ship, or to reposition the ship enough to allow water to flow back into the cove. An estimate of the frequency of core damage due to this scenario is developed in the following.

Ships that arrive at the breakwater but do not make it into the intake cove are potential candidates for breakwater blockage. It is assumed that all of these ships ground somewhere on the breakwater. Therefore, the breakwater blockage initiating frequency is

$$B_i = A_i - C_i \quad (F.5.4.9)$$

B_i is the number of ships per year that arrive at the breakwater, but fail to either be swept over the breakwaters or to negotiate the channel (see Table F.5.4-10). A weighting factor of 0.75 and 0.25 will be used as before to calculate the weighted average B_i with respect to storm



1
2
3
4
5
6
7
8
9
10

conditions. The calculations are summarized in Table F.5.4-11. The frequency of breakwater blockage is expressed as

$$\phi_{BB} = b \cdot P_{OR} \cdot P_{CB} \quad (F.5.4.10)$$

where

ϕ_{BB} = frequency of breakwater blockage (per year).

b = breakwater blockage initiating frequency (ships per year).

P_{OR} = probability that a ship that fails to arrive in the intake cove, given arrival at the breakwater, has proper orientation to ground in channel.

P_{CB} = probability that ship seals off flow of water through channel, given ship grounds in channel.

It is unlikely for a ship to ground in the intake channel. It would need to approach the breakwater at the opening of the channel. Also, it must be aligned properly with the channel so as not to ground outside of the channel. It will be conservatively assumed that $P_{OR} = 0.25$. It is also unlikely for a ship to totally seal off the flow of water even if it does ground in the channel. All that is needed is a flow rate of greater than 11,000 gpm to ensure the long-term operation of an ASW pump. Even if flow was reduced to a level below this, there would still be time to



take some sort of action. At worst, the ship would completely seal off the flow of water. We will conservatively assume $P_{CB} = 0.10$.

$$\phi_{BB} = (5.87 \times 10^{-5}) \cdot (0.25) \cdot (0.10)$$

$$\phi_{BB} = 1.47 \times 10^{-6} \text{ per year}$$

The frequency of this event leading to unavailability of the ASW system can now be calculated as

$$\phi = \phi_{SE} \cdot P_{FR}$$

where

P_{FR} = probability that the plant fails in ASW recovery attempts.

To estimate P_{FR} , we note that within the minimum time of 36 hours in the case of complete blockage, the plant may be able to take some action as described earlier. Since only a relatively small flow is needed for the action to be successful, a $P_{FR} = 0.25$ is assumed. Therefore,

$$\phi = (1.47 \times 10^{-6}) (0.25) = 3.67 \times 10^{-7} \text{ per year}$$

Considering possible recovery by aligning fire water to charging pumps to prevent RCP seal LOCA, as discussed in the previous section, the frequency of core damage due to this scenario is

$$\phi_c = \phi (1.27 \times 10^{-2})$$

$$= (3.67 \times 10^{-7}) (1.27 \times 10^{-2}) = 4.67 \times 10^{-9} \text{ per year}$$



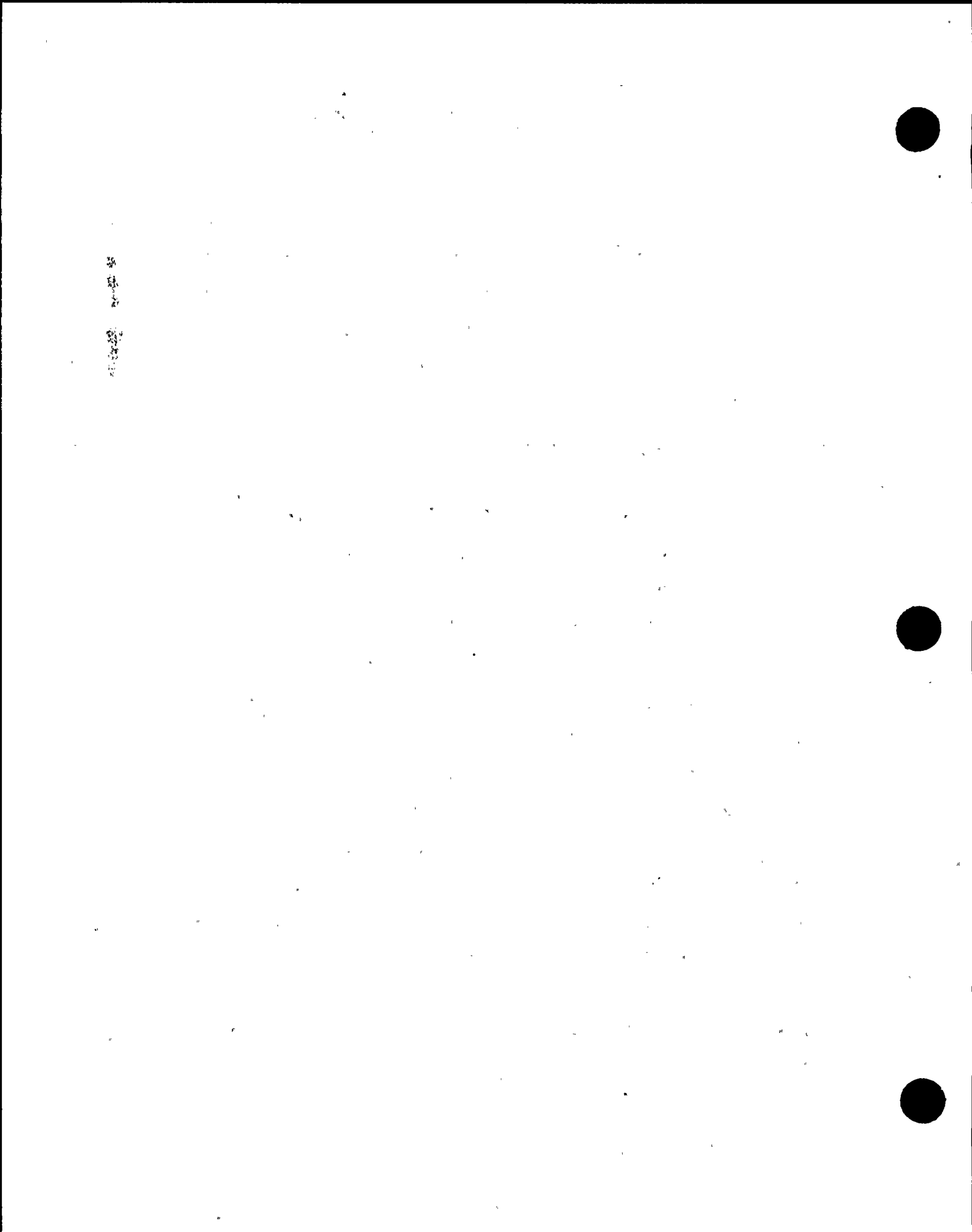
F.5.4.5 Hazard Posed by Debris, Oil, and Cargo

It can be postulated that shipping can also endanger the function of the ASK pumps if an accident at sea causes debris or oil or other buoyant material to drift into the intake cove, without a ship actually grounding on the breakwater or entering the intake cove. However, the design of the intake structure precludes this hazard. Figure F.5.4-2 shows the first wall of the intake structure between the sea and the bar racks. As can be seen, this wall extends more than 5 feet below the mean lower low water level. Therefore, any buoyant material would be screened out.

Any scenarios involving nonbuoyant materials would be bounded by the intake impact and blockage scenarios discussed in earlier sections.

F.5.4.6 Conclusions

Various scenarios involving shipping hazards to the plant were analyzed. Scenarios involving ship breakthrough over the breakwater in its normal state (not degraded by heavy wave action) were shown to be not possible due to the speed required to generate the kinetic energy needed to physically force a passage. Scenarios involving oil spills and other floating debris were also shown to have no consequence. Analysis scenarios involving a degraded breakwater, therefore greatly increasing the possibility of a ship arriving in the intake cove, resulted in a core damage frequency of 1.87×10^{-8} per year. Scenarios involving a ship blocking the flow of water into the intake cove result in a core damage frequency of 4.67×10^{-9} per year. Both of these frequencies are much



smaller than other core damage scenario frequencies and do not therefore merit further study.

F.5.4.7 References

- F.5.4-1. "Units 1 and 2, Diablo Canyon Power Plant Final Safety Analysis Report Update," Pacific Gas and Electric Company, Sections 2.2 and 2.4, Rev. 3, September 1987.
- F.5.4-2. Kircher, C., H. M. Despang, and R. J. Morris, "Frequency of Vessel Impact with the Diablo Canyon Intake Structure," Jack R. Benjamin & Associates, Inc., 156-010-HF01, December 1982.



4
1
2



3
4



5
6

TABLE F.5.4-1. SUMMARY OF LARGE-VESSEL TRAFFIC IN THE VICINITY OF DIABLO CANYON IN 1981

Vessel Category ¹	Deadweight Tons (DWT)	Range of Maximum Draft (feet)	Assumed ² Operational Draft (feet)	Passages in 1981
1 ³	600-1,800 ⁴	10-15	6.7	235
2	1,000-6,000	15-20	10.0	39
3	4,000-12,000	20-25	13.3	124
4	8,000-25,000	25-30	16.7	592
5	13,000-35,000	30-35	20.0	2,971
6	25,000-50,000	35-40	23.3	1,247
7	40,000-80,000	40-45	26.7	653
8	70,000-110,000	45-50	30.0	133
9 - 12	> 100,000	50-70	30.0	750
13 ⁵		10-20	3-4	286
Total				7,030

NOTES:

- Categories are defined on the basis of maximum draft. Vessels of different types (tankers, cargo ships, etc.) are grouped together according to their maximum draft.
- Draft reduced to account for empty or partially loaded vessels.
- Offshore support vessels only; no commercial self-propelled vessels were detected in this category.
- For this vessel category, displacement tons are used rather than deadweight tons. The traffic analysis detected no vessels between 250 and 600 displacement tons.
- Barges only.



24

25



26

27



TABLE F.5.4-2. ANNUAL LARGE-VESSEL
 TRAFFIC IN THE VICINITY OF DIABLO CANYON
 (1988 - 2025)

Vessel Category	Annual Passages, N_i
1	349
2	58
3	184
4	879
5	4,411
6	1,851
7	970
8	197
9 - 12	1,113
13	424
Total	10,438



5
2



3



TABLE F.5.4-3. ARRIVAL FREQUENCY
OF VESSELS AT BREAKWATER

Vessel Category, i	A_i (groundings/year)
1	2.02×10^{-6}
2	3.36×10^{-7}
3	1.07×10^{-6}
4	5.10×10^{-6}
5	2.56×10^{-5}
6	1.07×10^{-5}
7	5.62×10^{-6}
8	1.15×10^{-6}
9 - 12	6.46×10^{-6}
13	2.46×10^{-6}
Total	6.05×10^{-5}

卷之三

七



TABLE F.5.4-4a. PROBABILITY OF VESSELS CROSSING BREAKWATER BOUNDARY,
GIVEN ARRIVAL AT BREAKWATER
(STORM-DEPENDENT CASE)

Vessel Category, i	F_{Ii} Fraction of Vessels Passing Through Channel (best estimate)*	F_{Iii} Fraction of Vessels Not in Channel Passing Over Breakwater (best estimate)*	F_i Total Fraction of Vessels Crossing Breakwater Boundary (best estimate)*
1	0.10	0.93	0.94
2	0.055	0.82	0.83
3	0.034	0.63	0.64
4	0.021	0.44	0.45
5	0.013	0.30	0.31
6	0.0071	0.16	0.16
7	0.0024	0.082	0.084
8	0.00	0.044	0.044
9 - 12	0.00	0.044	0.044
13			1

*As developed in Reference F.5.4-2.

第 一 章

第 一 章

TABLE F.5.4-4b. PROBABILITY OF VESSELS CROSSING BREAKWATER BOUNDARY,
GIVEN ARRIVAL AT BREAKWATER
(STORM-INDEPENDENT CASE)

Vessel Category, i	F_{Ii} Fraction of Vessels Passing Through Channel (best estimate)*	F_{IIi} Fraction of Vessels Not in Channel Passing Over Breakwater (best estimate)*	F_i Total Fraction of Vessels Crossing Breakwater Boundary (best estimate)*
1	0.10	0.65	0.69
2	0.055	0.41	0.44
3	0.034	0.17	0.20
4	0.021	0.069	0.088
5	0.013	0.030	0.043
6	0.0071	0.0085	0.016
7	0.0024	0.0027	0.0051
8	0.00	0.00099	0.00099
9 - 12	0.00	0.00099	0.00099
13			1

*As developed in Reference F.5.4-2.



62

71

83



85

94



TABLE F.5.4-5. STORM-INDEPENDENT
AND STORM-DEPENDENT
SHIP ARRIVAL FREQUENCY IN INTAKE COVE

Vessel Category, f	$(C_i)_{SI}$ Storm Independent	$(C_i)_{SD}$ Storm Dependent
1	3.218-7	3.724-7
2	3.140-8	4.450-8
3	5.404-8	1.010-7
4	1.412-7	3.258-7
5	4.094-7	1.093-6
6	8.581-8	2.405-7
7	1.502-8	5.939-8
8	1.13-10	5.040-9
9 - 12	6.39-10	2.842-8
13	4.680-7	4.680-7
Total	1.527-6	2.738-6

NOTE: Exponential notation is indicated
in abbreviated form; i.e., 3.218-7 =
 3.218×10^{-7} .



TABLE F.5.4-6. WEIGHTED AVERAGE SHIP
ARRIVAL FREQUENCY IN INTAKE COVE

Vessel Category, i	C_i
1	3.344-7
2	3.468-8
3	6.578-8
4	1.874-7
5	5.802-7
6	1.245-7
7	2.611-8
8	1.345-9
9 - 12	7.585-9
13	4.680-7
Total	1.830-6

NOTE: Exponential
notation is indicated
in abbreviated form;
i.e., 3.344-7 =
3.344 x 10⁻⁷.



TABLE F.5.4-7. SHIP CHARACTERISTICS
FOR PHYSICAL BREAKTHROUGH ANALYSIS

Deadweight (tons*)	Length (ft)	Beam (ft)	Operating Draft (ft)
20,000	600	75	26.7
40,000	700	100	30.0
80,000	800	100	30.0
120,000	900	150	30.0
160,000	900	150	30.0
200,000	1,050	150	30.0

*1 deadweight ton = 2,205 lbm = 1,000 kg



TABLE F.5.4-8. ENERGY REQUIRED TO
BREACH BREAKWATER

Deadweight (tons)	Energy Required (ft • lb _f)
20,000	6.08×10^8
40,000	8.1×10^8
80,000	8.1×10^8
120,000	1.21×10^9
160,000	1.21×10^9
200,000	1.21×10^9

TABLE F.5.4-9. RESULTS OF PHYSICAL BREAKTHROUGH ANALYSIS

	Speed Required (mph)					
	Deadweight (tons*)					
	20,000	40,000	80,000	120,000	160,000	200,000
Breach	20.3	16.6	11.7	11.7	10.2	9.1
Friction	47.4	51.2	47.9	45.1	45.1	41.8
Total	51.5	53.8	49.3	46.6	46.3	42.8

*1 deadweight ton = 2,205 lbm = 1,000 kg



22

100

100

TABLE F.5.4-10. STORM-INDEPENDENT AND
STORM-DEPENDENT BREAKWATER
BLOCKAGE INITIATING FREQUENCY

Vessel Category, i	$(B_i)_{SI}$ Storm Independent	$(B_i)_{SD}$ Storm Dependent
1	1.702-6	1.651-6
2	3.045-7	2.914-7
3	1.014-6	9.669-7
4	4.957-6	4.773-6
5	2.518-5	2.449-5
6	1.065-5	1.050-5
7	5.609-6	5.564-6
8	1.145-6	1.140-6
9 - 12	6.458-6	6.431-6
13	1.995-6	1.995-6
Total	5.902-5	5.781-5

NOTE: Exponential notation is indicated
in abbreviated form; i.e., 1.702-6 =
 1.702×10^{-6} .



TABLE F.5.4-11. WEIGHTED AVERAGE BREAKWATER
BLOCKAGE INITIATING FREQUENCY

Vessel Category, f	B_i
1	1.689-6
2	3.012-7
3	1.002-6
4	4.911-6
5	2.501-5
6	1.061-5
7	5.598-6
8	1.144-6
9 - 12	6.451-6
13	1.995-6
Total	5.871-5

NOTE: Exponential
notation is indicated
in abbreviated form;
i.e., 1.689-6 =
1.689 x 10⁻⁶.

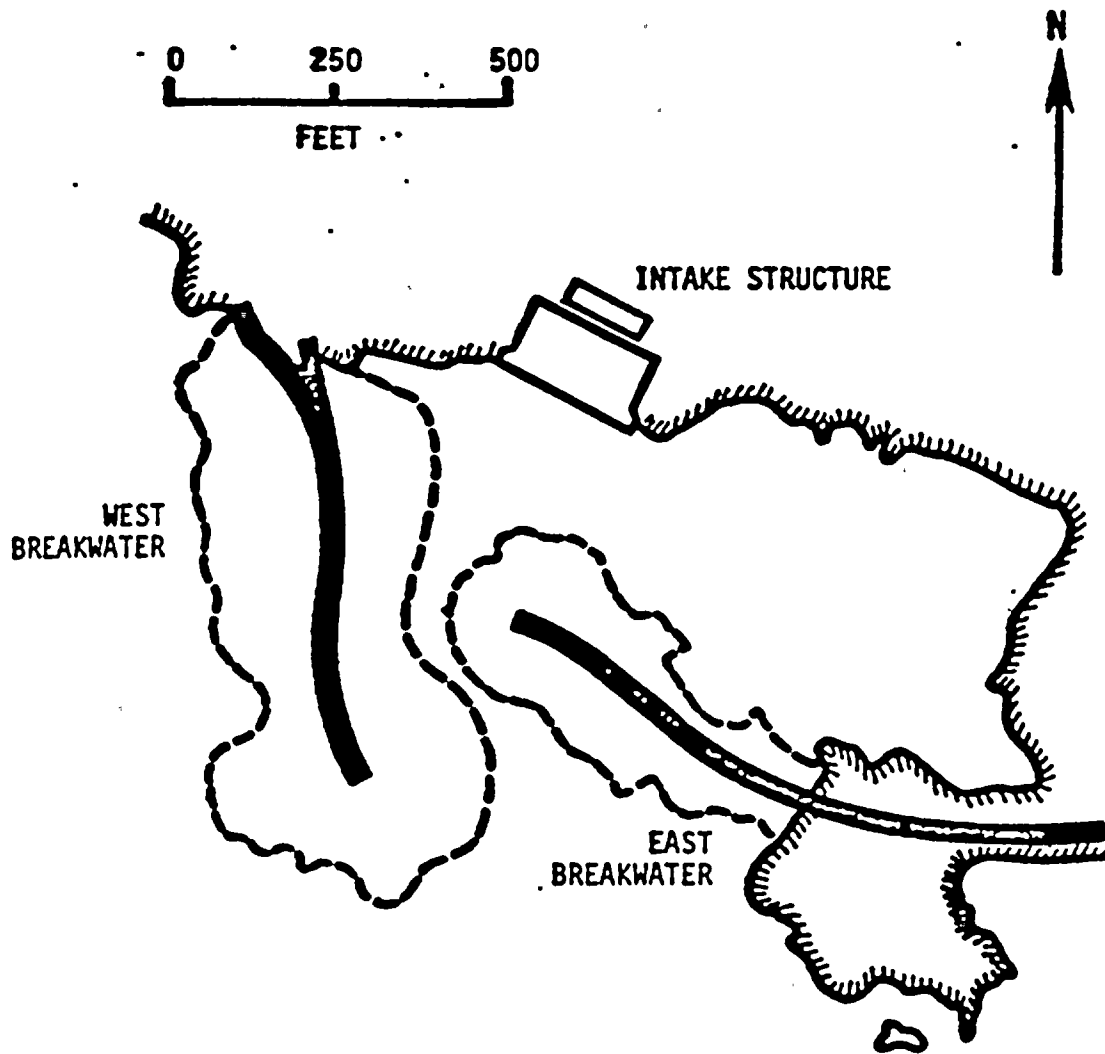


FIGURE F.5.4-1. DIABLO CANYON NUCLEAR POWER PLANT
BREAKWATER AND INTAKE STRUCTURE



100

100

100

100

100

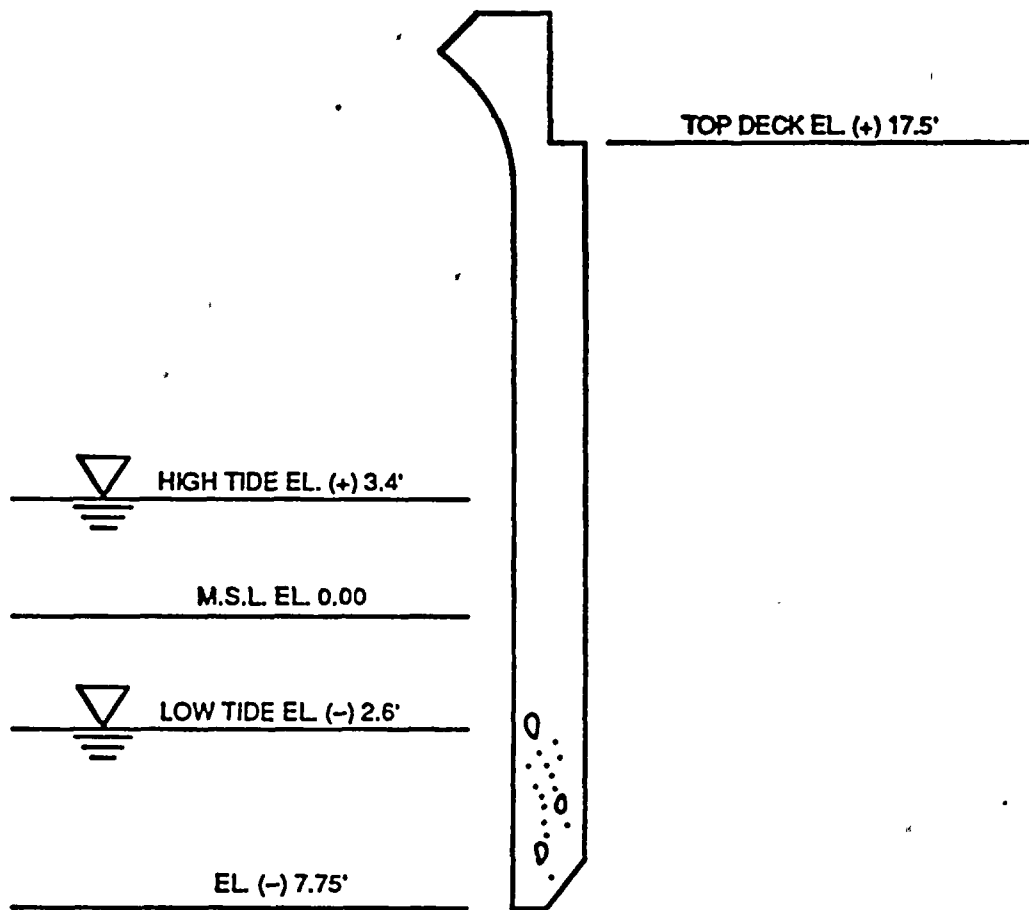


FIGURE F.5.4-2. CROSS-SECTION VIEW OF INTAKE STRUCTURE FRONT WALL



Vertical text on the left side, possibly bleed-through from the reverse side of the page.

F.5.5 HAZARDOUS CHEMICAL

F.5.5.1 Introduction

In this section, the hazard from toxic chemicals stored onsite is investigated.

The hazard from chemicals stored onsite is dominated by the potential effect of a spill on control room habitability.

F.5.5.2 Approach

For a toxic chemical to pose a threat to the control room habitability, a sequence of events must occur. The initiating event would be a chemical spill. This could be caused, for example, by a handling accident, container failure, or some other accident. After the material is released, it must be carried by some mechanism to the control room air intake. It will be assumed that the plant is at power at the beginning of the accident. When the chemical reaches the control room air intake, there are mitigating factors that prevent the operators from being incapacitated. The core melt scenario frequencies depend on the likelihood of successful operator intervention, and on the random equipment failure rate. (The chemicals taken into the control room will not directly fail any equipment.) The chemically-initiated core damage scenario frequency is described by the following expression:

$$\phi_{CD_i} = \phi_{IE_i} \cdot P_{A|IE_i} \cdot P_{CD|A_i} \quad \dots \quad (F.5.5.1)$$



Vertical text on the left side of the page, possibly bleed-through from the reverse side. The characters are faint and difficult to read, but appear to be arranged in a single column.

where

ϕ_{CD_i} = frequency of core damage because of chemical release (per year), for chemical i .

ϕ_{IE_i} = frequency of release (per year) of chemical i .

$P_{A|IE_i}$ = conditional probability of chemical arrival of intake, given release.

$P_{CD|A_i}$ = conditional probability of core damage, given chemical arrival at intake.

These frequencies will be developed in the following sections.

F.5.5.3 Hazardous Chemical Sources

An analysis was made to determine which chemicals stored onsite could pose a threat to the control room habitability (References F.5.5-1 and F.5.5.2). It was determined that anhydrous ammonia, aqueous ammonia, and chlorine could exceed the toxic limit values (TLV) and possibly incapacitate the operators if the chemicals were able to reach the air intakes and pass into the control room.

The anhydrous ammonia source, which could exceed the TLV, is located in a 72-scf pressurized container in the auxiliary building. According to Reference F.5.5-1, a spill from this tank would be mixed by the auxiliary building ventilation system and exhausted through the Unit 1 main plant vent. From there, if the wind and atmospheric stability conditions were right, it could diffuse down to the normal control room air intake, which is located approximately 24 meters away at a lower elevation and to the



Vertical text on the left side, possibly bleed-through from the reverse side of the page. The characters are faint and difficult to decipher, but appear to be arranged in a single column.

south. Assuming a complete spill and assuming that the control room remains unisolated, the TLV would begin to be exceeded 35 seconds after the chemical release. The odor threshold would be reached 31 seconds later. It could then take 1,489 more seconds (24.8 minutes) before the operators would be incapacitated. There would be plenty of time for the operators to take some type of action.

Aqueous ammonia is stored in a 6,000 gallon tank located in the Diablo Canyon Unit 2 condensate polisher buttress area. Reference F.5.5-1 analyzed an instantaneous release of the entire tank. No credit was given for the existence of the buttress area. Given favorable wind speed and direction and favorable atmospheric stability conditions, the chemical could arrive at the control room air intake. The TLV would begin to be exceeded in the control room 87 seconds from the time of the chemical release. The odor threshold would be reached 8 seconds later. It would take 325 more seconds (5.4 minutes) to incapacitate the operators. Again, this is assuming the operators fail to don breathing apparatus and that the control room remains unisolated.

Chlorine is stored in four 1-ton cylinders (2,000 lbs. each) at the intake structure top deck. These cylinders are approximately 427 meters south of the plant complex. One tank is normally fitted with piping for ready use in water treatment operations. The other cylinders are used, in turn, as each tank is used up. The water treatment operations are performed on a regular schedule each week (Mondays, Wednesdays, and Fridays). The amount of chlorine used per operation varies with the condition of the water.



1
2
3
4
5
6
7
8
9
10
11
12
13
14
15
16
17
18
19
20
21
22
23
24
25
26
27
28
29
30
31
32
33
34
35
36
37
38
39
40
41
42
43
44
45
46
47
48
49
50
51
52
53
54
55
56
57
58
59
60
61
62
63
64
65
66
67
68
69
70
71
72
73
74
75
76
77
78
79
80
81
82
83
84
85
86
87
88
89
90
91
92
93
94
95
96
97
98
99
100

It is possible for chlorine to slowly leak out of a cylinder and thus possibly affect the control room. The analysis of Reference F.5.5-1 considers a case in which there are assumed to be five chlorine cylinders leaking over a period of 4 hours. However, since the chlorine tanks are not connected together, it is highly unlikely to have leakage from all the cylinders. However, in terms of control room impact, a one-tank leakage scenario can be bounded by this five-tank analysis. Again, if the winds are favorable and the atmospheric conditions allow, the chemical may reach the control room air intake. The air intakes are equipped with chlorine detectors, which puts the control room in the isolation mode if chlorine is detected. Therefore, in the analysis of Reference F.5.5-1 credit was given for isolation in the analysis. It was assumed that isolation was successfully triggered at the chlorine setpoint level of 1 ppm and that isolation would be complete 8 seconds later.

Under these conditions, the TLV would begin to be exceeded 3,900 seconds after the chemical reaches the air intake. Incapacitation would occur 3,700 seconds later. The odor threshold would not be reached. Isolation would be complete 9 seconds after the chemical reaches the intake. The operators would have over 2 hours to take action, assuming that the detection and isolation of the chemical are successful.

A sudden release from one of the 1 ton cylinders has also been analyzed in Reference F.5.5-1. Given proper wind direction and atmospheric conditions, it is possible for the chemical to reach at the control room air intakes. According to the analysis of Reference F.5.5-1, the



Vertical text on the left side, possibly bleed-through from the reverse side of the page.

concentration at the control room intake would exceed 1 ppm 360 seconds after release. The control room ventilation system is designed to automatically go to mode 3 isolation when this concentration is detected. This will also warn the operators if they have not already been notified. Isolation would be assumed to take 8 seconds. The odor threshold of 3.5 ppm is exceeded in the control room 453 seconds after release. Incapacitation would occur 1,422 seconds after release. Therefore, the operators have $1422 - (360 + 8) = 1,054$ seconds (17.6 minutes) to take some sort of action (such as don a breathing mask and call for help or trip if necessary) after receiving the warning.

A third chlorine scenario is analyzed in Reference F.5.5-2. This involved an instantaneous spill from all five chlorine cylinders. This could occur if all five tanks were involved in a chlorine explosion. The TLV would be exceeded 402 seconds after the release of the chemical. Incapacitation would occur 293 seconds later. The control room would be isolated at 361 seconds after the release. The operators would have about 5.6 minutes to take action, assuming that the detection and isolation of the chemical are successful.

F.5.5.4 Frequency of Release, ϕ_{IE}

Reference F.5.5-3 was used to obtain the frequency of various chlorine release scenarios. According to Reference F.5.5.3, the frequency of "serious" release from 1-ton chlorine containers is 3.8×10^{-5} per year for normal operating/storage conditions and 5.5×10^{-6} per changeover. Further investigation indicated that only one of eight serious releases



could be considered rupture of the tank leading to sudden release in normal conditions. We also assumed, conservatively, that 25% of all changeover releases involved container rupture. Finally, based on an interview with plant personnel, it was determined that the frequency of changeover is about 12 per year. It was also assumed that if one tank ruptures there is a 50% chance of all the remaining tanks rupturing.

Based on the above information, the following initiator frequencies were developed for chlorine scenarios.

- Leakage of One Chlorine Tank

$$\begin{aligned}\phi_{C1} &= (4 \text{ tanks}) \left[(3.8 \times 10^{-5}) \left(\frac{7}{8} \right) \text{ leaks/tank year} \right] \\ &\quad + \left[(5.5 \times 10^{-6}) (0.75) \text{ leaks/changeover} \right] (12 \text{ changeovers/year}) \\ &= 1.8 \times 10^{-4} \text{ per year}\end{aligned}$$

- Rupture of One Chlorine Tank

$$\begin{aligned}\phi_{C2} &= (4 \text{ tanks}) \left[(3.8 \times 10^{-5}) \left(\frac{1}{8} \right) \text{ ruptures/tank year} \right] \\ &\quad + \left[(5.5 \times 10^{-6}) (0.25) \text{ rupture/changeover} \right] (12 \text{ changeovers/year}) \\ &= 3.6 \times 10^{-5} \text{ per year}\end{aligned}$$

- Rupture of All Four Chlorine Tanks

$$\begin{aligned}\phi_{C3} &= 0.5 \phi_{C2} \\ &= 0.5 (3.6 \times 10^{-5}) = 1.8 \times 10^{-5} \text{ per year}\end{aligned}$$



1

2
3
4
5
6
7
8
9
10
11
12
13
14
15
16
17
18
19
20
21
22
23
24
25
26
27
28
29
30
31
32
33
34
35
36
37
38
39
40
41
42
43
44
45
46
47
48
49
50
51
52
53
54
55
56
57
58
59
60
61
62
63
64
65
66
67
68
69
70
71
72
73
74
75
76
77
78
79
80
81
82
83
84
85
86
87
88
89
90
91
92
93
94
95
96
97
98
99
100

101
102
103
104
105
106
107
108
109
110
111
112
113
114
115
116
117
118
119
120
121
122
123
124
125
126
127
128
129
130
131
132
133
134
135
136
137
138
139
140
141
142
143
144
145
146
147
148
149
150
151
152
153
154
155
156
157
158
159
160
161
162
163
164
165
166
167
168
169
170
171
172
173
174
175
176
177
178
179
180
181
182
183
184
185
186
187
188
189
190
191
192
193
194
195
196
197
198
199
200

For the ammonia tanks, a value of 1.0×10^{-4} per year was used. This value is consistent with the frequency of chlorine cylinder failures developed above assuming the same number of changeovers (12 per year), which is high for the ammonia tanks.

F.5.5.5 Conditional Probability of Chemical Arrival at Air Intake Given Chemical Spill, PAIE

The conditional probability that a chemical would reach the intake is composed mainly of two factors: wind direction and atmospheric stability conditions.

For the anhydrous ammonia release, the wind must be from the north for the chemical to be able to reach the intake since the normal control room intake is south of the Unit 1 plant vent where the material would be released. Furthermore, the wind speed must not be too great and the stability conditions must be favorable, allowing the material to diffuse downward, since the plant vent is at a higher elevation (approximately at a 230-foot elevation) than the control room air intake (approximately at a 165-foot elevation).

The aqueous ammonia tank is located in the Unit 2 buttress area directly to the west of the turbine building. For a release to reach the normal air intakes, the wind must be from a generally westerly direction. The atmospheric conditions must also be favorable and allow the material to diffuse up over the turbine building and to the air intakes on the auxiliary building roof.



For chlorine, the wind direction would have to be from the south since the intake structure where the chlorine is located is 427 meters south of the plant. The atmospheric stability conditions would have to be favorable and allow the chlorine to diffuse around and over structures shielding the air intakes.

In this analysis, we will make the conservative assumption that, for all chemical release scenarios, the probability of favorable wind direction and atmospheric conditions (P_{AIR}) existing at the time of the release is 1.0.

F.5.5.6 Conditional Probability of Core Damage Given Chemical Arrival at Air Intake, PCD|A

The sequence of events following the arrival of toxic material at the control room air intake depend on whether

- Operators Detect Toxic Chemicals
- Control Room Air Intake Is Isolated (Manually or Automatically)
- Operators Don Breathing Apparatus
- Operators Become Incapacitated
- Operators Recover or Outside Help Becomes Available



19
20
21
22
23
24
25
26
27
28
29
30
31
32
33
34
35
36
37
38
39
40
41
42
43
44
45
46
47
48
49
50
51
52
53
54
55
56
57
58
59
60
61
62
63
64
65
66
67
68
69
70
71
72
73
74
75
76
77
78
79
80
81
82
83
84
85
86
87
88
89
90
91
92
93
94
95
96
97
98
99
100

- With Plant Trip (manual or spurious), Operators are Capable of Performing Necessary Actions To Bring the Plant to a Safe Shutdown Condition

Control room air intake is isolated automatically only in the case of chlorine scenarios. Even with isolation, because of infiltration of gas during isolation, the operators will become incapacitated after some time as calculated in Reference F.5.5-1 and summarized in Section F.5.5.3.

In all the scenarios, it is assumed that outside help is eventually needed. This help is very likely to be available shortly after the release since in some scenarios the time available before operators are incapacitated is considerable even without operators donning breathing masks. Even if outside help is not called for by the operators prior to becoming incapacitated, the new shift will arrive. The mean time to arrive after release is $1/2$ (8 hours) = 4 hours. As we will see, this time is shorter than the time before operator action is required if the plant is tripped.

In this analysis, we assume that following a chemical release the plant is tripped either manually by the operators or spuriously. This is of course conservative since the operators do not necessarily trip the plant in reaction to the chemical release, and spurious trip during the time between release and when operators recover or outside help becomes available is not very likely.



本 部 表

2

Given reactor trip, the key action required by the operators within 8 hours is replenishment of condensate storage tank (CST). This time is longer than the estimated 4-hour mean "operator recovery" time discussed above.

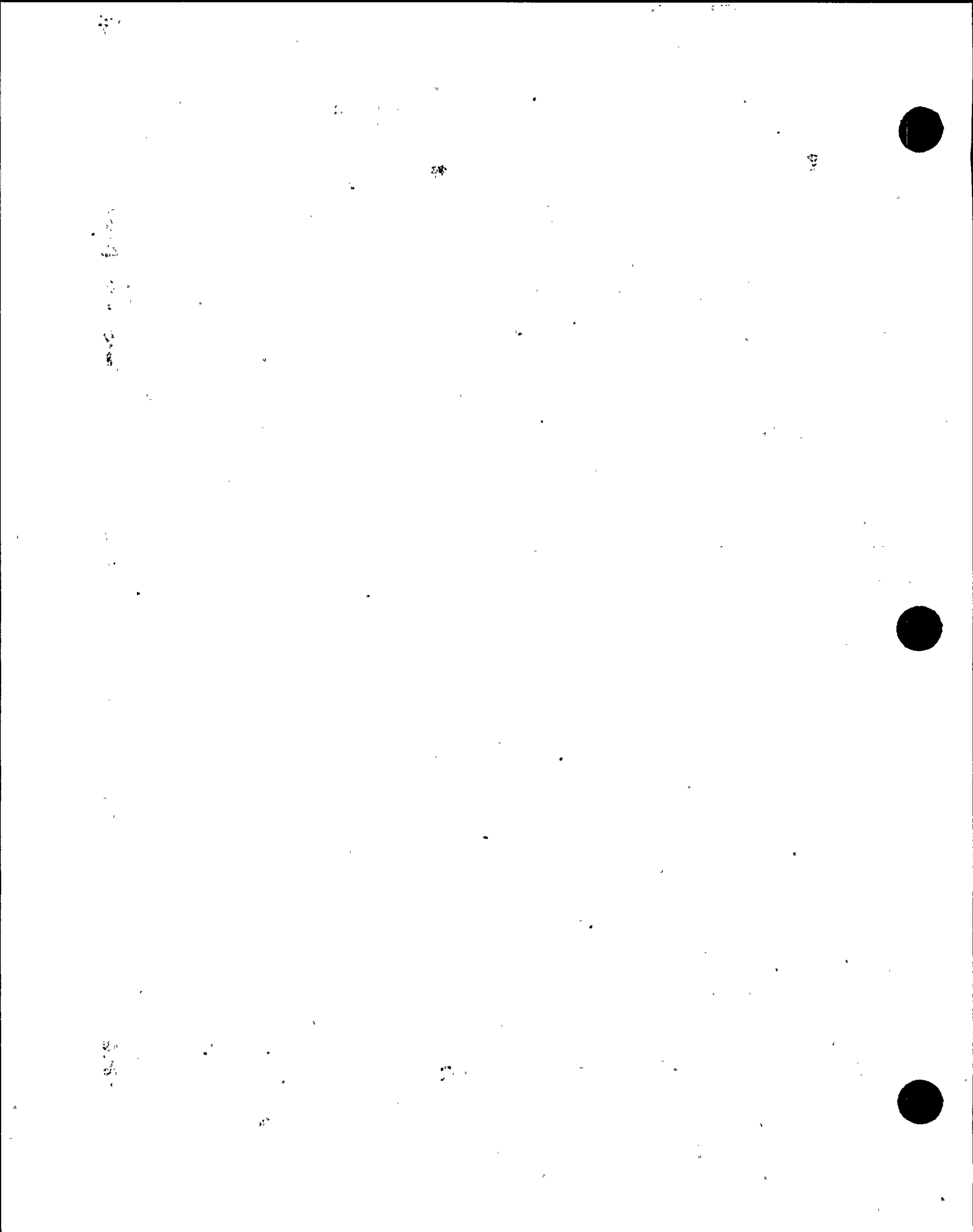
The probability of operator failure to replenish CST under conditions in which no hazardous material is present in the environment and the control room is estimated in the human actions analysis report (Appendix H) to be 4.4×10^{-3} . For the scenarios of interest here, we use a higher value of approximately 8×10^{-3} . If this action fails, core damage is assumed for all the scenarios regardless of type of chemical released and times available. Therefore,

$$P_{CD|A} = 8.0 \times 10^{-3}$$

The total core damage frequency for all scenarios is then

$$\begin{aligned}\phi_{CD} &= \left(1.8 \times 10^{-4} + 3.6 \times 10^{-5} + 1.8 \times 10^{-5} + 1.0 \times 10^{-4}\right. \\ &\quad \left.+ 1.0 \times 10^{-4}\right) \left(8.0 \times 10^{-3}\right) \\ &= \left(4.3 \times 10^{-4}\right) \left(8.0 \times 10^{-3}\right) \\ &= 3.5 \times 10^{-6} \text{ per year}\end{aligned}$$

Despite all the conservatisms in estimating the above frequency, it is still a small contributor to the total core damage frequency from other initiators.



F.5.5.7 References

- F.5.5-1. Pacific Gas and Electric Company, "Control Room Habitability - Onsite Toxic Chemical Analysis," Mechanical (HVAC) Calculation Number 86-13, Diablo Canyon Power Plant Units 1 and 2 Project, Rev. 2, July 29, 1987.
- F.5.5-2. Pacific Gas and Electric Company, "Chlorine Release Accident Analysis," Mechanical Calculation Number M-714, Diablo Canyon Power Plant Units 1 and 2 Project, Rev. 0, May 12, 1987.
- F.5.5-3. Pickard, Lowe and Garrick, Inc., proprietary data.
- F.5.5-4. "Units 1 and 2, Diablo Canyon Power Plant Final Safety Analysis Report Update," Pacific Gas and Electric Company, Section 9.4, Rev. 3, September 1987.



8

9

10

11

12

13

F.5.6 HURRICANE WIND AND TORNADO-INITIATED SCENARIOS

F.5.6.1 Introduction

Winds can affect critical structures at the plant site in at least two ways. If wind forces exceed the load capacity of a building or other external facility, the incident walls or framing might collapse or the structure might overturn from the excessive loading. If the wind is strong enough, as in a tornado or hurricane, it may be capable of lifting materials and thrusting them as missiles against some of these critical facilities. Critical components or other contents of facilities not designed to resist missile penetration might be damaged and lose their function. This section presents an analysis of the risk to the Diablo Canyon Nuclear Power Plant (DCNPP) from wind load and missiles generated by hurricanes or tornadoes.

F.5.6.2 Tornado, Wind, and Missile Hazard

A review of the analysis in Reference F.5.6-1 shows that the critical concrete structures at DCNPP can withstand at least a 200-mph wind without major damage (such as collapse of a wall or overturning of a structure). The annual frequency, ϕ , of excessive tornado wind (≥ 200 mph) on the structures can be found by the following relationship:

$$\phi = \phi_t \cdot \phi_v / t \quad (F.5.6.1)$$



Vertical text on the left side of the page, possibly a page number or header.

Vertical text on the left side of the page, possibly a page number or header.

where ϕ_t is the annual frequency of a tornado striking the plant and $\phi_{v|t}$ is the fraction of tornadoes with peak wind speed greater than 200 mph.

To estimate ϕ_t , we use the following expression (Reference F.5.6-2):

$$\phi_t = n \cdot \frac{W}{A} \quad (\text{F.5.6.2})$$

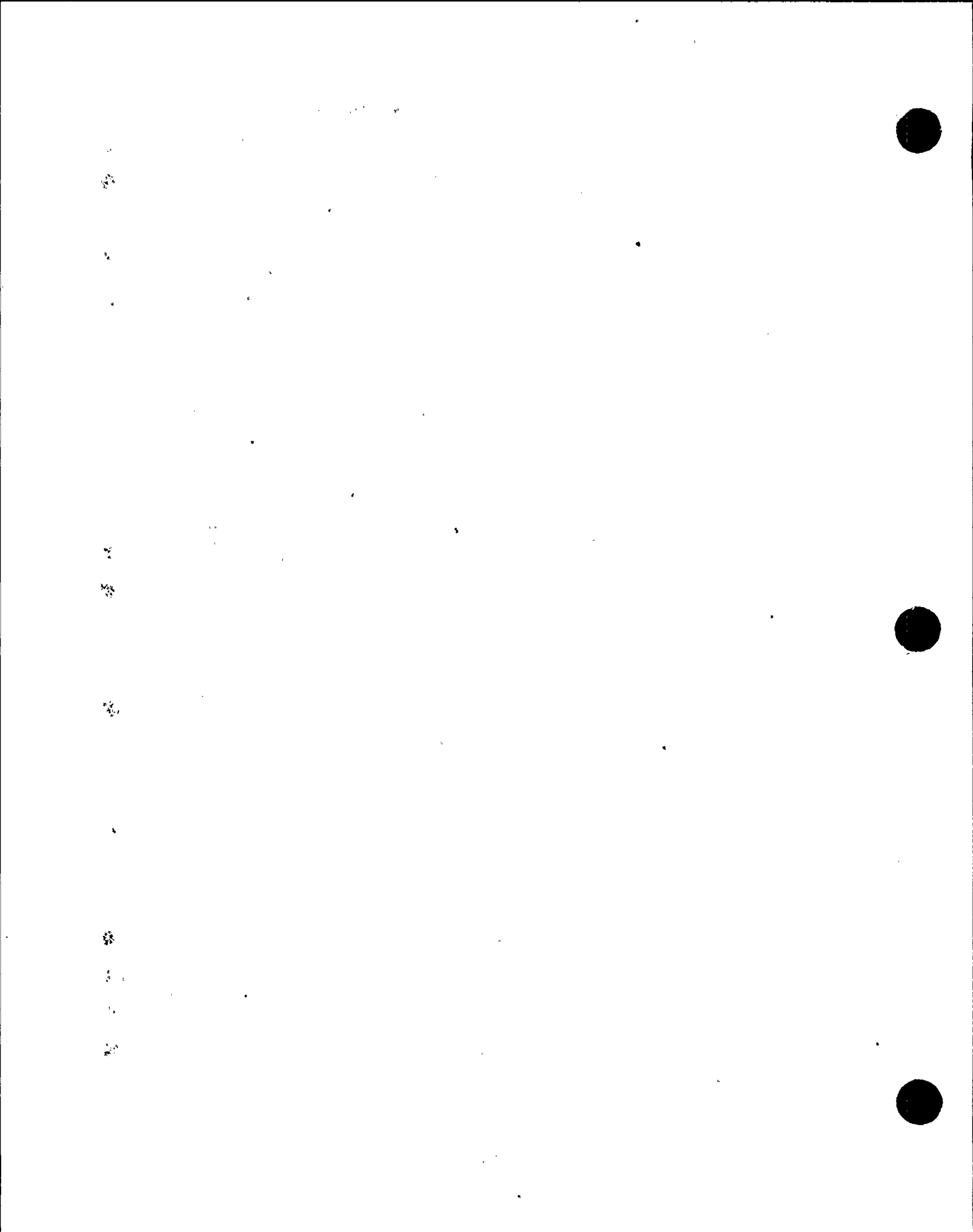
where W is the mean path area of a tornado in square miles, A is the area of interest within which it is assumed the tornado could strike the site, and n is the mean number of tornado occurrences per year in this area. According to Reference F.5.6-3, there is an average of four tornadoes within the state of California per year. This gives an annual occurrence density (n/A) of 0.25 tornadoes per 10,000 square miles.

Reference F.5.6-4 gives a mean path area (W) for California tornadoes of 0.140 square miles. Now, we can calculate ϕ_t as

$$\phi_t = \frac{n}{A} \cdot W = (2.5 \times 10^{-5})(0.140)$$

$$\phi_t = 3.50 \times 10^{-6} \text{ strikes per year}$$

An analysis of 4,582 tornadoes in the U.S., classified according to the Fujita intensity scale, is given in Reference F.5.6-5. Table F.5.6-1 shows the distribution of tornado wind speeds based on a Gamma distribution fit to the data for NRC tornado Region 2 where DCNPP is



located. Table F.5.6-2 shows the tornado wind speed exceedance probabilities that were developed from the data in Table F.5.6-1. Interpolating from Table F.5.6-2 for $V=200$ mph, gives $\phi_{v|t} = 0.0155$.

Therefore, the annual frequency of tornado wind speeds in excess of 200 mph at the plant is

$$\phi = \phi_t \cdot \phi_{v|t}$$

$$\phi = (3.5 \times 10^{-6})(0.0155) = 5.43 \times 10^{-8} \text{ per year}$$

The only critical structures that cannot withstand a 200-mph wind are the outdoor water storage tanks. They can, however, withstand at least a 150-mph wind (Reference F.5.6-1). For this case, $\phi_{v|t} = 0.0923$.

Hence,

$$\phi = \phi_t \cdot \phi_{v|t} = (3.5 \times 10^{-6})(0.0923) = 3.23 \times 10^{-7} \text{ per year}$$

With such low initiator frequencies, it is judged that tornado wind-initiated scenarios are insignificant contributors to the overall core melt frequency.

The analysis in Reference F.5.6-1 also shows that the critical concrete structures can withstand a 200-mph wind with missiles without major damage. Missile types considered were a 108-pound board, a 76-pound pipe, and a 4,000-pound automobile. The outside tanks could withstand up



to a 150-mph wind with missiles. Therefore, tornado missile-initiated scenarios are also judged to be insignificant contributors to the overall core melt frequency.

F.5.6.3 Hurricane Wind Hazard

The hurricane wind hazard can be approached in the same way that the tornado wind hazard was analyzed. For this analysis, it will be conservatively assumed that failure of the outdoor water storage tanks leads to core melt. As mentioned in the previous section, the other critical structures have higher wind resistance. The analysis, in Reference F.5.6-1 shows that the tanks can withstand a 165-mph wind without missiles and a 150-mph wind with missiles. It will be assumed that the wind fragility of the tanks is 150 mph. The annual frequency, ϕ , of excessive hurricane wind (≥ 150 mph) on the structures can be found by

$$\phi = \phi_h \cdot \phi_{v|h} \quad (\text{F.5.6.3})$$

where ϕ_h is the annual frequency of a hurricane striking the plant and $\phi_{v|h}$ is the fraction of hurricanes with peak wind speeds greater than 150 mph.

Reference F.5.6-6 indicates that no hurricanes (maximum sustained wind speed > 74 mph) and only three documented tropical storms (maximum sustained wind speed 39 to 73 mph) have entered the southwestern U.S. in this century. Reference F.5.6-4 shows that the annual probability of a



tropical storm occurring near San Diego is less than 0.05. The plant site, which is more than 200 miles away to the northwest, would have even less chance of experiencing a tropical storm. Since there is no record of hurricanes in this region, we will make the conservative assumption that the hurricane frequency, ϕ_h , at the plant site is equal to the tropical storm frequency near San Diego. Therefore, we use $\phi_h = 0.05$.

To calculate the fraction of hurricanes with wind speeds greater than 150 mph ($\phi_{v|h}$), wind speed data from the three recorded tropical storms are used to fit a probability distribution. The peak sustained wind speeds of the storms when they were on shore were 52 mph, 46 mph, and 57 mph (Reference F.5.6-6). These data were used to fit an extreme value distribution of the form

$$P(v \geq v_0) = 1 - \exp -e^{-\alpha(v_0 - \beta)} \quad (F.5.6.4)$$

where

$$\alpha = \frac{1.645}{s^2}^{\frac{1}{2}}$$

$$\beta = v - \frac{0.577}{\alpha}$$



where V and S^2 are the mean and variance of the data, respectively. From the data, α is 0.233 and B is 49.2. This gives the probability of exceeding $V_0 = 150$ mph of

$$P(V \geq V_0 = 150) = 1 - \exp^{-e^{-0.233(150-49.2)}}$$

$$P(V \geq V_0 = 150) = 6.37 \times 10^{-11}$$

This gives $\phi_{v|h} = 6.37 \times 10^{-11}$. Other parametric distributions such as lognormal and normal give smaller numerical values. The annual frequency of hurricane wind speeds in excess of 150 mph is therefore

$$\phi = \phi_h \cdot \phi_{v|h}$$

$$\phi = (0.05) \cdot (6.37 \times 10^{-11}) = 3.2 \times 10^{-12} \text{ per year}$$

With such a low initiator frequency, it is judged that hurricane-initiated scenarios are insignificant contributors to the overall core damage frequency.

F.5.6.4 References

- F.5.6-1. "Units 1 and 2, Diablo Canyon Power Plant Final Safety Analysis Report Update," Pacific Gas and Electric Company, Section 3.3, Rev. 3, September 1987.
- F.5.6-2. Thom, H. C. S., "Tornado Probability," Monthly Weather Review, No. 91, pp. 730-736, 1963.
- F.5.6-3. U.S. Department of Commerce, National Oceanic and Atmospheric Administration, "Storm Data," Vol. 28, No. 28, December 1986.
- F.5.6-4. State of California, Department of Water Resources, "Windstorms in California," Sacramento, California, December 1979.



F.5.6-5. Twisdale, L. A., "Tornado Data Characterization and Windspeed Risk," Journal of the Structural Division, Proceedings of ASCE, Vol. 104, No. ST10, October 1978.

F.5.6-6. Smith, W., "The Effects of Eastern North Pacific Tropical Cyclones on the Southwestern United States," U.S. Department of Commerce, NOAA Technical Memorandum NWS WR-197, August 1986.

F.5.6-7

1647P070188



TABLE F.5.6-1. TORNADO WIND SPEED FRACTIONS

F-Scale	Wind Speed Range (mph)	Frequency (NRC Tornado Region 2)
0	40 to 72	0.3559
1	72 to 112	0.3822
2	112 to 157	0.2008
3	157 to 206	0.0520
4	206 to 260	0.0080
5	260 to 318	0.0010
6	318 to 380	0.0001
<u>> 6</u>	<u>> 380</u>	0.0000

TABLE F.5.6-2. TORNADO WIND SPEED EXCEEDANCE PROBABILITIES

V (mph)	ϕ_v/t
40	1.0
72	0.6441
112	0.2619
157	0.0611
206	0.0091
260	0.0011
318	0.0001



Vertical text or markings along the left edge of the page, possibly bleed-through from the reverse side.

F.5.7 EXTERNAL FLOODING

F.5.7.1 Introduction

Potential accident sequences initiated by external floods at the Diablo Canyon Nuclear Power Plant are investigated, and the frequencies of the resulting core damage scenarios are calculated.

F.5.7.2 Flooding Sources

DCNPP is located on the California coast, approximately halfway between San Francisco and Los Angeles. It is subject to potential flooding from the ocean and from heavy rainfall.

The analysis of Reference F.5.7-1 identifies the flooding resulting from the simultaneous occurrence of a tsunami, high tide, storm waves, and a severely degraded breakwater to be the most severe flooding event from the ocean. Hurricane and line squall surge flooding (storm-generated, long-period waves) have not been observed on the California Pacific coastline, according to the same reference. However, the above tsunami-storm event would be even more severe than surge projections for the Atlantic and Gulf states, which encounter much more frequent and severe hurricanes than California (Reference F.5.7-1). Reference F.5.7-1 also shows that heavy rains will not cause sufficient ponding on the plant site to flood safety-related buildings; neither will it cause the only stream near the site (Diablo Creek) to overtop.



Vertical text or markings along the left edge of the page, possibly bleed-through from the reverse side.

Another possible flooding source would be the raw water reservoirs located on the hill behind the plant at Elevation 310 feet. There are two reservoirs, each holding about 2.25 million gallons each. Each reservoir is roughly egg shaped, with major and minor dimensions of approximately 270 feet and 190 feet. The reservoirs were made by excavating from bedrock and lining with 4" concrete and PVC liner. The lip of the reservoir is at Elevation 310 feet. There is usually between 1.5 to 3 feet of freeboard. The bottom of the reservoirs are concave and vary between Elevation 296.5 feet and Elevation 298.5 feet. The sides angle smoothly up to the lip from the bottom, over a distance of about 18 feet. Reservoir 1-A is closest to the plant. The impoundment is located at least 200 feet away from the edge of the hillside. The hillside slopes approximately 20 degrees down. The plant is located approximately 800 feet from Reservoir 1-A. It is unlikely that the reservoirs can fail in such a way to pose a threat to the plant; however, a worst case scenario will be presented.

To be conservative, it will be assumed that both reservoirs (Reservoir 1-B is behind 1-A, and is located nearly 500 feet from the edge of the hillside), lose all their water and that the entire volume of water flows toward the plant. The area covered by the flood is taken to be the triangle formed by the closest point of Reservoir 1-A to the plant (800 feet), and the north and south sides of the plant (800 feet). This area is approximately 320,000 square feet. If the entire reservoir inventory is applied to this area, the depth of flooding will be approximately 2 feet at the back of the plant. This depth of flooding is



Vertical text or markings along the left edge of the page, possibly bleed-through from the reverse side.

not expected to cause serious damage to the plant. In addition, the flood will only be temporary and not sustained.

According to Reference F.5.7-1, the roofs of the safety-related buildings are designed to handle a PMP of 4 inches per hour. If the rainfall intensity should exceed this drain capacity, overflow scuppers will still prevent ponding in the roof. Yard areas around safety-related buildings are also sloped to keep water away from the buildings. The Unit 1 plant has been in commercial operation since May 7, 1985, and the Unit 2 plant since March 13, 1986. Only one case of rainwater inleakage to a safety-related area occurred. This was at the diesel fuel oil transfer pump vault area. Rainwater was able to enter this area through the diesel fuel oil pipe chase (trench), which was not equipped with a waterproof cover. Under normal conditions, the drains in these rooms would remove the water. However, to prevent a recurrence of this problem, the diesel fuel oil transfer pump vault walls have been sealed at the junction of the diesel fuel oil pipe trench. Therefore, the potential of future flooding due to rainfall is negligibly small.

F.5.7.3 Flooding Frequency

Based on the discussion in the previous sections, the safety-related equipment subject to external flooding are the auxiliary saltwater (ASW) pumps located within the intake structure. There are two ASW pumps per unit. Each pump is housed in its own room. Each room is equipped with a normally closed watertight door. The pump rooms are equipped with snorkels to allow air in to remove heat from the ASW pump motors. These



1
2
3
4
5
6
7
8
9
10
11
12
13
14
15
16
17
18
19
20
21
22
23
24
25
26
27
28
29
30
31
32
33
34
35
36
37
38
39
40
41
42
43
44
45
46
47
48
49
50
51
52
53
54
55
56
57
58
59
60
61
62
63
64
65
66
67
68
69
70
71
72
73
74
75
76
77
78
79
80
81
82
83
84
85
86
87
88
89
90
91
92
93
94
95
96
97
98
99
100



snorkels allow the pump rooms to be waterproof up to +48 feet above the mean lower low water level (MLLW).

Two cases will be examined for possible flooding of the ASW pump rooms. One is when one or more pump room doors has been left open or fails during a tsunami event. In this case, flooding of the pump rooms will occur if the water level reaches the main deck level of the intake structure, which is at +20-feet MLLW. The other case is when a combined tsunami-storm wave height exceeds +48-foot MLLW.

The analysis of Reference F.5.7-1 summarizes the maximum water elevation calculations for two categories: one in which the breakwater is assumed to be intact and the other in which the breakwater is assumed to be degraded to 0 feet MLLW by previous wave action (see Table F.5.7-1).

The following equation will be used to calculate the frequency with which a particular water level is exceeded:

$$F = P_B \cdot (f_a \cdot f_b \cdot f_c \cdot f_d)_B + P_{NB} \cdot (f_a \cdot f_b \cdot f_c \cdot f_d)_{NB} \quad (F.5.7.1)$$

where

F = frequency of exceeding a given water level at the intake structure (+feet MLLW).

P_B = probability of breakwater being intact at time of a tsunami event.



P_{NB} = probability of breakwater being in a degraded state (0 feet MLLW) at time of a tsunami event.

f_a = probability of maximum astronomical tide at time of tsunami event.

f_b = frequency of tsunami event with a particular run-up level per year.

f_c = probability of maximum meteorological tide at time of tsunami.

f_d = probability of "once-a-year storm" occurring at time of tsunami event.

E = with breakwater.

N_B = without breakwater.

We will conservatively assume that the maximum astronomical and meteorological tides co-exist at the time of the tsunami event; i.e.,

$f_a = 1.0$ and $f_c = 1.0$. Equation (F.5.7.1) then reduces to

$$F = P_B \cdot (f_b \cdot f_d)_B + P_{NB} \cdot (f_b \cdot f_d)_{NB} \quad (F.5.7.2)$$

From Reference F.5.7-1, the breakwaters were in a damaged state for approximately 2 years from the fall of 1981 to the fall of 1983 because of storm damage. The original Diablo Canyon breakwaters were built in



Vertical text on the left side, possibly bleed-through from the reverse side of the page. The characters are small and difficult to read, but appear to be arranged in a column.

1971. Therefore, the observed availability of the breakwaters is $P_B = 0.90$. Consequently, $P_{NB} = 1 - P_B = 0.10$.

For the water level to exceed +20 feet MLLW, the combined tide, tsunami, and storm effects must exceed +20 feet MLLW. With the breakwater in place, the water level without tsunami is comprised of +5.3 feet for astronomical tide, +1.0 foot for meteorological tide, +12.15 feet for storm wave effects, giving +18.45-foot MLLW. Therefore, the tsunami must exceed +1.55 feet to result in the +20-foot MLLW level being exceeded. The frequency with which this is exceeded is approximately 5.9×10^{-2} per year, as extrapolated from Reference F.5.7-2 by taking 10^{-6} per year as the lowest frequency of tsunamis at the site (see Figure F.5.7-1). This reference includes only the effects of distantly generated tsunamis on the west coast of the United States. To include the effect of locally generated tsunamis, we will conservatively increase the frequency of infrequent tsunamis by a factor of 2. In the case of +1.55 feet tsunamis however, we will use the value based on Figure F.5.7-1. That is,

$$(f_b)_B = 5.9 \times 10^{-2} \text{ per year}$$

The probability of the once-per-year storm occurring at the same time depends on how long the storm lasts. According to Reference F.5.7-1, the once-per-year storm has an effective duration of approximately 2 days.



1000

1000

1000

1000

1000

1000

Therefore,

$$(f_d)_B = \frac{2 \text{ days}}{365 \text{ days}} = 5.5 \times 10^{-3}$$

With the breakwater gone, the water level without tsunami is composed of +5.3 feet for astronomical tide, +1.0 foot for meteorological tide, and +29.52 feet for storm effects, giving +35.82-foot MLLW. In this case, no tsunami is needed to exceed +20 feet MLLW, so $(f_b)_{NB}$ is deleted from the equation. As before, the probability of storm occurrence is $(f_d)_{NB} = 5.5 \times 10^{-3}$.

Therefore, the annual frequency of exceeding +20 feet MLLW is

$$\begin{aligned} F_{20} &= 0.90 (5.9 \times 10^{-2}) (5.5 \times 10^{-3}) \\ &\quad + 0.10 (5.5 \times 10^{-3}) \\ &= 2.9 \times 10^{-4} + 5.5 \times 10^{-4} \\ F_{20} &= 8.4 \times 10^{-4} \text{ per year} \end{aligned}$$

For water level to exceed +48 feet MLLW, the combined tide, tsunami, and storm effects must exceed +48 feet MLLW. With the breakwater in place, the water level without tsunami is composed of +5.3 feet for astronomical tide, +1.0 foot for meteorological tide, and +12.15 feet for storm wave effects, giving +18.45-foot MLLW. For the combined tsunami, storm, and tide to exceed +48 feet MLLW, the tsunami height must exceed +29.55 feet. Based on distantly generated tsunamis, the frequency with which this is exceeded is taken to be 1×10^{-6} per year, which is the



10

11

12

13

14

15

16

minimum tsunami frequency used in this analysis (see Figure F.5.7-1). To account for the effect of locally generated tsunamis, we increase this frequency by a factor of 2.

Therefore, we have

$$(f_b)_B = 2.0 \times 10^{-6} \text{ per year}$$

With the breakwater gone, the water level without tsunami is composed of +5.3 feet for astronomical tide, +1.0 foot for meteorological tide, and +29.52 feet for storm wave effects, giving +35.82-foot MLLW. For the combined water level to exceed +48 feet MLLW, the tsunami height must therefore exceed +12.18 feet. From Figure F.5.7-1, the frequency is approximately 4.5×10^{-4} per year considering the distantly generated tsunamis. Increasing this frequency by a factor of 2 to account for locally generated tsunamis, we have

$$(f_b)_{NB} = 9.0 \times 10^{-4} \text{ per year}$$

The probability of storm occurrence is, again,

$$(f_d)_B = (f_d)_{NB} = 5.5 \times 10^{-3}$$



Vertical text or markings along the left edge of the page, possibly bleed-through from the reverse side.

Therefore, the annual frequency of exceeding +48 feet MLLW is

$$\begin{aligned} F_{48} &= 0.90 (2.0 \times 10^{-6}) (5.5 \times 10^{-3}) \\ &\quad + 0.10 (9.0 \times 10^{-4}) (5.5 \times 10^{-3}) \\ &= 9.9 \times 10^{-9} \text{ per year} + 4.9 \times 10^{-7} \text{ per year} \\ F_{48} &= 5.0 \times 10^{-7} \text{ per year} \end{aligned}$$

F.5.7.4 Flooding Fragility of Safety-Related Structures

The plant site is located +85 feet above mean sea level (MSL), or, alternatively, +87.6 feet above mean lower level water level (MLLW). The only safety-related equipment located within flooding range are the ASW pumps in the intake structure. There are four ASW pumps, two per unit. One can service both units if necessary. Each pump is located in its own watertight compartment within the intake structure at the -2.1-foot MSL level (-4.7-foot MLLW). The intake structure is protected from flooding up to its main deck level of +20-foot MLLW. Above that level, water can also enter into the intake structure via the penetrations for the traveling screens on the roof and through the personnel entrance into the structure, which leads down a flight of stairs to the -4.7-foot MLLW level.

There is a gate at the doorway, but this is not a barrier to water. However, even if water should enter the intake structure from these access points, the pumps will not be endangered because of the watertight compartments. Flooding will only occur in this situation if the watertight access door has been inadvertently left open or if the door



1
2
3
4
5
6
7
8
9
10
11
12
13
14
15
16
17
18
19
20
21
22
23
24
25
26
27
28
29
30
31
32
33
34
35
36
37
38
39
40
41
42
43
44
45
46
47
48
49
50
51
52
53
54
55
56
57
58
59
60
61
62
63
64
65
66
67
68
69
70
71
72
73
74
75
76
77
78
79
80
81
82
83
84
85
86
87
88
89
90
91
92
93
94
95
96
97
98
99
100



101
102
103
104
105
106
107
108
109
110
111
112
113
114
115
116
117
118
119
120
121
122
123
124
125
126
127
128
129
130
131
132
133
134
135
136
137
138
139
140
141
142
143
144
145
146
147
148
149
150
151
152
153
154
155
156
157
158
159
160
161
162
163
164
165
166
167
168
169
170
171
172
173
174
175
176
177
178
179
180
181
182
183
184
185
186
187
188
189
190
191
192
193
194
195
196
197
198
199
200



fails, allowing seawater to enter. The first case is not likely because access to the ASW pump rooms is monitored by the control room. There is an alarm in the control room that will sound if any of the watertight doors are open. Plant procedures direct security personnel to investigate if the door is open without authorization (Reference F.5.7-3). Also, given a tsunami warning, the ASW pump room alarm is checked. If a door is open in this situation, the operators may or may not be allowed to close the door, depending on the circumstances (Reference F.5.7-4). To compute the frequency of occurrence of the first scenario, an estimate is needed for the probability of flooding the pump room via the watertight doors, given a tsunami. This can be estimated by

$$\begin{aligned}
 P_{WE} = & (1 - P_{DO}) \cdot P_{NW} & (F.5.7.3) \\
 & + P_{DO} \cdot (1 - P_{NA}) \cdot (1 - P_{FC}) \cdot P_{NW} \\
 & + P_{DO} \cdot (1 - P_{NA}) \cdot P_{FC} + P_{DO} \cdot P_{NA}
 \end{aligned}$$

where

P_{WE} = probability that water enters a pump room through its watertight door, given a tsunami.

P_{DO} = probability that watertight door is open at the time of a tsunami.

P_{NW} = probability that watertight door fails, allowing seawater to enter pump room.



P_{NA} = probability that plant does not receive a tsunami warning.

P_{FC} = probability that operators are not able to close watertight door, given the door is open during a tsunami warning.

We will conservatively assume the operator is not able to close a watertight door if it is open during a tsunami warning. Therefore, $P_{FC} = 1.0$. Equation (3) then reduces to

$$P_{KE} = (1 - P_{DO}) \cdot P_{NW} + P_{DO} \quad (F.5.7.4)$$

To estimate P_{NW} , the flood fragility of the watertight door, we will assume that it is lognormally distributed with a 50th percentile value of 0.05 and a 95th percentile value of 0.50. This covers a sufficiently large range of fragility with a very conservative upper bound for a door that is designed to withstand the hydraulic load in the event of pump room flooding. The mean of this distribution for P_{NW} is 0.133. Therefore, we are assuming a 13.3% chance of mechanical failure of the watertight door.

P_{DO} , the probability that the watertight door of a pump room is open when a tsunami hits, can be computed from

$$P_{DO} = f_{OD} \cdot P_{DM} \cdot P_{OF} \cdot T_{bd} \quad (F.5.7.5)$$



1

2

3

4

5

6

7

8

9

10

11

12

13

14

where

f_{OD} = frequency with which the watertight door is opened per hour.

P_{DN} = probability that door is inadvertently left open following personnel entry into pump room.

P_{OF} = probability that control room operators fail to realize that watertight door is open without authorization.

T_{bd} = time before control room operators respond to watertight door open alarm, given failure to realize that door is open without authorization.

A review of plant procedures for maintenance and surveillance testing on the ASW pumps gives a frequency of about 1.4×10^{-3} /hour for opening the door of a pump room. The door is also opened at least once per day for a visual inspection of the pump. This gives a combined frequency of 4.3×10^{-2} /hr for opening a pump room door (f_{OD}).

The probability of leaving the door open, P_{DN} , is a human error of omission and is taken to be 4.7×10^{-3} per demand. This value is based on comparisons with similar activities from the human actions analysis discussed in Appendix H of this report. The probability that the control room operators fail to realize that a watertight door is open without authorization (P_{OF}) is taken to be 0.22, based on Appendix H analysis.



Vertical text on the left side, possibly a page number or header, including characters like '一', '二', '三', '四', '五', '六', '七', '八', '九', '十'.

Small horizontal text or number in the center-right area.

The time it takes the operators to realize that a watertight door is open without authorization, given that they did not first notice when the door should have been closed (e.g., at the end of an inspection), is no more than 24 hours (since visual inspection of the pumps occurs at least once every 24 hours). Therefore, we have

$$P_{DO} = (4.3 \times 10^{-2}/\text{hr}) \cdot (4.7 \times 10^{-3}) \cdot (0.22) \cdot (24 \text{ hours})$$

$$P_{DO} = 0.0011$$

Returning to Equation (F.5.7.4), we have for the probability that water enters the pump room through the watertight door, given a tsunami,

$$P_{WE} = (1 - 0.0011) \cdot (0.133) + 0.0011$$

$$P_{WE} = 0.134$$

Besides flooding the intake structure, there is a second way water can enter the ASW pump compartments. This is through the snorkels that penetrate the top of each pump compartment. These snorkels allow air to circulate into the compartments to ventilate the pump motors. The snorkels are high enough to be safe from flooding up to the +48-foot MLLW level. Therefore, if the sea level exceeds this level, the pump rooms can become flooded.

F.5.7.5 Flooding-Initiated Scenarios

Two flooding scenarios will be considered. The first one is when the water level exceeds +20-foot MLLW when one or more ASW pump room



watertight doors are open or fail. The other is when the water level exceeds +48-foot MLLW and water floods the pump compartments through the snorkels.

To compute the frequency of occurrence of the first scenario, we combine the conditional fragility, P_{WE} , calculated in the previous section, with the scenario initiating frequency, F_{20} . Therefore, the frequency of this scenario is

$$\begin{aligned} f &= (\text{frequency of flooding at +20-foot MLLW}) \\ &\quad \cdot (\text{probability that water is able to enter pump room}) \\ &= (8.4 \times 10^{-4} \text{ per year}) \cdot (0.134) \\ f &= 1.13 \times 10^{-4} \text{ per year} \end{aligned}$$

The consequence of flooding one pump room is reduced by the fact that only one out of the four pumps is needed to service both units.

We will assume that if one ASW door fails (human error or mechanical failure) there is a higher chance that another door also fails. The frequency of flooding all four pump rooms can therefore be estimated by

$$f = F_{20} \cdot P_{WE} \cdot P_{2/1} \cdot P_{3/2} \cdot P_{4/3}$$

where

$P_{2/1}$ = conditional probability that two doors fail, given that one is known to fail.



$P_{3/2}$ = conditional probability that three doors fail, given that two are known to fail.

$P_{4/2}$ = conditional probability that four doors fail, given that three are known to fail.

We will conservatively assume $P_{2/1} = 0.5$ and $P_{3/2} = P_{4/2} = 1.0$

Therefore,

$$f_1 = (8.4 \times 10^{-4} \text{ per year}) \cdot (0.134) \cdot (0.50) \cdot (1.0) \cdot (1.0)$$

$$f_2 = 5.6 \times 10^{-5} \text{ per year}$$

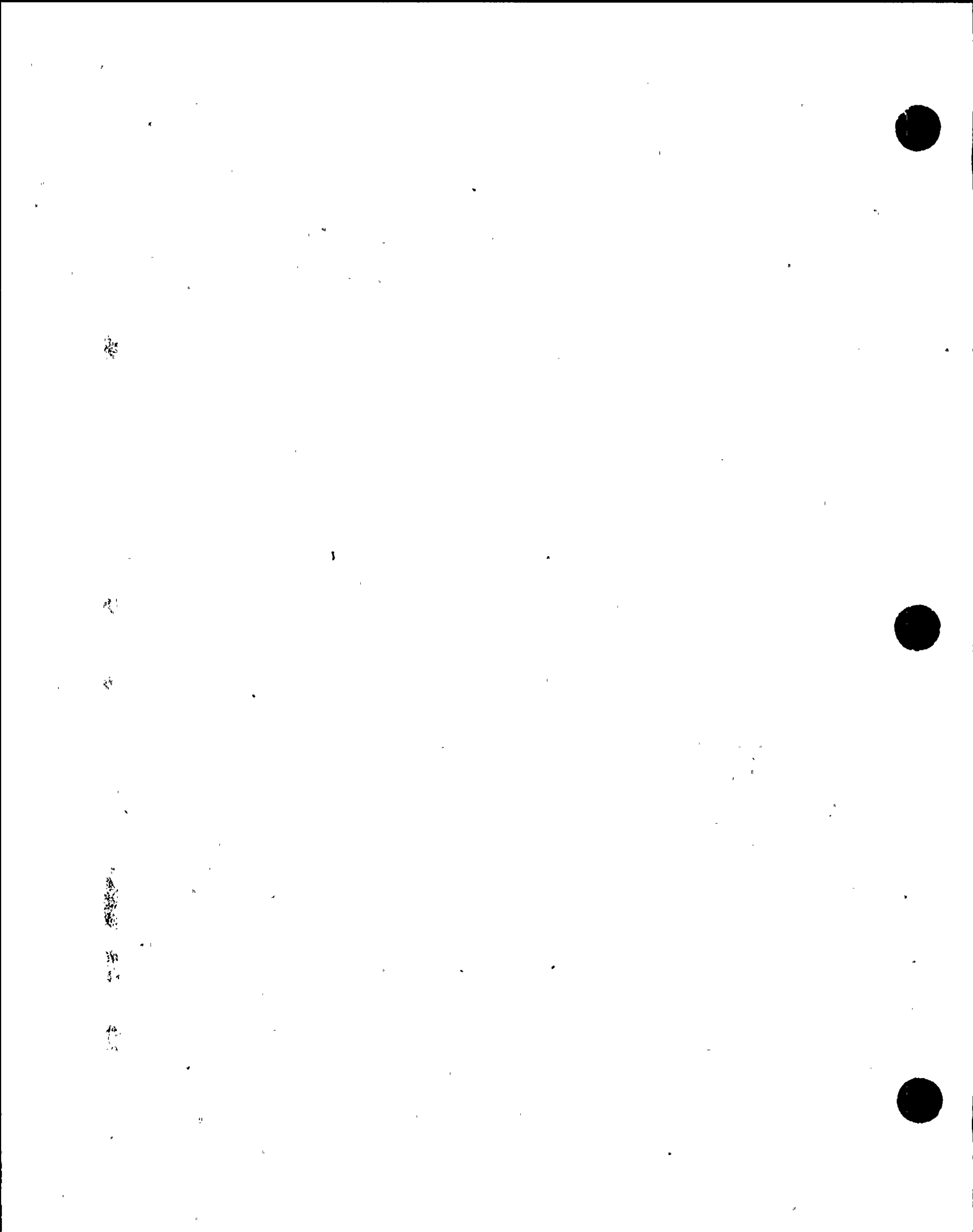
The frequency of occurrence of the second scenario has been computed in Section F.5.7.2. The result is

f_2 = frequency of flooding ASW pump rooms through the snorkels

= frequency of water level exceeding +48-foot MLLW

$$f_2 = 5.0 \times 10^{-7} \text{ per year}$$

In this scenario, all four pump rooms will be flooded through the snorkel penetrations.



The total frequency if flooding all four AWS pumps is

$$\begin{aligned}\phi &= f_1 + f_2 \\ &= 5.6 \times 10^{-5} + 5.0 \times 10^{-7} \\ &= 5.65 \times 10^{-5} \text{ per year}\end{aligned}$$

However, loss of all ASW pumps does not automatically lead to core damage since there is a possibility of aligning fire water to the charging pumps, thus preventing RCP seal failure. The likelihood of recovery of this type is estimated to be 1.27×10^{-2} . The flooding initiated core damage failure frequency, therefore, is

$$\begin{aligned}\phi_c &= \phi (1.27 \times 10^{-2}) \\ &= (5.65 \times 10^{-5}) (1.27 \times 10^{-2}) = 7.18 \times 10^{-7} \text{ per year}\end{aligned}$$

which is negligible compared with other contributors.

F.5.7.6 References

- F.5.7-1. "Units 1 and 2, Diablo Canyon Power Plant Final Safety Analysis Report Update," Pacific Gas and Electric Company, Sections 2.4, 3.4, and 3.8, Rev. 3, September 1987.
- F.5.7-2. Houston, J. R., and A. W. Garcia, "Type 16 Flood Insurance Study: Tsunami Predictions for the West Coast of the Continental United States," Hydraulics Laboratory, U.S. Army Engineer Waterways Experiment Station, December 1978.
- F.5.7-3. Pacific Gas and Electric Company, Diablo Canyon Power Plant, Units 1 and 2, Annunciator Response Procedure, PK01-02, Rev. 6, April 7, 1986.
- F.5.7-4. Pacific Gas and Electric Company, Department of Nuclear Plant Operations, Diablo Canyon Power Plant Units 1 and 2 Emergency Procedure, EP M-5, "Tsunami Warning," Rev. 5, August 16, 1982.

Vertical text on the left side of the page, possibly a page number or header.



TABLE F.5.7-1. EXTREMES OF RUNUP AT THE INTAKE STRUCTURE

Agent Producing Water Level Change	WITH BREAKWATER		WITHOUT BREAKWATER	
	Maximum Runup (feet) Above MLLW Datum		Maximum Runup (feet) Above MLLW Datum	
	Prolonged	Transitory	Prolonged	Transitory
Astronomical Tide	+ 5.3		+ 5.3	
Meteorological Tide	+ 1.0		+ 1.0	
Storm Wave (1 year) Standing Wave Set-up Wave Height	+ 3.15	6.66	+ 11.52	18
Prolonged Water Elevation	+ 9.45		+ 17.82	
Wave Crest Height				18
Maximum Water Elevation Without Tsunami	+ 18.45		+ 35.82	



F.5.7-18

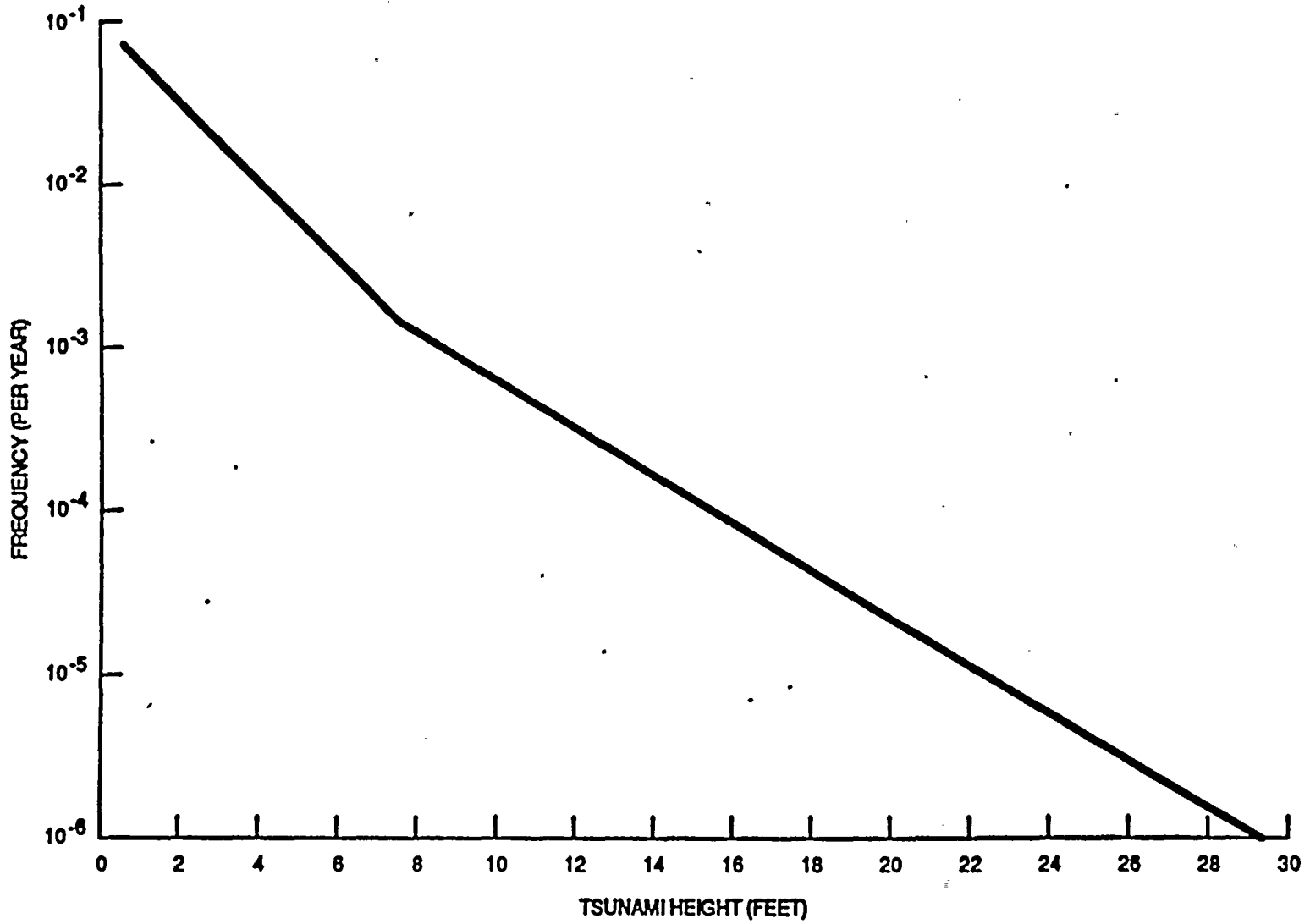


FIGURE F.5.7-1. TSUNAMI FREQUENCY-MAGNITUDE CURVE FOR
LATITUDE $35^{\circ} 12' 44''$ OF CALIFORNIA WEST COAST



Vertical text or markings along the left edge of the page, possibly bleed-through from the reverse side.

H.2 DATA ANALYSIS APPROACH

This section provides a discussion of the techniques used in developing the Diablo Canyon Unit 1 data base. As mentioned earlier, the data was developed by updating generic information with Diablo Canyon-specific information, using Bayesian techniques.

Familiarity with certain basic concepts of Bayesian analysis is essential in understanding the content of this section. These concepts are briefly reviewed in the following.

The methodology used to develop the data for this study is based on the Bayesian interpretation of probability and the concept of "probability of frequency" (Reference H.2-1). In this context, for example, component failure rates are treated as measurable quantities whose uncertainty is dependent on the state of knowledge of the investigation. The "state of knowledge" is presented in the form of a probability distribution over the range of possible values of that quantity. The probability associated with a particular numerical value of an uncertain but measurable quantity indicates the likelihood that the numerical value is the correct one.

A key issue in developing state-of-knowledge distributions for the parameters of the PRA models is to assure that the information regarding each parameter, its relevance, and its value as viewed by the analyst are presented correctly and that various pieces of information are integrated coherently. "Coherence" is preserved if the final outcome of the process is consistent with every piece of information used and with all



assumptions made. This is done by utilizing the fundamental tool of probabilistic inference; i.e., Bayes' theorem (Reference H.2-2).

Mathematically, Bayes' theorem is written as

$$P(x|E, E_0) = k^{-1} L(E|x, E_0)P(x|E_0) \quad (H.2.1)$$

where

$P(x|E, E_0) \equiv$ probability of x being the true value of an unknown quantity in light of new evidence E and prior body of knowledge E_0 .

$L(E|x, E_0) \equiv$ likelihood of the new evidence E assuming that the true value is x .

$P(x|E_0) \equiv$ probability of x being the true value of the unknown quantity based on the state of knowledge E_0 prior to receiving E .

Finally, k is a normalizing factor defined as

$$k \equiv \int_{\text{all } x} L(E|x, E_0)P(x|E_0)dx \quad (H.2.2)$$

In the context of a plant-specific PRA, there are three types of information available for the frequency of elemental events.

E_0 = general engineering knowledge such as that of the design and manufacture of equipment.

E_1 = the historical information from other plants similar to the one in question.

E_2 = the past experience in the specific plant being studied.



1
2
3

4
5
6
7

8

9

The information of types E_0 and E_1 together constitute the "generic" information, and E_2 is the "plant-specific" or "item-specific" information.

Diablo Canyon Unit 1 has had relatively little commercial operating experience to date. Therefore, the data developed for the DCPRA, although based on generic as well as plant-specific information, are dominated by the generic data. However, any additional plant-specific information collected in the course of operating Diablo Canyon units in the future can be incorporated into the existing data by applying Bayes' theorem.

It is very important to note that the information E_0 brings an element of plant specificity in the generic data developed for a plant-specific PRA. In general, decisions regarding the relevance and applicability of different pieces of information in developing each generic distribution are made based on type E_0 information. Therefore, a piece of information may be judged as being relevant in developing the generic data in one PRA and not in another. As a result, generic distributions for different plant-specific studies could be significantly different.

H.2.1 COMPONENT FAILURE RATES

H.2.1.1 Generic Failure Rate Distributions

To discuss the way the failure rate distributions were developed based on different types of information, we consider the following cases.



100

100

100

100

100

100

100

- Type 1. Failure data from operating experience at various nuclear power plants.
- Type 2. Failure rate estimates or distributions contained in various industry compendia, such as WASH-1400 (Reference H.2-3) and IEEE-500 (Reference H.2-4).

By type 1 information, we mean a set of failure and success data collected from the performance of similar equipment in various power plants. Reference H.2-5, for example, provides a detailed list of reported valve failures at various U.S. commercial nuclear power plants for a 2-year period. Also given in this reference are the number of demands and total operating time for the valves at each power plant.

Type 2 information, which could be called processed data, are estimates ranging from the opinion of experts with engineering knowledge about the design and manufacturing of the equipment to estimates based on observed performance of the same class of equipment in various applications. For instance, Reference H.2-4 provides failure estimates based on the opinion of several experts. Estimates of Reference H.2-5, on the other hand, are based on recorded failures of equipment at various nuclear power plants.

Normally, type 2 data are either a point estimate usually referred to as the "best estimate," or a range of values centered about a "best estimate." In some cases, a distribution is provided covering a range of values for the failure rate with the mean or median representing the "best estimate" of the source. For instance, IEEE-500 provides a "low," "high," and "recommended" for the failure rates under normal conditions



30

31

32

33

34

35

36

37

38

39

40



and a "maximum" value under extreme environments. WASH-1400, on the other hand, assesses a probability distribution for each failure rate to represent the variability of the available data from source to source. Such distributions are normally centered around a median value judged to be most representative of the equipment in question for nuclear applications.

The methodology used to develop the Diablo Canyon Unit 1 failure rate data uses both types of information to generate generic probability distribution for the failure rates. Such distributions represent variability of the failure rates, from source to source (for type 2 information) and/or from plant to plant (for type 1 information). Obviously, as applied to Diablo Canyon Unit 1, these distributions are in fact, prior state-of-knowledge curves for the failure rate of components. The following discussion helps to understand the distinction and serves as a prelude to the discussion of the methodology.

Suppose that we have 100 plants and that for each plant the exact value of the failure rate of a particular type of pump is known. Let λ_i be the failure rate of the pump at the i th plant. Suppose further that the λ_i 's can be grouped into a limited number of discrete values, say λ_1^* , through λ_5^* , with 20 of the λ_i 's being equal to λ_1^* , 35 equal to λ_2^* , 25 equal to λ_3^* , 15 equal to λ_4^* , and finally, 5 equal to λ_5^* . The frequency distribution of the λ_i 's is then given by the histogram shown in Figure H.2-1.



1
2
3
4

5
6
7

8

9

10

This histogram represents the "population variability" of the λ_j 's because it shows how the failure rate of the particular type of pumps under consideration varies from plant to plant. It is an exact and true representation of the variability of the failure rate at the 100 plants in the population without any uncertainty or ambiguity because the distribution is based on presumed perfectly known failure rates at each and every one of those plants.

Consider now, the case where only estimates and not the exact values of the failure rates are available for some but not all of the 100 plants in the population. With this state of knowledge, obviously we are not able to know the exact population variability distribution (Figure H.2-1). The question is how one can use this more limited information to estimate the population variability curve and how close the estimate will be to the true distribution as given in Figure H.2-1.

To answer the question, first note that the desired distribution is a member of the set of all histograms. Because of our limited information, we are uncertain as to which member of that set is in fact the true distribution. This situation can be represented by a probability distribution over the set of all possible histograms expressing our state of knowledge about the nature of the true histogram.

For instance, if the entire space, H , of all possible histograms is composed of only n histograms; i.e., if

$$H \equiv \{h_1, h_2, \dots, h_n\}$$



47

7



88

89

90

91

92

93



where h_i represents the i th histogram, the evidence regarding the pump failure rates at different power plants can be used to assess a probability distribution over H as follows

$$P(H) = \{p_1, p_2, \dots, p_N\} \quad \text{with} \quad \sum_{i=1}^n p_i = 1 \quad (\text{H.2.3})$$

where p_i is the chance that h_i is the true histogram.

Figure H.2-2 depicts the situation where the variable λ is considered to be continuous and the desired distribution is a density function.

For a perfect state of knowledge, we would be able to say which h_i is the true distribution; consequently, the corresponding p_i would be equal to 1 and all others equal to 0. However, based on the state of knowledge expressed by Equation (H.2.3), our estimate of the true histogram is

$$\bar{h} = \sum_{i=1}^n p_i h_i \quad (\text{H.2.4})$$

which is called the "expected distribution." Another histogram of interest is one which is assigned the highest chance of being the true histogram. We call that the "most likely distribution," h_m , and we have

$$p_m = \max \{p_i \quad i=1, \dots, n\} \quad (\text{H.2.5})$$



1

2

3

4

5

6

7

8

9

10

11

12

13

14

15

16

17

18

19

20

21

22

23

24

25

The problem of obtaining P , defined by Equation (H.2.3), is formulated in the Bayesian context as follows [see Equation (H.2.1)]

$$P(h_i|E) = k^{-1} L(E|h_i)P_0(h_i) \quad (H.2.6)$$

where $P_0(h)$ is the prior state of knowledge regarding the set H defined by Equation (H.2.3) and $P(h_i|E)$ is the posterior state of knowledge in light of the evidence E . The evidence is incorporated via the likelihood term $L(E|h_i)$ which is the probability of observing the evidence given that the true histogram is h . Finally, k is a normalizing factor defined as [see Equation (H.2.2)]

$$k = \sum_{i=1}^n L(E|h_i) P_0(h_i) \quad (H.2.7)$$

The expected distribution, Equation (H.2.4), is our estimate of the true population variability of the failure rate. It shows how the failure rates of similar pumps are distributed among plants in the population. Now if all we know about a specific pump before we have any experience with it is that it is one member of the population, the population variability curve also becomes our state-of-knowledge distribution for the failure rate of that specific pump. In other words, generic distributions representing the population variability can also be used to predict the expected behavior of any member of the population if no other information is available.

...

...

...

...

...



For this reason, the generic frequency distributions developed based on type 1 and type 2 information are used as the state-of-knowledge distributions for the components at the Diablo Canyon Unit 1 plant prior to incorporating the site-specific information.

The following sections describe how types 1 and 2 information can be used to develop generic distribution.

H.2.1.1.1 Generic Distributions Based on Actual Performance Records (Type 1)

The following discussion is based on the method presented in Reference H.2-6. Consider the case where the following set of information is available about the performance of a generic component in N plants

$$I_1 = \{ \langle k_i, T_i \rangle; i=1, \dots, N \} \quad (H.2.8)$$

where k_i is the number of failures of the component in the i th plant in a specific period of time, T_i .

The desired information is, $\phi(\lambda)$, the distribution of the failure rate of the component, λ , in light of evidence I_1 . This distribution represents the variation of λ from one plant to another, and is analogous to Figure H.2-1.

Following our discussion in Section H.2.1.1, we would like to express a posterior state of knowledge about the true nature of the function $\phi(\lambda)$.



To make matters practical, it is assumed that $\phi(\lambda)$ belongs to a particular parametric family of distributions. Let θ be the set of m parameters of $\phi(\lambda)$

$$\theta = \{\theta_1, \dots, \theta_m\} \quad (\text{H.2.9})$$

For each value of θ , there exists a distribution $\phi(\lambda|\theta)$ and vice versa. Therefore, the state-of-knowledge distribution over the space of all possible $\phi(\lambda|\theta)$ s is the state of knowledge over all possible values of θ and vice versa.

Bayes' theorem in this case is written as [see Equation (H.2.6)]

$$P(\theta|I_0 I_1) = k^{-1} L(I_1|\theta, I_0) P_0(\theta|I_0) \quad (\text{H.2.10})$$

where

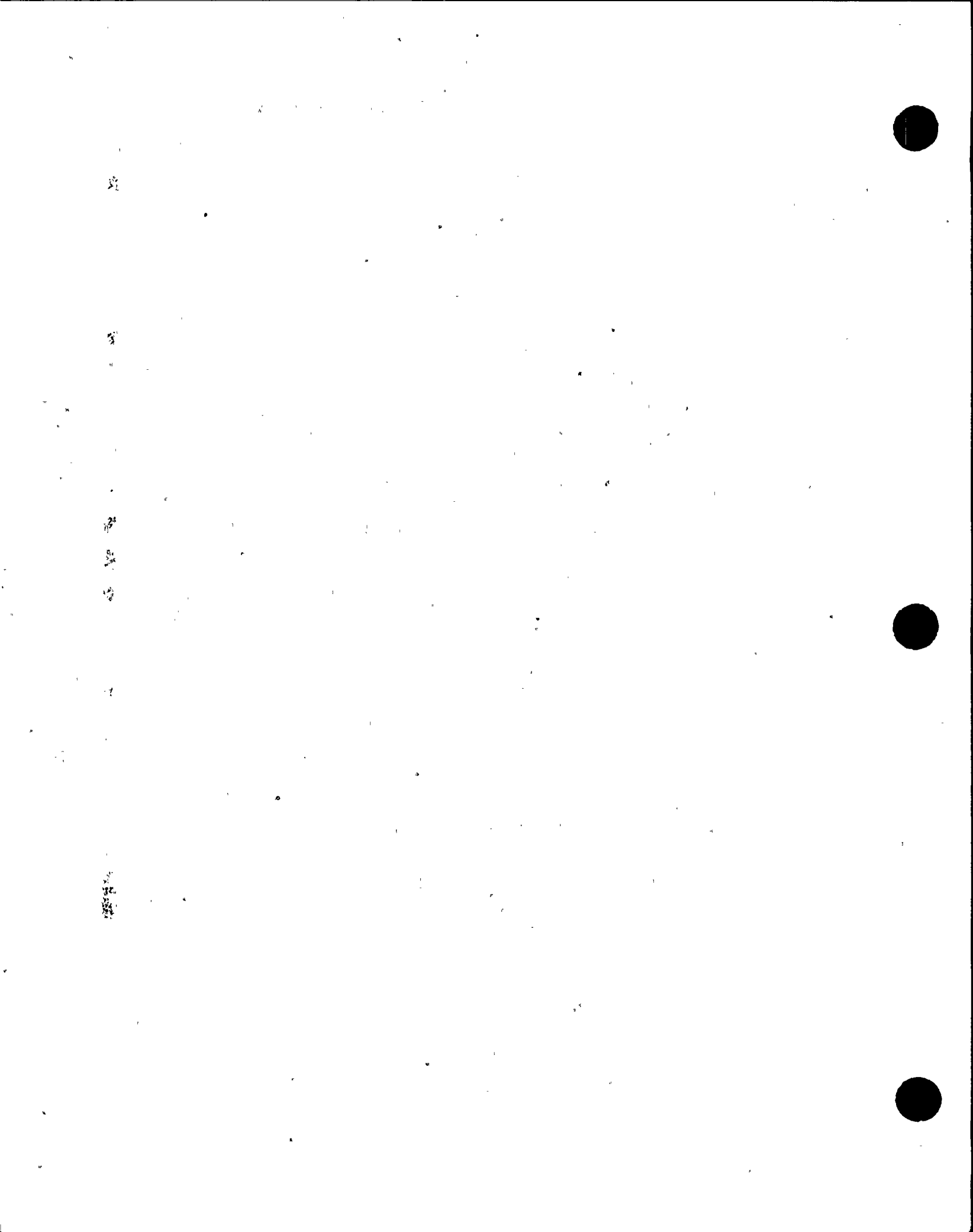
$P(\theta|I_0 I_1)$ = posterior state of knowledge about θ in light of evidence I_1 and prior information I_0 .

$L(I_1|\theta, I_0)$ = the likelihood of evidence I_1 given that the actual set of parameters of $\phi(\lambda)$ is θ .

$P_0(\theta|I_0)$ = prior state of knowledge about θ based on general engineering knowledge I_0 .

and k is a normalizing factor

$$k = \int_{\theta} L(I_1|\theta, I_0) P_0(\theta|I_0) d\theta$$



The likelihood term is the (conditional) probability of observing the evidence, I_1 , given that the data are based on an underlying population variability curve $\phi(\lambda|\theta)$ with θ as the value of its parameters

$$L = P(\langle k_i, T_i \rangle; i=1, \dots, N | \theta, I_0) \quad (H.2.11)$$

Note that L is also conditional on the prior state of knowledge I_0 .

If we assume that the length of operating hours, T_i 's, at different plants are independent of one another and that the observed failures, k_i 's, also have no dependence (according to our model, each k_i is based on a different underlying failure rate) the joint probability distribution given by Equation (H.2.11) can be reduced to the product of the marginal distributions as follows

$$L(I_1 | \theta, I_0) = \prod_{i=1}^N P_i(k_i, T_i | \theta, I_0) \quad (H.2.12)$$

where

$P_i(k_i, T_i | \theta, I_0) \equiv$ probability of observing k_i failures of the equipment in question during the period T_i in the i th plant assuming that the set of parameters of the underlying population variability curve is θ .



52

53

54

55

If the failure rate, λ_i , at the i th plant is known exactly, using a Poisson model, the likelihood of observing k_i in T_i can be calculated from

$$P(k_i, T_i | \lambda_i) = \frac{(\lambda_i T_i)^{k_i}}{k_i!} \exp(-\lambda_i T_i) \quad (\text{H.2.13})$$

However, λ_i is not known. All we know is that λ_i is one of possibly many values of variable λ which represents the variation of the failure rate from plant to plant. In addition, according to our model, λ is distributed according to $\phi(\lambda | \theta)$ with θ being unknown. For this reason, we calculate the probability of observing the evidence, $\langle k_i, T_i \rangle$, by allowing the failure rate to assume all possible values. This is achieved through averaging Equation (H.2.13) over the distribution of λ

$$\begin{aligned} P_i(k_i, T_i | \theta, I_0) &= \int_0^{\infty} P_i(k_i, T_i | \lambda) \phi(\lambda | \theta) d\lambda \\ &= \int_0^{\infty} \frac{(\lambda T_i)^{k_i}}{k_i!} e^{-\lambda T_i} \phi(\lambda | \theta) d\lambda \end{aligned} \quad (\text{H.2.14})$$

Depending on the parametric family chosen to represent $\phi(\lambda | \theta)$, the integration in Equation (H.2.14) can be carried out analytically or by



100

100

100

100



numerical techniques. For example, if $\phi(\lambda|\theta)$ is assumed to be a gamma distribution which has the following form

$$\phi(\lambda|\alpha, \beta) = \frac{\beta^\alpha}{\Gamma(\alpha)} \lambda^{\alpha-1} e^{-\beta\lambda} \quad (\text{H.2.15})$$

with α and β , both nonnegative, as its parameters, the integral can be done analytically resulting in (Reference H.2-5)

$$P_i(k_i, T_i|\alpha, \beta) = \binom{T_i}{k_i} \left(\frac{\beta^\alpha}{\Gamma(\alpha)} \right) \left(\frac{\Gamma(\alpha+k_i)}{(\beta+T_i)^{\alpha+k_i}} \right) \quad (\text{H.2.16})$$

In developing failure rate distributions, $\phi(\lambda|\theta)$ is assumed to be lognormal with μ and σ as its parameters

$$\phi(\lambda|\mu, \sigma) = \frac{1}{\sqrt{2\pi} \sigma \lambda} \exp \left\{ -\frac{1}{2} \left(\frac{\ln \lambda - \ln \mu}{\sigma} \right)^2 \right\} \quad (\text{H.2.17})$$

In this case, Equation (H.2.14) is calculated numerically.

The total likelihood for all N plants can now be found by using Equation (H.2.14) in Equation (H.2.12)

$$L(I_1|\theta, I_0) = \prod_{i=1}^N \left\{ \int_0^\infty d\lambda \phi(\lambda|\theta) \frac{(\lambda T_i)^{k_i}}{k_i!} \exp(-\lambda T_i) \right\} \quad (\text{H.2.18})$$



1
2
3
4
5



6
7

8



The posterior distribution resulting from using the likelihood of Equation (H.2.18) in Bayes' theorem, Equation (H.2.10), is a probability distribution over the m -dimensional space of θ . Any point, θ , in this space has a one-to-one correspondence with a distribution, $\phi(\lambda|\theta)$, in the space of $\phi(\lambda|\theta)$. Figure H.2-3 is an example of $P(\theta|I_0, I_1)$ constructed for $\theta = \{\alpha, \beta\}$; the two parameters of gamma distribution based on the pump data from all U.S. nuclear power plants (Reference H.2-7).

The "expected distribution" is obtained from [see Equation (H.2.4)]

$$\bar{\Phi}(\lambda) = \int_{\theta} \phi(\lambda|\theta) P(\theta|I_0, I_1) d\theta \quad (\text{H.2.19})$$

The quantity $\bar{\Phi}(\lambda)$ "summarizes" the information about λ and is used in this study as the model for generic failure distributions.

Sometimes it is also useful to obtain the "most likely distribution" [see Equation (H.2.4)]. According to the definition, the most probable distribution of λ is the one whose parameters maximize $P(\theta|I_0, I_1)$.

These parameters are, therefore, the solution of the following system of m equations

$$\left. \frac{\partial P(\theta|I_0, I_1)}{\partial \theta_i} \right|_{\theta_{i, \max}} = 0; \quad i=1, \dots, m \quad (\text{H.2.20})$$



The methodology discussed above also applies to failure on demand type of data where the evidence is of the form

$$I_1 = \{ \langle k_i, D_i \rangle, i=1, \dots, N \} \quad (H.2.21)$$

where k_i and D_i are the number of failures and demands in the i th plant, respectively. This can be done if the Poisson distribution used in Equation (H.2.14) is replaced by the binominal distribution

$$P(K_i, D_i | \lambda) = \frac{D_i!}{k_i!(D_i - k_i)!} \lambda^{k_i} (1-\lambda)^{D_i - k_i} \quad (H.2.22)$$

Example

For motor-operated valve failure to start on demand, the following data from six plants were available.

Plant	Number of Failures (k)	Number of Demands (D)
1	10	1.65×10^4
2	14	1.13×10^4
3	7	1.73×10^3
4	42	6.72×10^3
5	3	1.26×10^3
6	31	9.72×10^3

These data, which form a set of type 1 information, I_1 , were used in mode 1 of the computer code BEST4 (Reference H.2-8), which calculates Equations (H.2.14) and (H.2.18) and generates $\Phi(\lambda)$ based on



Vertical text or markings on the left side of the page, possibly bleed-through from the reverse side.

Equation (H.2.19). The result was a 20-bin discrete probability distribution with the following characteristics:

5th Percentile: 6.10×10^{-4}
50th Percentile: 1.05×10^{-3}
95th Percentile: 3.19×10^{-3}
Mean: 2.26×10^{-3}

H.2.1.1.2 Generic Distributions Using Estimates of Available Sources of Generic Data (Type 2)

As mentioned earlier, generic data frequently are not in the fundamental form given by Equations (H.2.7) and (H.2.21). Rather, most sources report point or interval estimates or even distributions for failure rates (type 2 information). These estimates are either judgmental (expert opinion), or based on standard estimation techniques used by the analysts to translate raw data into point or interval estimates, and sometimes into a full distribution.

An example of such estimation techniques is the well known maximum likelihood estimator given by

$$\lambda_M = \frac{k}{T} \quad (\text{H.2.23})$$

where k is the total number of failures in T units of operating time. Most data sources report λ_M and not k and T .



1
2
3
4
5



To develop a model for constructing generic distributions using this type of data, the following cases are considered.

H.2.1.1.2.1 Estimating an Unknown Quantity Having a Single True Value.

The following method is adopted from Reference H.2-9. Suppose there are M sources, each providing its own estimate of λ , which has a single true, but unknown value λ_t . An example is the failure rate of a particular component at a given plant. The true value of that failure rate, λ_t , will be known at the end of the life of the component. Before then, however, the failure rate may be estimated by one or more experts familiar with the performance of the component. Let

$$I_2^* = \{\lambda_i^*; i=1, \dots, M\} \quad (\text{H.2.24})$$

be the set of such estimates where λ_i^* is the estimate of the i th expert for λ_t .

The objective is to use information I_2^* and obtain a state-of-knowledge distribution for λ_t . Obviously, when everything is known about λ_t , such a state-of-knowledge distribution is a delta function centered at λ_t

$$P(\lambda | \text{Perfect Knowledge}) = \delta(\lambda - \lambda_t) \quad (\text{H.2.25})$$

Note that in Equation (H.2.25), λ is used as a variable representing the unknown failure rate.



12

13

14



15

16

17



Assuming a prior state of knowledge, $P_0(\lambda)$, about the quantity λ , Bayes' theorem can be utilized to incorporate information I_2^* into the prior and obtain an "updated" state of knowledge about λ

$$P(\lambda | \lambda_1^*, \dots, \lambda_N^*) = k^{-1} L(\lambda_1^*, \dots, \lambda_N^* | \lambda) P_0(\lambda) \quad (\text{H.2.26})$$

For N independent sources of information the likelihood term, $L(\lambda_1^*, \dots, \lambda_N^* | \lambda)$ can be written as

$$L(\lambda_1^*, \dots, \lambda_N^* | \lambda) = \prod_{i=1}^N P_i(\lambda_i^* | \lambda) \quad (\text{H.2.27})$$

where

$P_i(\lambda_i^* | \lambda)$ = the probability that the estimate of the i th source is λ_i^* , when the true value of the unknown quantity is λ .

The case of dependent sources of information is discussed in Reference H.2-9. Obviously, if the i th source is a perfect one,

$$P_i(\lambda_i^* | \lambda) = \delta(\lambda_i^* - \lambda) \quad (\text{H.2.28})$$

which means the estimate, λ_i^* , is the true value. The posterior, $P(\lambda | \lambda_1^*, \dots, \lambda_N^*)$, in this case will be entirely determined by the estimate of this source

$$P(\lambda | \lambda_1^*, \dots, \lambda_N^*) = \delta(\lambda - \lambda_i^*) \quad (\text{H.2.29})$$



Vertical text or markings on the left side of the page, possibly bleed-through from the reverse side.

In another extreme, when it is believed that the source is totally unreliable,

$$P_i(\lambda_i^*|\lambda) = C \quad (H.2.30)$$

where C is a constant. This means that if the true value is λ , the estimate of the *i*th source can be anything. Using a likelihood of this form in Equation (H.2.26), will show that the estimate of this source, as expected, has no effect on shaping the posterior state of knowledge.

The likelihood term in this approach is the most crucial element. It reflects the analysts' degree of confidence in the sources of information, their accuracy, and the degree of applicability of their estimates to the particular case of interest.

As can be seen, the subjective nature of evaluating and "weighting" of the evidence from different sources fits very well in the above formulation. This becomes clearer in discussing the following models for the likelihood functions in Equation (H.2.27).

Suppose in estimating the true value of λ_t the *i*th source makes an error of magnitude E. Two simple models relating λ_t , E, and λ_t^* are

$$\lambda_i^* = \lambda_t + E \quad (H.2.31)$$

$$\lambda_i^* = \lambda_t \cdot E \quad (H.2.32)$$

22

22

22



In the model of Equation (H.2.31), if a normal distribution is assumed for the error term of the estimate of each source, the likelihood function will be a normal distribution with mean equal to $\lambda_t + b_i$, where b_i is the expected error or, in other words, a "bias" term about which the error of the i th source is propagated.

Formally, we have

$$P(\lambda_i^* | \lambda_t) = \frac{1}{\sqrt{2\pi} \sigma_i} \exp \left\{ -\frac{1}{2} \left(\frac{\lambda_i^* - (\lambda_t + b_i)}{\sigma_i} \right)^2 \right\} \quad (\text{H.2.33})$$

The variance of the likelihood, σ_i^2 , is the variance of the error distribution. Values of b_i and σ_i are assessed by the data analyst subjectively and reflect the credibility and accuracy of the source as viewed by the data analyst. Sometimes, certain information provided by the source such as the uncertainty bound for the estimate can be used to assess σ_i .

If, in addition to a normal likelihood function, a normal prior distribution representing the state of knowledge of the data analyst is assumed for λ_t with mean λ_0 and variance σ_0^2 , the posterior distribution in Equation (H.2.26) will also be normal with mean, λ_p , given by

$$\lambda_p = \sum_{i=1}^N w_i (\lambda_i^* - b_i) \quad (\text{H.2.34})$$



卷
末

and variance

$$\sigma_p^2 = \left(\sum_{i=1}^N \frac{1}{\sigma_i^2} \right)^{-1} \quad (\text{H.2.35})$$

where w_i , defined as

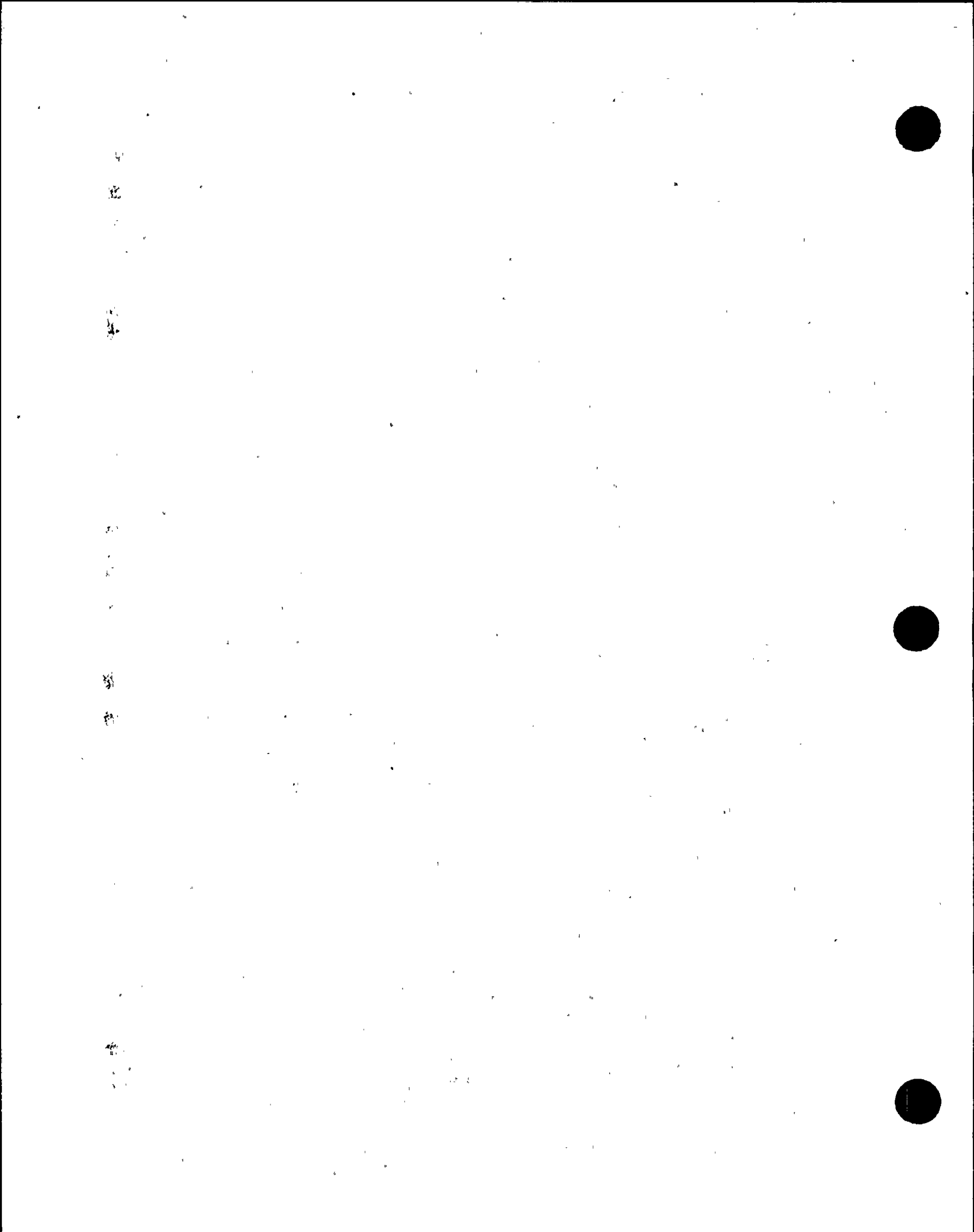
$$w_i = \left(\frac{\sigma_p}{\sigma_i} \right)^2 \quad (\text{H.2.36})$$

is the weight given to the i th source.

Note that

$$\sum_{i=1}^N w_i = 1 \quad (\text{H.2.37})$$

The mean, therefore, is a weighted average of the individual estimates after correcting for their expected biases. Also, as can be seen from Equation (H.2.36), smaller values of σ_i result in higher weights, implying that the source which is believed to make errors of smaller magnitudes (σ_i is the variance of E) is assigned a higher weight; something which is intuitively expected. Extreme cases are when $\sigma_i = 0$ (highest degree of confidence in the i th estimate), for which $w_i = 1$, and when $\sigma_i = \infty$ (no confidence at all) for which $w_i = 0$.



If, instead of the model of Equation (H.2.31), the model of Equation (H.2.32) is applied and the logarithm of the error is assumed to be normally distributed, the likelihood function for the i th source becomes a lognormal distribution

$$P_i(\lambda_i^* | \lambda_t) = \frac{1}{\sqrt{2\pi} \sigma_i \lambda_i^*} \exp \left\{ -\frac{1}{2} \left(\frac{\ln \lambda_i^* - (\ln \lambda_t + \ln b_i)}{\sigma_i} \right)^2 \right\} \quad (\text{H.2.38})$$

where $\ln b_i$ is the logarithmic mean error about the logarithm of the true value, $\ln \lambda_t$, and σ_i is the multiplicative standard deviation. Again, $P_i(\lambda_i^* | \lambda_t)$ is the probability that the estimate of the i th source is λ_i^* when the true value of the failure rate is λ_t . Some evidence in support of the lognormality of $P_i(\lambda_i^* | \lambda_t)$ are provided in References H.2-9 and H.2-10.

By using the model of Equation (H.2.38) for individual likelihoods in Bayes' theorem, Equation (H.2.26), and assuming a lognormal prior distribution for λ_t the posterior state of knowledge will also be a lognormal with the following median value

$$\lambda_{50,p} = \sum_{i=1}^N \left(\frac{\lambda_i^*}{b_i} \right)^{w_i} \quad (\text{H.2.39})$$

where w_i is defined as in Equation (H.2.36).

The median, then, is a weighted geometric average of the individual estimates after correcting for the multiplicative biases. Note that the



usual arithmetic and geometric average methods frequently used in the literature are special cases of these Bayesian normal and lognormal models. For instance, Reference H.2-4 uses the following geometric average of the estimates provided by several experts

$$\bar{\lambda} = \left(\prod_{i=1}^N \lambda_i \right)^{1/N} \quad (\text{H.2.40})$$

which assumes equal weights ($W_i = \frac{1}{N}$), no bias ($b_i = 1$), no prior information, and does not show any uncertainty about the resulting value.

Example

Reference H.2-5 provides a point estimate of 5.60×10^{-3} for the demand failure rate of motor-operated valves. We would like to use this estimate and obtain a state-of-knowledge distribution for the MOV failure rates. We use the lognormal model of Equation (H.2.38) to express our confidence in the estimated value

$$P(\lambda_1^* | \lambda_t) = \frac{1}{\sqrt{2\pi} \sigma_1 \lambda_1^*} \exp \left\{ -\frac{1}{2} \left(\frac{\ln \lambda_1^* - (\ln \lambda_t + \ln b_1)}{\sigma_1} \right)^2 \right\} \quad (\text{H.2.41})$$

where λ_1^* is the estimate (5.60×10^{-3}) and λ_t is the assumed true value of the failure rate which remains an unknown variable at this point. Our subjective judgment about the magnitude of error of the data source is expressed by assigning numerical values to the "bias" term b_1 and the logarithmic standard deviation σ_1 .



1
2
3
4
5
6
7
8
9
10
11
12
13
14
15
16
17
18
19
20
21
22
23
24
25
26
27
28
29
30
31
32
33
34
35
36
37
38
39
40
41
42
43
44
45
46
47
48
49
50
51
52
53
54
55
56
57
58
59
60
61
62
63
64
65
66
67
68
69
70
71
72
73
74
75
76
77
78
79
80
81
82
83
84
85
86
87
88
89
90
91
92
93
94
95
96
97
98
99
100



101
102
103
104
105
106
107
108
109
110
111
112
113
114
115
116
117
118
119
120
121
122
123
124
125
126
127
128
129
130
131
132
133
134
135
136
137
138
139
140
141
142
143
144
145
146
147
148
149
150
151
152
153
154
155
156
157
158
159
160
161
162
163
164
165
166
167
168
169
170
171
172
173
174
175
176
177
178
179
180
181
182
183
184
185
186
187
188
189
190
191
192
193
194
195
196
197
198
199
200



We assume that there is no systematic bias ($b_1=1$). We estimate σ_1 with the aid of range factor (RF) which is a more understandable quantity. Unless otherwise indicated, the range factor here is defined as the ratio of the 95th to the 50th percentiles of the lognormal distribution. Therefore, given the range factor, the value of σ_1 is obtained from the following equation

$$\sigma_1 = \frac{\ln RF}{1.645} \quad (H.2.42)$$

For our example, we assume a range factor of 3. Normally, such a range factor represents a relatively high degree of confidence and means that the source's estimate could be a factor of 3 higher or smaller than the true failure rate and such a statement is made with 90% confidence.

Using this range factor in Equation (H.2.42) results in a value of 0.67 for σ_1 .

If we now use the likelihood of Equation (H.2.41) in Bayes' theorem, Equation (H.2.26), and assume a flat prior distribution, $P_0(\lambda_t)$, the posterior distribution will be

$$P(\lambda | \lambda_1^* = 5.6 \times 10^{-3}) = 106.65 \exp \left\{ -\frac{1}{2} \left(\frac{\ln \lambda - \ln 5.6 \times 10^{-3}}{0.67} \right)^2 \right\} \quad (H.2.43)$$

which has the following characteristics:

5th Percentile: 1.87×10^{-3}

50th Percentile: 5.6×10^{-3}



探 査 記 録 簿

95th Percentile: 1.68×10^{-2}

Mean: 7.01×10^{-3}

H.2.1.1.2.2 Estimating Distributions Using Point Estimates of Various

Sources. We now go back to our original problem which was estimating the generic failure rate distribution $\phi(\lambda|\theta)$. This time, however, we assume that instead of having the set of $\langle k_i, T_i \rangle$ defined in Equation (H.2.8) from various plants, we are given one estimate, λ_i^* , for each plant. That is, the evidence is of the form

$$I_2 = \{\lambda_i^* \mid i=1, \dots, N\} \quad (H.2.44)$$

The model to be used is a combination of the methods presented in Sections H.2.1.3.1 and H.2.1.3.2.1 and is fully discussed in References H.2-7 and H.2-11. A particular family of parametric distributions, $\phi(\lambda|\theta)$, is assumed for λ and the information I_2 is used in Bayes' theorem to obtain a posterior distribution over the entire set of possible values of θ and consequently over all possible distributions $\phi(\lambda|\theta)$. Formally

$$P(\theta|I_2, I_0) = k^{-1} L(I_2|\theta, I_0) P_0(\theta|I_0) \quad (H.2.45)$$

See the set of definitions immediately following Equation (H.2.10) for interpretation of the terms in Equation (H.2.45).



Vertical text on the left side, possibly a page number or title, written in a traditional East Asian style.

The total likelihood function in the present case when λ_i 's are independently estimated can be written as [see Equation (H.2.12)]

$$L(I_2|\theta, I_0) = \prod_{i=1}^N P_i(\lambda_i^*|\theta, I_0) \quad (\text{H.2.46})$$

where

$$P_i(\lambda_i^*|\theta, I_0) \equiv \text{probability that the estimate provided for the } i\text{th plant is } \lambda_i^* \text{ if the parameter of the population variability distribution of the failure rates is } \theta. \quad (\text{H.2.47})$$

To make matters clearer, note that we are assuming that the i th source of data is providing an estimate for the failure rate at a particular plant and all we know is that failure rates vary from plant to plant according to the variability curve $\phi(\lambda|\theta)$. Each λ_i , therefore, is an estimate of one point in that distribution. As a result, there are two sources of variability in the estimates. First, estimates of individual sources are not necessarily perfect; i.e., they could involve errors and biases as discussed in Section H.2.1.1.2.1. Second, even if all the sources were perfect, the estimates would still be different due to the actual variation of the failure rate from plant to plant.

Based on our discussion in the previous section, the confidence that we have in the accuracy of the estimate λ_i^* for the failure rate at



the i th plant can be modeled by a lognormal distribution [see Equation (H.2.38)]. Assuming no bias, we have

$$P_i(\lambda_i^* | \lambda_i) = \frac{1}{\sqrt{2\pi} \sigma_i \lambda_i^*} \exp \left\{ -\frac{1}{2} \left(\frac{\ln \lambda_i^* - \ln \lambda_i}{\sigma_i} \right)^2 \right\} \quad (\text{H.2.48})$$

where λ_i is the true value of the failure rate at the i th plant. Again, we really do not know λ_i but we assume that it belongs to $\phi(\lambda|\theta)$, the distribution representing the variability of λ_i 's from plant to plant. The relation between $P_i(\lambda_i^*|\theta, I_0)$ and $\phi(\lambda|\theta)$ is shown in Figure H.2-4.

Therefore, as we did in the case of Equation (H.2.14) we write

$$P_i(\lambda_i^*|\theta, I_0) = \int_0^{\infty} P_i(\lambda_i^*|\lambda) \phi(\lambda|\theta) d\lambda \quad (\text{H.2.49})$$

As it was mentioned earlier, in developing the failure rate distributions $\phi(\lambda|\theta)$ is assumed to be lognormal defined by Equation (H.2.17).

With this assumption, the integration in Equation (H.2.49) can be done analytically and the result is

$$P_i(\lambda_i^*|\theta, I_0) = \frac{1}{2\pi \sqrt{\sigma_i^2 + \sigma^2} \lambda_i^* \lambda} \exp \left\{ -\frac{1}{2} \frac{(\ln \lambda_i^* - \ln \mu)^2}{\sigma_i^2 + \sigma^2} \right\} \quad (\text{H.2.50})$$



Equation (H.2.45), Bayes' theorem, is now written as:

$$P(\theta|\lambda_1^*, \dots, \lambda_N^*) = k^{-1} \prod_{i=1}^N P_i(\lambda_i^*|\theta, I_0) P_0(\theta|I_0) \quad (\text{H.2.51})$$

The most probable and expected distributions of λ can be found in the same way as discussed in Section H.2.1.1.1. The expected distribution is calculated by using the result of Equation (H.2.48) in Equation (H.2.19). The parameters of the most likely distribution are shown to be solutions of the following system of equations (Reference H.2-12)

$$\ln \mu = \sum_{i=0}^N \frac{(\sigma_i^2 + \sigma^2)^{-1}}{\sum_{i=0}^N (\sigma_i^2 + \sigma^2)^{-1}} \ln \lambda_i^* \quad (\text{H.2.52})$$

$$\sum_{i=1}^N \left[\frac{1}{\sigma_i^2 + \sigma^2} - \left(\frac{(\ln \lambda_i^* - \ln \mu)}{\sigma_i^2 + \sigma^2} \right)^2 \right] = 0 \quad (\text{H.2.53})$$

For perfect sources of information (i.e., $\sigma_i = 0$), the above equations simplify and result in the following solution

$$\mu = \left(\prod_{i=1}^N \lambda_i^* \right)^{\frac{1}{N}} \quad (\text{H.2.54})$$

$$\sigma^2 = \frac{1}{N} \sum_{i=0}^N (\ln \lambda_i^* - \ln \mu)^2 \quad (\text{H.2.55})$$



1
2
3
4
5

Note that Equations (H.2.54) and (H.2.55) are similar to the conventional results for fitting a lognormal distribution to a set of estimates. It should also be mentioned that the results of this section apply to any set of failure rate estimates from various sources where a true variability is suspected to exist among the actual values being estimated by each source. For instance, if several generic sources of data provide estimates for a particular type of equipment and it is known or suspected that each source's estimate is based on a different subset of the population, the methods of this section can be applied to obtain a generic distribution representing the "source to source" variability of the failure rate.

Example

The following set of estimates are available for the demand failure rate of MOVs.

<u>Source</u>	<u>Estimate</u>
WASH-1400 (Reference H.2-3)	1.00×10^{-3}
N-1363 (Reference H.2-5)	5.60×10^{-3}
GCR (Reference H.2-12)	1.00×10^{-3}

To use the model of this section, we need to assign range factors to each source as a measure of our confidence in the estimate provided by that source. In this way, we will be able to determine $P_i(\lambda_i^* | \lambda_i)$, Equation (H.2.48), for each source.



Vertical text on the left side of the page, possibly bleed-through from the reverse side. The characters are faint and difficult to decipher, but appear to be arranged in a single column.

Following our discussion in the example of Section H.2.1.1.2.1, we assign a range factor of 3 to the estimate of N-1363. For the estimate of WASH-1400, we assign a range factor of 5 which results in a broader likelihood, $P_i(\lambda_i^*|\lambda_i)$, for that source and represents a less degree of confidence as compared to N-1363. This is due to the fact that the estimate of N-1363 appears to be based on a larger sample of MOV failures in nuclear applications than the estimate of WASH-1400. The latter provides a range factor of 3 for the lognormal distribution whose median (1.00×10^{-3}) we have taken as the estimate. Assigning a larger range factor of 5 also means that we believe WASH-1400 has overstated its confidence in the estimated median value.

The idea of broadening some of WASH-1400 distributions when used as generic curves was introduced in an early site-specific PRA study (References H.2-13 and H.2-14) where the WASH-1400 curves (as given) were used as generic prior distributions. It was then found that several posterior distributions, reflecting the evidence of the specific plant, lay in the tail region of the prior distributions on the high side. These results led us to the conclusion that the generic curves had to be broadened to reflect greater uncertainty.

References H.2-15 and H.2-16 provide further support to our decision. In Reference H.2-15, the authors review experimental results that test the adequacy of probability assessments, and they conclude that "the overwhelming evidence from research on uncertain quantities is that people's probability distributions tend to be too tight. The assessment of extreme fractiles is particularly prone to bias." Referring to the

Reactor Safety Study, they state "The research reviewed here suggests that distributions built from assessments of the 0.05 and 0.95 fractiles may be grossly biased."

Commenting on judgmental biases in risk perception, Reference H.2-16 states:

A typical task in estimating uncertain quantities like failure rates is to set upper and lower bounds such that there is a 98% chance that the true value lies between them. Experiments with diverse groups of people making many different kinds of judgments have shown that, rather than 2% of true values falling outside the 98% confidence bounds, 20 to 50% do so (Reference H.2-15). Thus, people think that they can estimate such values with much greater precision than is actually the case.

The numerical effect of using a larger range factor is illustrated in the following table

Distribution	5th Percentile	Median	Mean	95th Percentile	Range Factor
WASH-1400	3.3×10^{-4}	1.0×10^{-3}	1.2×10^{-3}	3.0×10^{-3}	3
Broadened Distribution	2.0×10^{-4}	1.0×10^{-3}	1.6×10^{-3}	5.0×10^{-3}	5

We see here that the medians are the same and the mean value increases slightly reflecting the extension of the high side tail of the curve.

For the cases where WASH-1400 was the only source used for a failure rate, the above methodology was used to generate a broader generic curve from the distribution of WASH-1400. The applied range factor, however, was not necessarily the same for each case. Several examples of this



第
一

第
二
第
三
第
四

第
五

第
六

situation can be found in the detailed failure rate description of Reference H.2-17.

Similarly, we assign a range factor of 10 for the GCR (Reference H.2-12) estimate. This reflects a lower degree of confidence in the estimate of Reference H.2-12.

These range factors can be used to obtain the corresponding σ_i values by using Equation (H.2.42). The results are $\sigma_1=0.67$, $\sigma_2=0.98$, and $\sigma_3=1.40$, for WASH-1400, N-1363, and GCR, respectively. These values as well as the estimate from the three sources were used as the main input to the mode 2 of the computer code BEST that calculates Equations (H.2.48) through (H.2.51) and obtains an expected curve based on an integration similar to Equation (H.2.19).

The resulting histogram has the following characteristics:

5th Percentile:	8.4×10^{-4}
50th Percentile:	1.5×10^{-3}
95th Percentile:	7.4×10^{-3}
Mean:	2.0×10^{-3}

H.2.1.1.3 Generic Distributions Based on a Mixture of Type 1 and Type 2 Data

An obvious extension of the situations discussed in Sections H.2.1.3.1 and H.2.1.3.2 is the case where a mixture of I_2 and I_1 information is



3

4

5

6

7

8



available. In this case, the equivalent of Equations (H.2.10) and (H.2.45) is

$$P(\theta|I_2, I_1, I_0) = k^{-1} L(I_2, I_1|\theta, I_0)P_0(\theta|I_0) \quad (\text{H.2.56})$$

If I_1 and I_2 are independent pieces of information

$$L(I_2, I_1|\theta, I_0) = L(I_2|\theta, I_0)L(I_1|\theta, I_0) \quad (\text{H.2.57})$$

where the terms in the right-hand side of the equation are defined by Equations (H.2.12) and (H.2.46).

The expected distribution of λ can now be found from

$$\bar{\phi}(\lambda) = \int_0^{\infty} \phi(\lambda|\theta) P(\theta|I_2, I_1, I_0) d\theta \quad (\text{H.2.58})$$

Example

As an example, we use the combination of the data given in the examples in Sections H.2.1.1.1 and H.2.1.1.2.2. This information was used as the main input to mode 3 of the computer code BEST4, which calculates Equations (H.2.56) through (H.2.58). The resulting discretized distribution has the following characteristics:

5th Percentile: 7.49×10^{-4}

50th Percentile: 2.84×10^{-3}



1
2
3
4
5
6
7
8
9
10
11
12
13
14
15
16
17
18
19
20
21
22
23
24
25
26
27
28
29
30
31
32
33
34
35
36
37
38
39
40
41
42
43
44
45
46
47
48
49
50
51
52
53
54
55
56
57
58
59
60
61
62
63
64
65
66
67
68
69
70
71
72
73
74
75
76
77
78
79
80
81
82
83
84
85
86
87
88
89
90
91
92
93
94
95
96
97
98
99
100

95th Percentile: 1.05×10^{-2}

Mean: 4.30×10^{-3}

H.2.1.1.4 Development of Generic Failure Rate Distributions

Developing a generic data base requires a thorough review, analysis, and tabulation of the available generic data for each of the identified component failure modes. The PLG generic data base is proprietary. It was updated to its current form during the Seabrook PRA (Reference H.2-18), and it is documented in Reference H.2-17, a PLG proprietary report. This PLG generic data base was used as the generic data basis for the Diablo Canyon Unit 1 PRA. In addition to generic data sources, several well documented site-specific failure rate data from power plants examined in previous or ongoing risk studies were used in the development of the generic data base. This assures that the final failure rate distributions accurately reflect all information currently available.

A practical difficulty in using the available generic estimates in the process of developing generic distributions was the lack of standardization in the generic literature. This dictates that utilizing generic sources involves much more than a simple catalog of published failure rate estimates. Each source presents its own unique set of advantages and drawbacks, and these factors must be carefully evaluated before a meaningful comparative analysis may be performed. Typical problems encountered include incompatibility between failure and test data, inclusion of failures due to other than hardware related causes,



Vertical text on the left side of the page, possibly bleed-through from the reverse side. The characters are faint and difficult to read, but appear to be arranged in a single column.

exclusion of failures due to licensing based reporting criteria, and a general lack of specific documentation of assumptions made, boundary conditions, and methodologies applied. Often it is simply not possible to discern the reasons for significant differences among several sources publishing data for the same component failure mode.

Because of the inherent difficulty in ascertaining the direct comparability among these various estimates, the only practical approach to the problem is the assignment of subjective "weighting factors" to each piece of data, based upon the perceived compatibility of the source with the desired failure rate information. These weights are assigned by assessing either a range factor or σ parameter for the likelihood functions for each source according to the models discussed in Section H.2.1.2. This process is computerized via the computer code BEST4, which takes as input various point estimates and corresponding subjective range factors as well as plant-specific experience of the component in question at various plants. The code then performs Bayesian calculations based on the models and generates an average distribution for the failure rate representing source to source and/or plant to plant variability of the data. This process involves several iterations in running the code and reviewing the results to ensure that the range of discrete probability distribution is a reasonable representation of the input information and that the binning of the distribution (20 bins or less) was done properly.

In other cases, where only one source of data was available for the component, failure rate distributions were represented as lognormal. In



Vertical text on the left side, possibly bleed-through from the reverse side of the page.

general, these failure rate distributions were derived by defining the median value and range factor as the two most physically meaningful parameters of the lognormal distribution (the range factor is defined here as the ratio of the 95th percentile to the median, or the square root of the ratio of the 95th and 5th percentiles). In order to provide traceable documentation of the data sources used in this analysis, the median value of such distributions was based on published data. The range factor was subjectively assigned such that the resulting 5th and 95th percentiles of the distribution represent realistic bounds for expected or observed component failure rates.

The relative magnitudes of the range factors developed for the various distributions were influenced by a set of consistent evaluation criteria. In general, range factors significantly greater than 10 (i.e., a span of more than 100 in failure frequency between the 5th and 95th percentiles) were considered to produce distributions so broad as to convey a nearly uninformed state of knowledge and, therefore, would be of marginal utility in any quantification process. The mean value of such a broad distribution, while defined mathematically, is virtually meaningless as a representation of expected component performance because, in truth, very little is known about how the entire population behaves. Some distributions were assigned range factors on the order of 10. Typically, these distributions were characterized by sparse generic data not closely correlated to the desired component failure mode and a relatively low degree of confidence in the available source. It is felt that a distribution this broad conveys only marginal knowledge as to the behavior of a population and is generally indicative of the application of good engineering judgment to minimal prior information.



1

2

3

4

5

6

7

8

9

10

Some distributions were assigned range factors on the order of 3 to 5 (i.e., spans of approximately 10 to 25 between the 5th and 95th probability percentiles). While these distributions are still relatively broad, they represent a higher degree of confidence in the failure rate estimate used as the median value.

Treatment of the generic distributions from IEEE STD-500 (Reference H.2-4) is discussed in the following. This reference contains data for electronic, electrical, and sensing components. The reported values were mainly synthesized from the opinions of some 200 experts (a form of the Delphi procedure was used). Each expert reported a "low," "recommended," and "high" value of the failure rate under normal conditions and a "maximum" value which would be applicable under all conditions (including abnormal ones). The pooling of the estimates was done using geometric averaging technique, e.g.,

$$\lambda_{\max} = \left(\prod_{i=1}^N \lambda_{(\max, i)} \right)^{1/N} \quad (\text{H.2.59})$$

This method of averaging was considered a better representation of the expert estimates, which were often given in terms of negative powers of 10. In effect, the usual arithmetic averages of the exponents were used, which, as discussed in Section H.2.1.1.2.1, is a special case of the Bayesian model presented in this report.

Reference H.2-4 does not recommend a distribution. The method of averaging, however, suggests that the authors have in mind a lognormal



Vertical text or markings along the left edge of the page, possibly bleed-through from the reverse side.

distribution. Our task now is to determine this distribution from the given information.

The recommended value is suggested to be used as a "best" estimate. The word "best" is, of course, subject to different interpretations. We have decided to use it as the median value mainly for two reasons. First, for skewed, lognormal type distributions, the median is a more representative measure of central tendency than the mean, which is very sensitive to the tails of the distribution. Thus, we suspect that the experts who submitted their "recommended" estimates actually had in mind median values. Experimental evidence (Reference H.2-19) also indicates that assessors tend to bias their estimates of mean values toward the medians. The second reason is that this choice is conservative, since the mean value of our resulting distribution is then larger than the "recommended" value. The "maximum" value is taken to be the 95th percentile of the lognormal distribution.

For the majority of the components for Diablo Canyon Unit 1 PRA, generic component failure rates were taken from the PLG generic data base (Reference H.2-17). In a few cases, additional generic distributions had to be developed for some specific types of equipment. Reference H.2-17 provides detailed documentation of the generic distributions used in this study. The mean values of the generic distributions are listed in this appendix, in conjunction with the Diablo Canyon Unit 1-specific failure rate distributions.



11

12

13

14

15

16

17

18



19

20

21

22



H.2.1.2 Data Specialization

Data specialization or the development of plant-specific failure rate distribution is achieved by applying Bayes' theorem as

$$P(\lambda|E_2) = k^{-1} L(E_2|\lambda) \cdot P_0(\lambda) \quad (\text{H.2.60})$$

where $P(\lambda|E_2)$ is the plant-specific failure rate distribution reflecting the plant-specific experience E_2 , and the generic distribution $P_0(\lambda)$ is the prior state of knowledge about the failure rate of the component in question. The likelihood term, $L(E_2|\lambda)$, takes the form of a Poisson distribution when λ is the rate of failure per unit time and the evidence E_2 is k failures in T time units

$$P(k, \lambda | T) = \frac{(\lambda T)^k}{k!} e^{-\lambda T} \quad (\text{H.2.61})$$

If λ is a demand failure frequency and E_2 is k failures in D demands, then $L(E_2|\lambda)$ is a binomial distribution

$$P(k, \lambda | D) = \frac{D!}{(D-k)! k!} (1-\lambda)^{D-k} \lambda^k \quad (\text{H.2.62})$$

The magnitude of the effect of adding plant-specific data depends on the relative strength of the data compared with the prior level of confidence expressed in the form of the spread of the prior distribution. Typically both the location and the spread of the posterior or updated distribution is affected by the plant-specific evidence. The mean value of the updated distribution could be higher or lower than the mean of the



Vertical text or markings along the left edge of the page, possibly bleed-through from the reverse side.

generic prior but adding the plant-specific data normally reduces the spread of the distribution, as shown in the following example. The generic distribution for the MOV demand failure frequency presented in the example of Section H.2.1.1.3 was updated with 15 failures in 5,315 demands. Calculations were performed using mode 4 of the computer code BEST4. The following table compares some basic characteristics for the generic prior and updated distributions.

Distribution	Mean (per demand)	5th Percentile	Median	95th Percentile
Generic	4.30×10^{-3}	7.49×10^{-4}	2.84×10^{-3}	1.05×10^{-2}
Updated	2.87×10^{-3}	1.57×10^{-3}	2.57×10^{-3}	3.85×10^{-3}

H.2.2 COMMON CAUSE FAILURE PARAMETERS

In the DCPRA, such dependent failures as common cause failures at the systems level are treated either explicitly by means of identifying causes of dependent failure and incorporating them into the systems or event sequence models or implicitly by using certain parameters to account for their contribution to the unavailability of the systems. Examples of the first category are the sharing of common components, fires, floods, and certain types of human error during test and maintenance. This section deals with the second category, addressing common cause failures that are not covered in the first category, such as design errors, construction errors, procedural deficiencies, and unforeseen environmental variations.



1
2
3
4
5
6
7
8
9
10
11
12
13
14
15
16
17
18
19
20
21
22
23
24
25
26
27
28
29
30
31
32
33
34
35
36
37
38
39
40
41
42
43
44
45
46
47
48
49
50
51
52
53
54
55
56
57
58
59
60
61
62
63
64
65
66
67
68
69
70
71
72
73
74
75
76
77
78
79
80
81
82
83
84
85
86
87
88
89
90
91
92
93
94
95
96
97
98
99
100



The parametric model used in this study to quantify the effect of the second category of dependent failures is known as the alpha factor method (Reference H.2-20). The following is an overview of the method and the Bayesian technique used in developing state-of-knowledge distributions reflecting various sources of uncertainty in estimating the parameters of the method.

H.2.2.1 Overview of the Alpha Factor Method

In modeling common cause failures we have assumed that there is a certain degree of exchangeability in the way that common cause events impact multiple redundant components. For example, the frequency of failure of components A and B in a system of three identical and redundant components, A, B, and C, is assumed to be the same as the frequency of failure of components B and C due to common cause.

$$Q_{AB} = Q_{BC} = Q_{AC} = Q_2 \quad (\text{H.2.63})$$

In other words, the frequency of multiple component failures depends only on the number and not on the particular combination of components involved. Given this exchangeability or symmetry assumption, the unavailability of a system due to common cause failures can be written in terms of a set of basic frequencies defined as

$$Q_k \equiv \text{frequency of simultaneous failure of } k \text{ components.}$$

Currently, available system success and failure data do allow us to estimate Q_k 's directly. The α -factor model develops estimates for



Q_k 's in terms of the total component failure rate typically available from generic sources of data and a set of parameters obtainable from component failure data.

To describe the model, we consider a system of m identical redundant components and define

α_k = fraction of failure events involving k components due to common cause.

Using the "basic parameters" Q_k defined as

Q_k = frequency of failure of k components due to common cause,

we can see that

$$\alpha_k = \binom{m}{k} \frac{Q_k}{Q_t} \quad k=1, \dots, m \quad (\text{H.2.64})$$

where

$$Q_t \equiv \sum_{k=1}^m \binom{m}{k} Q_k \quad (\text{H.2.65})$$

is the total frequency of all events involving one or more component failures.



Using the system of equations given by Equation (H.2.64), we can write

$$Q_k = \frac{m}{\binom{m}{k}} \frac{\alpha_k}{\alpha_t} Q_t \quad (\text{H.2.66})$$

Also, as a function of Q_k 's, the total failure frequency of a component, Q_c , is

$$Q_c = \sum_{k=1}^m \binom{m-1}{k-1} Q_k \quad (\text{H.2.67})$$

From Equations (H.2.66) and (H.2.67), we get

$$Q_c = \sum_{k=1}^m \binom{m-1}{k-1} \frac{m}{\binom{m}{k}} \frac{\alpha_k}{\alpha_t} Q_t \quad (\text{H.2.68})$$

or

$$Q_t = \frac{\alpha_t}{\sum_{k=1}^m k \alpha_k} Q_c \quad (\text{H.2.69})$$

From Equations (H.2.66) and (H.2.69), we get

$$Q_k = \frac{m}{\binom{m}{k}} \frac{\alpha_k}{\sum_{k=1}^m k \alpha_k} Q_c \quad (\text{H.2.70})$$

海

For a system of three components ($m=3$), the following forms hold.

$$Q_1 = \frac{\alpha_1}{\alpha_t} Q_c \quad (\text{H.2.71})$$

$$Q_2 = \frac{\alpha_2}{\alpha_t} Q_c \quad (\text{H.2.72})$$

$$Q_3 = 3 \frac{\alpha_3}{\alpha_t} Q_c \quad (\text{H.2.73})$$

where

$$\alpha_t = \alpha_1 + 2\alpha_2 + 3\alpha_3$$

If the system success is two out of three, then the system unavailability due to hardware failure can be written as

$$Q(2/3) = 3Q_1^2 + 3Q_2 + Q_3 \quad (\text{H.2.74})$$

Rewriting Equation (H.2.74) in terms of α_k 's and Q_c yields

$$Q(2/3) = 3\left(\frac{\alpha_1}{\alpha_t}\right)^2 Q_c^2 + 3 \frac{\alpha_2}{\alpha_t} Q_c + 3 \frac{\alpha_3}{\alpha_t} Q_c \quad (\text{H.2.75})$$



Estimators for the parameters of the alpha-factor model are developed in the following. The evidence that is typically available on common cause failures is of the form

$$E = \{n_k \quad k=1, \dots, m\}$$

where

n_k = number of events involving k failures due to common cause.

The likelihood of observing this evidence, given a set of values for α_k 's is

$$L(n_1, n_2, \dots, n_m | \alpha_1, \alpha_2, \dots, \alpha_m) = \frac{\Gamma(n_1 + n_2 + \dots + n_m)}{\Gamma(n_1) \dots \Gamma(n_m)} \sum_{k=1}^m \alpha_k^{n_k} \quad (\text{H.2.76})$$

Note that

$$\sum_{k=1}^m \alpha_k = 1 \quad (\text{H.2.77})$$

Using the likelihood of Equation (H.2.76) in Bayes' theorem results in the posterior distribution of $\{\alpha_k \quad k=1, \dots, m\}$

$$\pi(\alpha_1, \dots, \alpha_m | E) = N L(E | \alpha_1, \dots, \alpha_m) \pi_0(\alpha_1, \dots, \alpha_m) \quad (\text{H.2.78})$$

where N is a normalization factor.



Since the likelihood is multinomial, using a Dirichlet prior distribution of the form

$$\pi_0(\alpha_1, \dots, \alpha_m) = \frac{\Gamma(A_1 + A_2 + \dots + A_m)}{\Gamma(A_1)\Gamma(A_2)\dots\Gamma(A_m)} \prod_{k=1}^m \alpha_k^{A_k - 1} \quad (\text{H.2.79})$$

results in another Dirichlet distribution as the posterior, which has the same form as Equation (H.2.79) with the following parameters

$$A'_k = A_k + n_k \quad k=1, \dots, m \quad (\text{H.2.80})$$

The marginal distribution of α_k is a beta distribution with mean and mode given by

$$\text{mean: } \bar{\alpha}_k = \frac{A_k + n_k}{\sum_{k=1}^m (A_k + n_k)} \quad k=1, \dots, m \quad (\text{H.2.81})$$

$$\text{mode: } \alpha_k^* = \frac{A_k + n_k - 1}{\sum_{k=1}^m (A_k + n_k - 1)} \quad k=1, \dots, m \quad (\text{H.2.82})$$

For a uniform prior

$$A_k = 1 \quad k=1, \dots, m \quad (\text{H.2.83})$$



Then

$$a_k^* = \frac{n_k}{\sum_{k=1}^m n_k} \quad k=1, \dots, m \quad (\text{H.2.84})$$

which is the maximum likelihood estimator of α_k 's.

H.2.2.2 Assessment of Uncertainty

Point estimators developed in the previous section only provide single values for the parameters of the α -factor model. However, since the estimates are typically based on limited information, the true value of a parameter may actually differ from the point estimate. The objective of uncertainty analysis is to assess the range of values of each parameter based on the available information and various sources of uncertainty. Variation of the value of a parameter could be due to one or a combination of the following reasons:

1. Size of the data sample.
2. Uncertainty in data classification.
3. Variation among the plants in equipment systems and operational philosophy.



1
2
3
4
5
6
7
8
9
10
11
12
13
14
15
16
17
18
19
20
21
22
23
24
25
26
27
28
29
30
31
32
33
34
35
36
37
38
39
40
41
42
43
44
45
46
47
48
49
50
51
52
53
54
55
56
57
58
59
60
61
62
63
64
65
66
67
68
69
70
71
72
73
74
75
76
77
78
79
80
81
82
83
84
85
86
87
88
89
90
91
92
93
94
95
96
97
98
99
100



101
102
103
104
105
106
107
108
109
110
111
112
113
114
115
116
117
118
119
120
121
122
123
124
125
126
127
128
129
130
131
132
133
134
135
136
137
138
139
140
141
142
143
144
145
146
147
148
149
150
151
152
153
154
155
156
157
158
159
160
161
162
163
164
165
166
167
168
169
170
171
172
173
174
175
176
177
178
179
180
181
182
183
184
185
186
187
188
189
190
191
192
193
194
195
196
197
198
199
200

201
202
203
204
205
206
207
208
209
210
211
212
213
214
215
216
217
218
219
220
221
222
223
224
225
226
227
228
229
230
231
232
233
234
235
236
237
238
239
240
241
242
243
244
245
246
247
248
249
250
251
252
253
254
255
256
257
258
259
260
261
262
263
264
265
266
267
268
269
270
271
272
273
274
275
276
277
278
279
280
281
282
283
284
285
286
287
288
289
290
291
292
293
294
295
296
297
298
299
300



The following sections describe how each of the above sources of uncertainty was treated in this study.

H.2.2.2.1 Assessment of Uncertainty due to Data Sample Size

The first of these sources of uncertainty is a well-known subject in statistics. Larger sets of failure and success data would result in estimates with higher degrees of confidence simply because they are more representative of the general population. For instance, in Equation (H.2.84), the larger the total number of failure events given by the term

$$n_t = \sum_{k=1}^m n_k$$

the more accurate the estimated value of α . The mathematical models presented in Equations (H.2.76) and (H.2.78) provide the mechanism for handling this source of uncertainty.

H.2.2.2.2 Assessment of Uncertainty due to Data Classification

An important source of uncertainty is the judgments that are made in the process of classification of data for use in quantifying common cause parameters. Treatment of this type of uncertainty and several other aspects of data classification that have direct impact on the assessment of common cause parameters are discussed below.



1

2

3

4

5

6

7

8

9

10

11

12

Of fundamental importance in a meaningful assessment of the contribution of common cause events to the system unavailability is a detailed review and systematic classification of failure events experienced in the nuclear industry. The data used for this study are based on review and classification of several thousand failure events reported by U.S. nuclear power plants, as well as Diablo-specific component failure events. The data classification approach was that of Reference H.2-21. In short, events were classified into one of two categories of dependent and independent events. Dependent events are those that involve several component abnormalities that are casually related. All other events are classified as independent. Abnormal states of components are classified as either failed or functionally unavailable when, in both cases, the component is not capable of performing its function according to a given success criterion. The failed state applies to cases when, to restore the component to operability, some kind of repair or replacement action on the component is necessary. A functionally unavailable component, however, is capable of operating, but the function normally provided by the component is unavailable due to loss of such input as motive power, command signal, cooling water, air, etc.

Sometimes, although a given success criterion has been met and the component has performed its function according to the success criterion, some abnormalities are observed that indicate that the component is not in its perfect or nominal condition. Although a component in such a state may not be regarded as unavailable, there may exist the potential of the component becoming unavailable, with time, due to changing conditions or due to more demanding operational modes. Events involving these potentially unavailable states provide valuable information about



1
2
3
4
5
6
7
8
9
10
11
12
13
14
15
16
17
18
19
20
21
22
23
24
25
26
27
28
29
30
31
32
33
34
35
36
37
38
39
40
41
42
43
44
45
46
47
48
49
50
51
52
53
54
55
56
57
58
59
60
61
62
63
64
65
66
67
68
69
70
71
72
73
74
75
76
77
78
79
80
81
82
83
84
85
86
87
88
89
90
91
92
93
94
95
96
97
98
99
100

causes and mechanisms of propagation of failures and thus should not be ignored. The concept of potentially unavailable states also serves a practical need for consistent classification of "grey area" cases and difficult-to-classify situations. The "potentially unavailable" component state category is defined for this situation. It refers to the cases in which the component is capable of performing its function according to a success criterion, but an incipient or degraded condition, as defined below, exists.

- Degraded. The component is in such a state that it exhibits reduced performance but insufficient degradation for declaring the component unavailable according to the specified success criterion. Examples of degraded states are relief valves opening prematurely outside the technical specification limits but within a safety margin and pumps producing less than 100% flow but within a stated performance margin.
- Incipient. The component is in a condition that, if left unremedied, could ultimately lead to a degraded or unavailable state. An example is the case of an operating charging pump that is observed to have excessive lube oil leakage. If left uncorrected, the lube oil would reach a critical level and result in severe damage to the pump.

A key to distinguishing between degraded and incipient conditions is the knowledge that an incipient condition has not progressed to the point of a noticeable reduction in actual performance, as is the case with a degraded condition.



Vertical text or markings along the left edge of the page, possibly bleed-through from the reverse side.

It is important to recognize that potentially unavailable is not synonymous with hypothetical. Both incipient and degraded conditions are indicative of observed, real component states that, without corrective action, would likely lead to unavailable component states.

Dependent events were further grouped into events in which the cause of failure of the component(s) of interest is the failure of another component (component-caused events) and those in which the cause(s) of failure(s) is something other than the state of another component (root-caused events). Finally, events in the dependent category were screened, based on a set of criteria for applicability to PRA-type systems analysis in general and the DCPRA in particular. The criteria for screening the generic data are defined in Reference H.2-17. The events that are not screened out in this process are named "common cause events" and are used to estimate the common cause model parameters.

In estimating the parameters of the α -factor model, a particular system size must be considered. The next step is to calculate the number of component failures for each of the various "system impact" categories. System impact category refers to the number of components being affected in an event. For instance, if, in an event, two components are failed, the system impact category for that event is 2. We explain this step with the aid of a hypothetical example.

Suppose that we want to estimate the common cause contribution to the unavailability of a system of three identical redundant components. Therefore, we need to estimate α_1 , α_2 , and α_3 in addition to the

1

2

3

4

5

6

7

8

9

10



failure rate of the component. Suppose, further, that the data after screening indicate that there have been 88 independent events, involving 70 actual and 18 potential failures. In addition, assume that there have been three common cause events:

- Event 1. In plant X, two components failed due to a common cause. The event occurred in a system of two components. However, the cause of failure was such that, if a similar event occurred in our example system, it would most likely affect all three components.
- Event 2. Two components failed in plant Y within a short period of time, but it cannot be determined, based on the event description, whether the two failures shared the same failure cause. Moreover, it is judged that the event would have the same impact if it occurred in our example system.
- Event 3. One component failed and another was in a degraded condition (potential failure) due to the same cause in plant Z. The impact of the event is judged to be the same in our example plant.

Event 1 involves a situation in which the data from a two-component system should be "extrapolated" by postulating the impact of the cause of the event on a three-component system. Therefore, with regard to the "system impact" of this event, there are two hypotheses: (1) the cause only affects two of the three components, and (2) it affects all three. Weights can be assigned to each of the two hypotheses that reflect the analyst's judgment regarding the two hypotheses. In Table H.2-1, this



1
2
3

4

5
6



situation is represented by weights of 0.05 and 0.95 assigned to the first and second hypothesis, respectively.

Event 2 also involves two hypotheses: (1) two components were affected independently, and (2) the event is a common cause failure of two components. In Table H.2-1, a weight of 0.9 is assigned to the first hypothesis, while the second one is given a weight of 0.1.

In event 3, we are dealing with a common cause situation. However, only one component actually failed, while the state of the other one was "potentially failed." We assign a weight of 0.10 to the hypothesis that two components failed. Consequently, a probability of 0.9 is assigned to the alternative hypothesis.

Table H.2-1 summarizes the information obtained for the common cause events in the form of effective number of failures in each impact category.

Note that in our example for the independent events, the effective number of failures is $70 + (0.1)(18) = 71.8$, where 0.1 is the weight given to potential failures.

Based on the information provided in Table H.2-1, the number of events in various impact categories are: $n_1 = 71.8 + 1.1$, $n_2 = 1.05$, and $n_3 = 0.95$. Therefore,

$$\begin{aligned}n_t &= n_1 + n_2 + n_3 \\ &= 74.90\end{aligned}$$

Using these values in the maximum likelihood estimator of Equation (H.2.84) gives

$$\alpha_1 = \frac{n_1}{n_t} = 0.9733$$

$$\alpha_2 = \frac{n_2}{n_t} = 0.0140$$

$$\alpha_3 = \frac{n_3}{n_t} = 0.0127$$

Note that $\alpha_1 + \alpha_2 + \alpha_3 = 1$, as expected. The above values for n_1 , n_2 , and n_3 can be used directly in the Bayesian formulation Equations (H.2.76) and (H.2.79) with an appropriate prior to obtain the combined effect of uncertainty on data classification as well as on the data sample size discussed earlier in this section.

H.2.2.2.3 Plant-to-Plant Variability of the Alpha Factor Parameters

The third source of uncertainty is the variation of the value of the parameters from plant to plant. This type of variability stems from the fact that similar equipment and systems in various plants may show inherently different failure rates due to a variety of reasons, such as minor design differences within the same category of equipment and variation in system designs and operating philosophies leading to different coupling mechanisms.

12

有 五 張 紙 一 張 紙 一 張 紙 一 張 紙 一 張 紙



There are two approaches for dealing with this issue. One approach is to assess the variability of the parameters, based on statistical evidence from all plants without screening events and based on their applicability to the situation under consideration. This results in a wider range of possible values for the parameters. In the second approach, failure events from various plants are reclassified and events not considered to be applicable to the plant or system of interest are excluded from the data base. The result is the formation of a data sample much larger than one based only on the records of the specific plant under consideration. The resulting uncertainty range for the estimated parameters will obviously be smaller in this case compared with a distribution representing differences in plants. This reduction in uncertainty is the result of applying the additional information about the specific characteristics of the system being analyzed. This was the approach taken in this study to quantify the common cause parameters.

H.2.2.3 Generic Common Cause Parameter Data Base

Based on the approach described in the previous section, the generic data are normally screened for applicability to the particular systems analyses being considered. In that sense, the industrywide data are specialized to the Diablo Canyon plant even at the "generic" level. The generic data used for this study and the result of Diablo-specific event screening are documented in Section H.6. The data base included common cause events for several key components, such as reactor trip breakers, diesel generators, pumps, and valves. Mean values of the generic



22

23

24

25

26

27

28

29

30

31

distributions are provided in Section H.3 in conjunction with the updated distributions.

H.2.3 COMPONENT MAINTENANCE DATA

Maintenance activities that remove components from service and alter the normal configurations of mechanical or electrical systems can provide a significant contribution to the overall unavailability of those systems. This section describes how generic and plant-specific maintenance data were used to develop distributions for component maintenance unavailability.

These distributions apply to maintenance performed during normal operation or in some cases at hot shutdown (but not during cold shutdown). These include both regularly scheduled preventive maintenance activities and also unplanned maintenance events. The specific causes leading to these maintenance activities can include repairs of component failures experienced during operation, repairs of failures discovered during periodic testing, removal of components from service for unplanned testing or inspection, minor adjustments, and hardware modifications.

To quantify maintenance unavailabilities, both the frequency and the mean duration of maintenance are necessary. The frequency defines the rate at which components are removed from service, while the mean duration is the



第 一 章

總 論

一、概 論

二

average amount of time that the component will be out of service. The unavailability due to maintenance is calculated according to

$$Q_M = \frac{f \cdot \tau}{1 + f \cdot \tau} \quad (\text{H.2.85})$$

where f is the maintenance frequency and τ is the mean maintenance duration or, equivalently, the mean time to repair. Note that when $f \cdot \tau$ is significantly less than 1, then

$$Q_M = f \cdot \tau \quad (\text{H.2.86})$$

In order to obtain a state-of-knowledge distribution for the maintenance-related unavailability Q_M , one thus needs state-of-knowledge distributions for both f and τ . Such distributions were developed as described in the following.

H.2.3.1 Frequency of Maintenance

The component maintenance frequency distributions for this study were developed by updating generic maintenance frequency distributions using plant-specific maintenance frequency data from Diablo Canyon Unit 1. The method of updating was the same as that used in updating failure rates (which was described in Section H.2.1.2 on data specialization). Generic maintenance frequency distributions were developed for 17 different categories of components based on the component type and normal service duty (i.e., operating or standby). The basis for these distributions is described in the PLG proprietary data book (Reference H.2-17), and the



Vertical text or markings along the left edge of the page, possibly bleed-through from the reverse side.

component categories are presented in Figure H.2-5. The results of the updating process are presented in Appendix H.3.4.3.

H.2.3.2 Duration of Maintenance

As defined in this data base, the duration of a maintenance event includes the entire time period during which the affected component is unavailable for operation. This is defined to be the period starting when the component is originally isolated or otherwise removed from service and ending when the component is returned to service in an operable state. In many cases, this duration may be only weakly dependent on the actual time required for maintenance personnel to effect the needed repairs.

Generic distributions for mean maintenance durations were developed for 12 categories of components based on the component type and the inoperability limitations imposed by plant technical specifications. The basis for these distributions is described in the PLG proprietary data book (Reference H.2-17), and the component categories are presented in Figure H.2-6. The distributions for plant-specific mean maintenance durations were developed by updating these generic distributions with Diablo Canyon data on component repair times. The technique used to update these distributions is described below.

The computer code BEST4 (Reference H.2-8), which is used for Bayesian estimation of parameters, is intended for estimation of event frequencies based on a number of events, k , and a time period, T . To use this code



to estimate mean maintenance durations, the plant-specific data on maintenance duration have to be converted to equivalent values of k and T . To do this, we made use of the fact that, according to the Poisson model for component failures, the mean value of a failure rate λ can be estimated by

$$\hat{\lambda} = \frac{k}{T} \quad (\text{H.2.87})$$

where k is the number of failures observed in T time units. The variance of this estimator is given by

$$\text{Var}(\hat{\lambda}) = \text{Var}\left(\frac{k}{T}\right) = \frac{1}{T^2} \cdot \text{Var}(k) \quad (\text{H.2.88})$$

If k has a Poisson distribution, then

$$\text{Var}(k) = \lambda T \approx \hat{\lambda} T = k \quad (\text{H.2.89})$$

so Equation (H.2.88) can be rewritten as

$$\text{Var}(\hat{\lambda}) = \frac{1}{T^2} \cdot \text{Var}(k) \approx \frac{k}{T^2} \quad (\text{H.2.90})$$

By substituting \bar{m} (the mean observed maintenance duration at Diablo Canyon Unit 1) for $\hat{\lambda}$ in Equations (H.2.87) and (H.2.90), we then computed appropriate values of k and T by solving the following equations:

$$\frac{k}{T} = \hat{\lambda} = \bar{m} \quad (\text{H.2.91})$$



Vertical text on the left side, possibly a page number or title, written in a small, dark font.

Now, solving for k and T in Equations (H.2.89) and (H.2.90) we get:

$$T = \frac{\bar{m}}{\text{Var}(\bar{m})} = \frac{\bar{m}}{1/n \cdot \sigma_m^2} = \frac{n \cdot \bar{m}}{\sigma_m^2} \quad (\text{H.2.95})$$

and

$$k = T \cdot \bar{m} = \frac{n \cdot (\bar{m})^2}{\sigma_m^2} \quad (\text{H.2.96})$$

Using these values for k and T with the corresponding prior distributions (generated as described in Section H.2.3.2), BEST4 was used to develop plant-specific posterior distributions for mean maintenance durations at Diablo Canyon. In several cases, an adjustment to this procedure was necessary. First, in instances with only one event (for which the computed value of σ_m^2 equaled zero) or instances involving a small number of events whose durations happened to be very close together (in which case the computed value of σ_m^2 was extremely small), more reasonable estimates of σ_m^2 were developed judgmentally, based on the values of σ_m^2 computed for other similar components. Second, it was assumed that the few durations that were longer than the allowed technical specifications represented data collection errors, so that durations were truncated at the technical specification limit. Finally, for components that were not subject to technical specifications, a few events were omitted from the data base; these events had extremely long durations (e.g., a year or more) atypical of the majority of the



Vertical text or markings along the left edge of the page, possibly bleed-through from the reverse side.

maintenance events for the components. The results of this process are presented in Section H.3.4.3.

H.2.4 INITIATING EVENTS FREQUENCIES

The initiating events are divided into two groups according to the method used for quantifying their frequencies. The first set is composed of those events for which the available data from other nuclear power plants are judged to be relevant. This includes essentially all initiating events except those involving failure of systems that have configurations unique to the Diablo Canyon Unit 1 plant, requiring a plant-specific analysis of those systems.

The methodology used to develop the generic and plant-specific distribution of the frequencies of the initiating events in the first group is similar to one used for component failure rates, as described in Section H.2.1. The details of the development of the generic frequencies and the compiled raw data are described in Reference H.2-17.

The details of the development of the frequency of the initiating events in the second group (i.e., those requiring plant-specific analysis of the systems involved) are presented in Sections D.2 and E.10 of this report.

H.2.5 REFERENCES

- H.2-1. Pickard, Lowe and Garrick, Inc., "Methodology for Probabilistic Risk Assessment of Nuclear Power Plants," PLG-0209, June 1981.
- H.2-2. Lindley, D. V., Introduction to Probability and Statistics. Part 1: Probability, Part 2: Inference, Cambridge University Press, 1970.



1

2

3

4

5

6

7

- H.2-3. U.S. Nuclear Regulatory Commission, "Reactor Safety Study: An Assessment of Accident Risks in U.S. Commercial Nuclear Power Plants," Appendix III, "Failure Data," WASH-1400 (NUREG/75-014), October 1975.
- H.2-4. Nuclear Power Engineering Committee of the IEEE Power Engineering Society, "IEEE Guide to the Collection and Presentation of Electrical, Electronic and Sensing Component Reliability Data for Nuclear Power Generation Stations," IEEE STD-500, June 1977.
- H.2-5. Hubble, W. H., and C. F. Miller, "Data Summaries of Licensee Event Reports of Valves at U.S. Commercial Nuclear Power Plants," NUREG/CR-1363, EGG-EA-5125, June 1980.
- H.2-6. Kaplan, S., "On a 'Two Stage' Bayesian Procedure for Determining Failure Rates from Experiential Data," IEEE Transactions on Power Apparatus and Systems, Vol. PAS-102, No. 1, January 1983.
- H.2-7. Mosleh, A., "On the Use of Quantitative Judgment in Risk Assessment: A Bayesian Approach," Ph.D. Dissertation, University of California, Los Angeles, 1981. Available from University Microfilms International, Ann Arbor, Michigan.
- H.2-8. Pickard, Lowe and Garrick, Inc., "Bayesian Estimation Computer Code 4 (BEST4) Users Manual," PLG-0460, December 1985.
- H.2-9. Mosleh, A., and G. Apostolakis, "Models for the Use of Expert Opinions," Proceedings, Workshop on Low-Probability/High-Consequence Risk Analysis, Arlington, Virginia, June 15-17, 1982, Plenum Press, New York, 1983.
- H.2-10. Dalkey, N. C., An Experimental Study of Group Opinion, The RAND Corporation, RM-5888-PR, Santa Monica, California, 1969.
- H.2-11. Mosleh, A., and G. Apostolakis, "Combining Various Types of Data in Estimating Failure Rate Distributions," Transactions of the 1983 Winter Meeting of the American Nuclear Society, San Francisco, California, 1983.
- H.2-12. Hannaman, G. W., "GCR Reliability Data Bank Status Report," General Atomic Company, GA-A14839 UC-77, July 1978.
- H.2-13. Pickard, Lowe and Garrick, Inc., Westinghouse Electric Corporation, and Fauske & Associates, Inc., "Zion Probabilistic Safety Study," prepared for Commonwealth Edison Company, September 1981.
- H.2-14. Apostolakis, G., "Data Analysis in Risk Assessments," Nuclear Engineering and Design, Vol. 71, pp. 375-381, 1982.
- H.2-15. Lichtenstein, S., B. Fischhoff, and L. D. Phillips, "Calibration of Probabilities: The State of the Art," Decision Making and Change in Human Affairs, J. Jungermann and G. de Zeeuw, Editors, D. Reidel Publishing Co., Dordrecht, Holland, 1977.



- H.2-16. Slovic, P., B. Fischhoff, and S. Lichtenstein, "Facts Versus Fears: Understanding Perceived Risk," Societal Risk Assessment, R. C. Schwing and W. A. Albers, Jr., Editors, Plenum Press, 1980.
- H.2-17. Mosleh, A., et al., "A Data Base for Probabilistic Risk Assessment of LWRs," Pickard, Lowe and Garrick, Inc., PLG-0500, 1987.
- H.2-18. Pickard, Lowe and Garrick, Inc., "Seabrook Station Probabilistic Safety Assessment," prepared for Public Service Company of New Hampshire and Yankee Atomic Electric Company, PLG-0300, December 1983.
- H.2-19. Peterson, C., and A. Miller, "Mode, Median, and Mean as Optimal Strategies," Journal of Experimental Psychology, Vol. 68, pp. 363-367, 1964.
- H.2-20. Mosleh, A., "A Multi-Parameter Common-Cause Failure Model," Pickard, Lowe and Garrick, Inc., January 1987.
- H.2-21. Pickard, Lowe and Garrick, Inc., "Classification and Analysis of Reactor Operating Experience Involving Dependent Events," prepared for Electric Power Research Institute, Interim Report, PLG-0400, NP-3967, June 1985.



TABLE H.2-1. EXAMPLE OF THE CALCULATION OF THE EFFECTIVE NUMBER OF FAILURES FOR VARIOUS SYSTEM IMPACT CATEGORIES

	Plant	Impact Vector				
		P ₀	P ₁	P ₂	P ₃	N/A
Event 1	Plant X	0	0	1	0	0
	Example Plant	0	0	0.05	0.95	0
Event 2	Plant Y	0	2(0.1)	0.9	0	0
	Example Plant	0	2(0.1)	0.9	0	0
Event 3	Plant Z	0	0.9	0.1	0	0
	Example Plant	0	0.9	0.1	0	0
Total for Example Plant 8		0	1.1	1.05	0.95	0



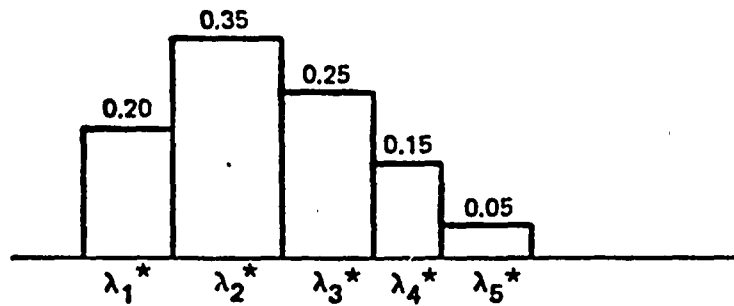


FIGURE H.2-1. POPULATION VARIABILITY OF THE FAILURE RATE

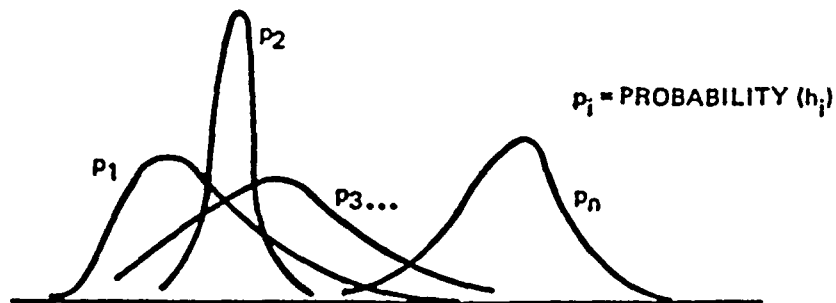


FIGURE H.2-2. STATE-OF-KNOWLEDGE DISTRIBUTION OVER THE SET OF FREQUENCY DISTRIBUTIONS



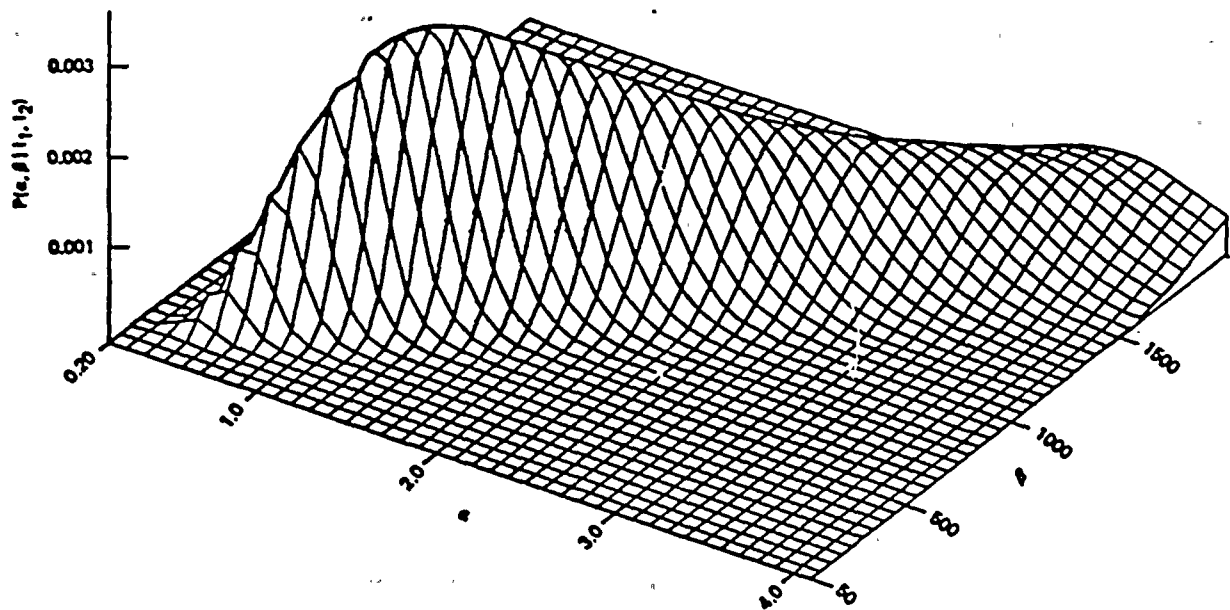


FIGURE H.2-3. POSTERIOR DISTRIBUTION FOR THE PARAMETERS OF THE DISTRIBUTION OF PUMPS' FAILURE TO START ON DEMAND RATES

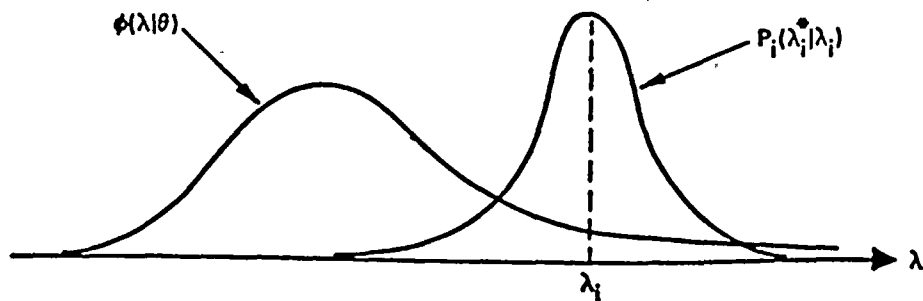


FIGURE H.2-4. THE RELATION BETWEEN THE POPULATION VARIABILITY CURVE AND UNCERTAINTY ABOUT INDIVIDUAL ESTIMATES



H.2-68

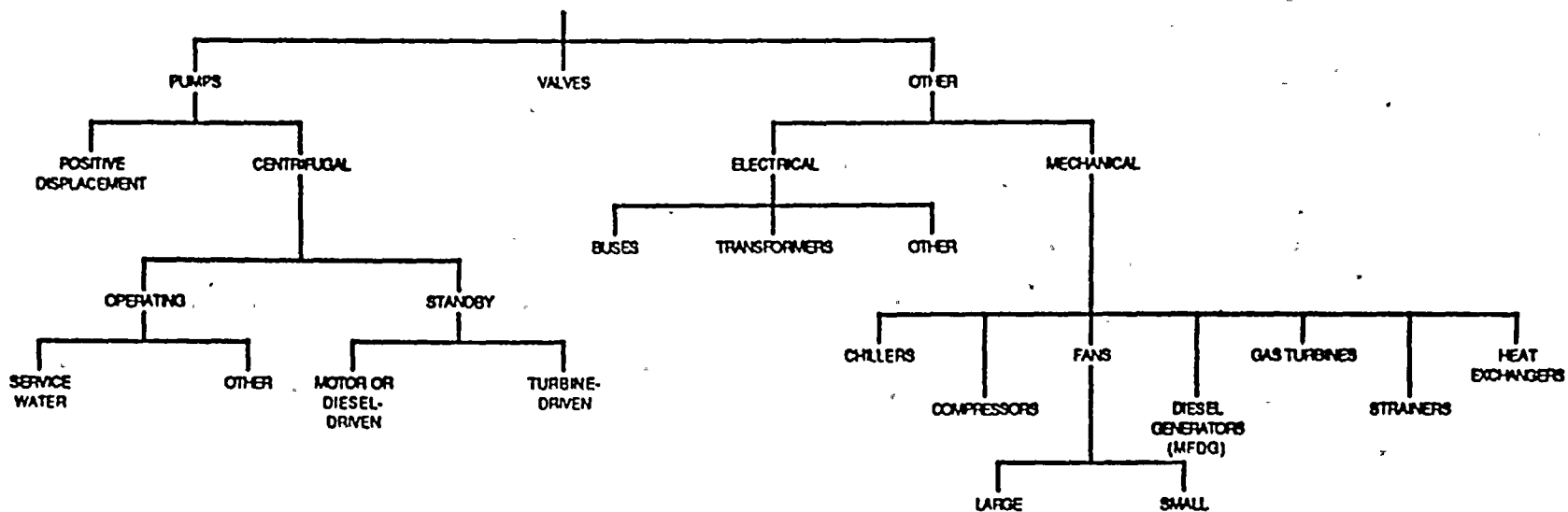


FIGURE H.2-5. CATEGORIZATION OF COMPONENT TYPES FOR GENERIC MAINTENANCE FREQUENCY DISTRIBUTIONS



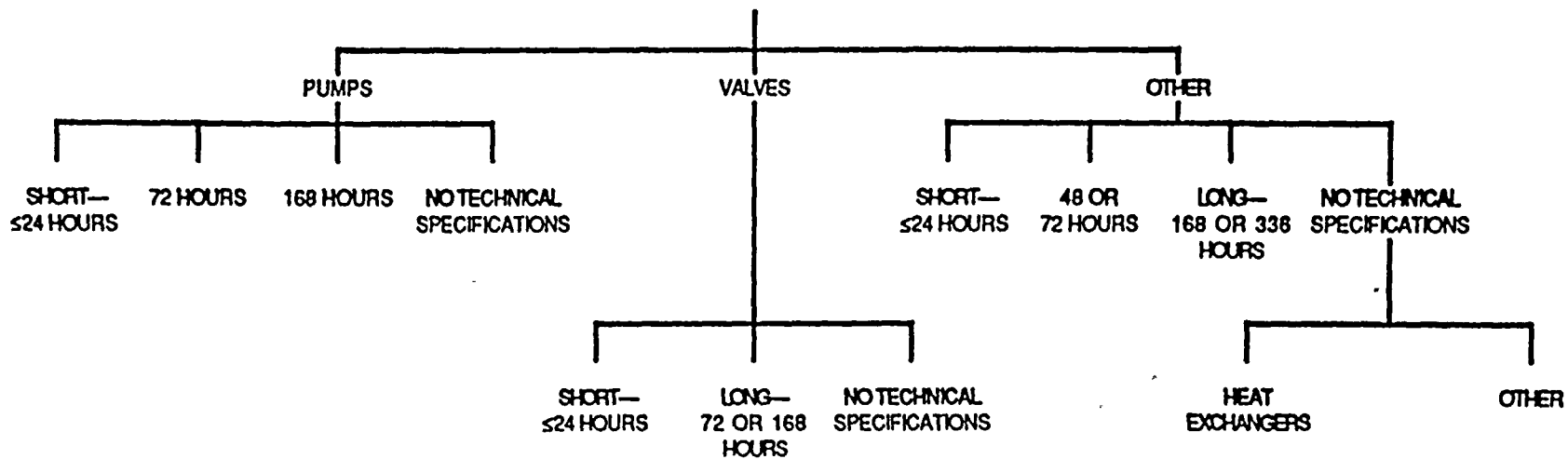


FIGURE H.2-6. CATEGORIZATION OF COMPONENTS BY TECHNICAL SPECIFICATION FOR GENERIC MEAN MAINTENANCE DURATION DISTRIBUTIONS

